THE ASEAN JOURNAL OF RADIOLOGY

September-December 2010
Volume XVI Number III
ISSN 0859 144X

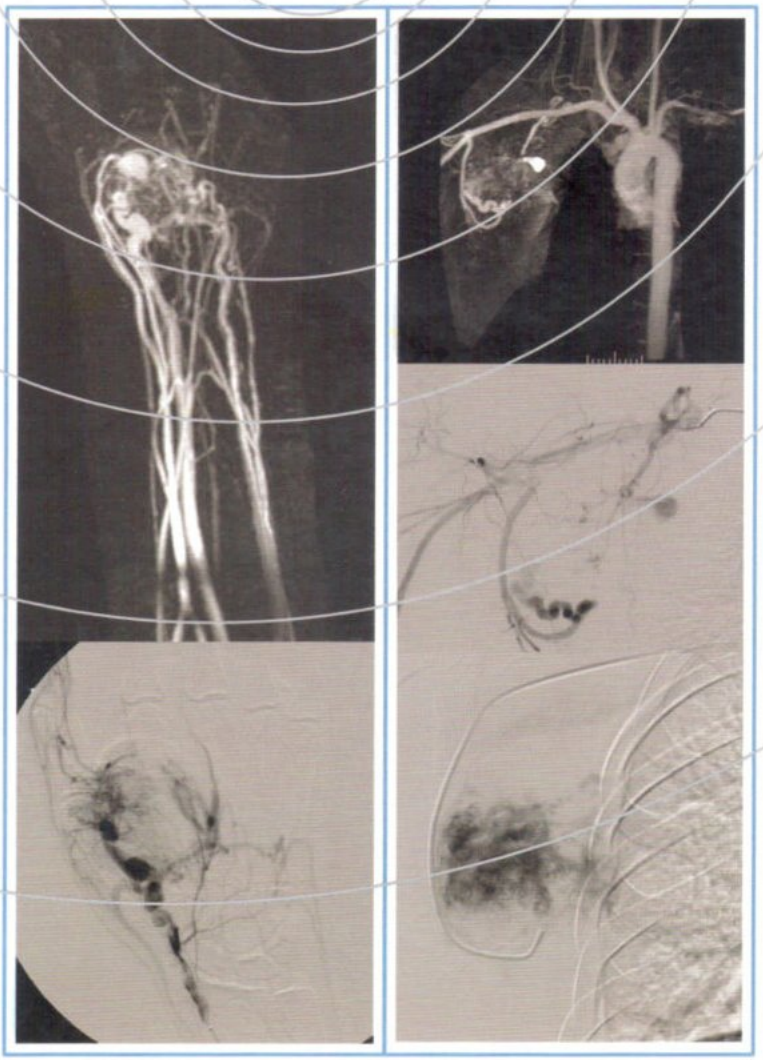

Published by

Royal College of Radiologists of Thailand

and

Radiological Society of Thailand

Bangkok, Thailand.

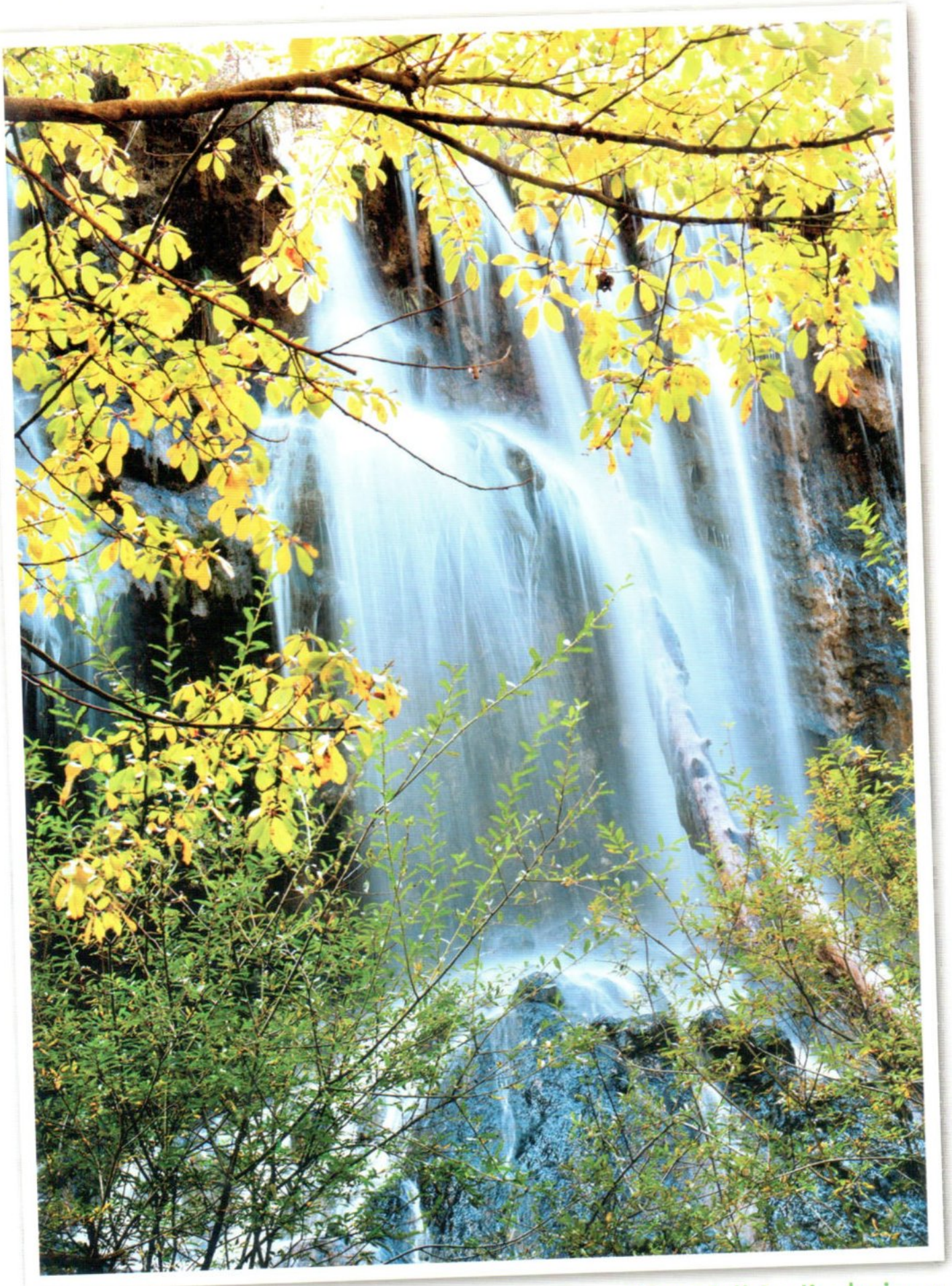

Waterfall in Jiuzhaigou

By Thanwa Sudsang, MD

THE ASEAN JOURNAL OF RADIOLOGY
September-December 2010, Volume XVI No.III

The Committee of Royal College of Radiologists of Thailand

Apr 2009 - Mar 2011

President:	Permyot	Kosolbhand
Vice-president:	Yongyut	Kongthanarat
Secretariat General:	Poonsook	Jitnuson
Vice-secretary General:	Pongdej	Pongsuwan
Treasurer:	Krisdee	Prabhasavat
Academic president:	Sirintara	Singhara Na Ayudya
House Master&Social Programme:	Chutakiat	Kruatrachue
Secretary:	Piyaporn	Apisarnthanarak
Registrar:	Alongkorn	Kiatdilokrath
Committee:	Chorfa	Kaewjinda
	Pimjai	Siriwongpairat
	Chamaree	Chuapatcharasopon
	Pisit	Wattanaruangkowit

The Committee of Radiological Society of Thailand

Apr 2009 - Mar 2011

President:	Permyot	Kosolbhand
Vice-president:	Yongyut	Kongthanarat
Secretariat General:	Poonsook	Jitnuson
Treasurer:	Krisdee	Prabhasavat
Academic president:	Amphai	Uraiverotchanakorn
House Master&Social Programme:	Chutakiat	Kruatrachue
Secretary:	Piyaporn	Apisarnthanarak
Committee:	Chorfa	Kaewjinda
	Chamaree	Chuapatcharasopon
	Alongkorn	Kiatdilokrath
	Pisit	Wattanaruangkowit
	Surat	Vinijsorn

The Journal of the Royal College of Radiologists & Radiological Society of Thailand

(2009 - 2011)

Office:

1. Department of Radiology, Faculty of Medicine, Ramathibodi Hospital 270, Rama VI Road, Toong Phayathai, Ratchathewi, Bangkok, 10400.
   Tel 02-201-1259 #110, Fax 02-201-1297, E-mail Sirintarapongpech2@hotmail.com
2. The Royal college of Radiologists & Radiological society of Thailand. 9th Floor, Royal Golden Jubilee Building, 2 Soi Soonvijai, Petchburi Road, Bankok, 10320
   Tel 02-716-5963, Fax 02-716-5964, E-mail rcrtthailand@gmail.com

Contents

Original Article

Case Report

THE ASEAN JOURNAL OF RADIOLOGY 2010; 16(3): 147-165 147

Original Article

Angiographic Classification and Embolotherapeutic Outcome of High-Flow Arteriovenous Malformations of the Body and Extremities: 4 Years Experience in Ramathibodi Hospital

Jiemjit Tapaneeyakorn, MD.
Keerati Hongsakul, MD.

Body intervention unit, Department of Radiology, Faculty of Medicine, Ramathibodi Hospital, Mahidol University, Bangkok 10400, Thailand

Abstract

Objective: To determine angiographic classification of the high-flow peripheral AVMs and to assess embolotherapeutic outcome in Ramathibodi Hospital.

Materials and Methods: Data from angiograms of the 16 consecutive patients with 18 AVMs were classified by two independent interventionists according to Cho et al classification into arteriovenous fistulae (type I), arteriolovenous fistulae (type II), arteriolovenulous fistulae with non-dilated fistula (type IIIa) and arteriolovenulous fistulae with dilated fistula (type IIIb). The embolotherapeutic outcome was assessed into cure, partial remission, no remission and aggravation. Complications were determined into major and minor conditions.

Result: For classification in 18 AVMs, 55.6% were type IIIb, 16.7% were IIIa, 16.7% were type II, 5.6% were combined type I and IIIb and 5.6% were combined type IIIa and IIIb. The embolotherapeutic outcome was assessed in 12 AVMs that 75 % were partial remission and 25 % had no remission. One patient had major complication (ulna artery dissection). Others had minor complications including pain, skin necrosis and transient erection of penis.

Conclusion: Type IIIb AVM was found as the most common type of high-flow peripheral AVMs. Transcatheter arterial embolization with/without superselection is a primary therapeutic modality in management of patients with peripheral AVM to improve, possible cure or as a presurgical intervention to reduce bleeding and maximize successful resection.

Keywords: Angiographic, Classification, Embolotherapeutic outcome, Arteriovenous malformation

Introduction

Vascular malformations are classified by Mulliken et al in 1982 according to endothelial characteristic and flow dynamic of the lesion into high-flow type such as arteriovenous malformation (AVM), and low-flow type, such as capillary, venous, lymphatic, and mixed malformation.[1-3] High-flow AVMs are rare and less common than low-flow malformations, but management of the high-flow AVMs is often more problematic.

Many patients remain asymptomatic through early life, becoming clinically significant at variable times dependent upon the location and size of the communicating arteries and veins. The symptoms include pain, local hyperhidrosis, ulceration, and bleeding. When massive, they may cause high-output cardiac failure.[4-9]

Currently, initial diagnostic modalities include Color Doppler Imaging (CDI) and Magnetic Resonance Imaging (MRI). CDI is an essential tool in the diagnostic work up of the AVMs. Accurate measurements of flow volumes and resistive indexes can be helpful in the initial evaluation and also are important noninvasive parameters for follow-up after therapy.[10-13] MRI has proven to be a mainstay in the initial diagnostic evaluation, as well as in assessing the efficacy of endovascular therapy.[14] Digital Subtraction angiography (DSA) is the best modality for diagnosis and follow-up, due to ability to assess hemodynamic flow and true comparison.

The angiographic description of AVMs is composed of feeding arteries, the complex network of arteriovenous shunts (referred to as the nidus), and draining veins.[5,15] A few reports have provided the descriptions or classifications of AVMs. In 1993, Houdart et al. classified intracranial AVMs into 3 types based on the morphology of the nidus: type I (arteriovenous), type II (arteriolovenous), or type III (arteriolovenulous).[5,8,16] In 2006, Cho et al.[5] modified this classic classification for use with peripheral AVMs into 4 types based on angiography [Fig.1] because the original system did not account for a unique feature of some AVMs - the blush type on angiography. Also some types of AVMs can be treated by direct puncture, whereas intracranial AVMs cannot. Type I is arteriovenous fistulae; type II, arteriolovenous fistulae; Type IIIa, arteriolovenulous fistulae with non-dilated fistula; and type IIIb, arteriolovenulous fistulae with dilated fistula.

Historically, surgery was the primary treatment for AVMs, but the cure rate was low. Recently, embolization with various embolic agents has been suggested as the primary therapeutic modality for improvement, cure or presurgical intervention to reduce bleeding and maximize successful resection.[3,4,17,18] In embolization, permanent occlusion of the nidus should be the goal. The technique can be applied though transarterial, transvenous or direct puncture approaches. Many endovascular occlusive agents are used including autologous clot, Gelfoam, Polyvinyl alcohol particles (PVA), various metallic coils with or without fibers, tissue adhesives glue (IBCA/NBCA), detachable balloons, Ethibloc, Sotradecol and ethyl alcohol.[3,13,18-21]

Due to the rarity of high-flow peripheral AVMs and embolotherapy is the primary standard treatment. The primary purpose of this study was to determine the angiographic classification of high-flow peripheral AVMs found in Ramathibodi Hospital. The secondary purpose was to assess embolotherapeutic outcome of peripheral high-flow AVMs in Ramathibodi Hospital.

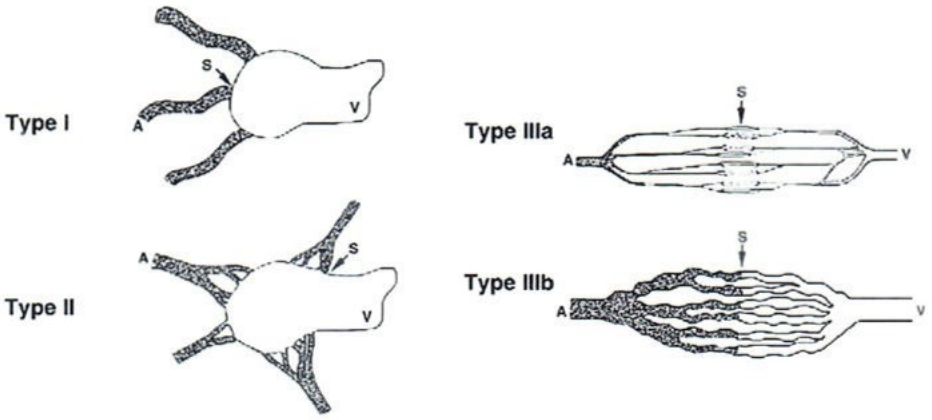

Fig.1 A diagram for the 4 types of AVMs based on angiogram of nidus morphology according to Cho et al. Type I (arteriovenous fistulae) AVMs: no more than 3 separate arteries shunt to the initial part of a single venous component. Type II (arteriolovenous fistulae): multiple arterioles shunt to the initial part of a single venous component, in which the arterial components show a plexiform appearance on angiography. Type IIIa (arteriolovenulous fistulae with non-dilated fistula): fine multiple shunts are present between arterioles and venules and appear as a blush or fine striation on angiography. Type IIIb (arteriolovenulous fistulae with dilated fistula): multiple shunts are present between arterioles and venules and appear as a complex vascular network on angiography. In types I and II, the first identifiable venous structure downstream of the shunt is the initial part of the draining vein. In types IIIa and IIIb, multiple venulous components of the fistula unit collect to a draining vein. A: arterial compartment of the fistula unit, V: venous compartment of the fistula unit, S: shunt

Materials and Methods

Patients

This was a retrospective study, approved by our institutional research ethic committee. We reviewed the angiographic data of patients who were diagnosed with body and/or extremity AVMs during a 4-years period from January 2004 to December 2007, searched from all databases at the Intervention Unit of the Department of Radiology, Ramathibodi Hospital.

The inclusion criteria included all patients, age 0-60 years, diagnosed with body and/or extremity AVMs by angiography at the Intervention Unit of the Department of Radiology, Ramathibodi Hospital. Patients with missing or inadequate data were excluded.

This study included 16 consecutive patients with 18 peripheral AVMs.

Diagnostic Angiography and Embolotherapy Technique

- Written consent for the procedure was obtained from all patients after a discussion about the advantages and risks of the procedure.
- Risk of allergy to contrast media was evaluated. If the patient was at risk, premedication with oral and intravenous steroids was administered.
- Coagulogram (Partial thrombin time; PTT

and prothrombin time; PT), platelet count and serum creatinine were evaluated at the admitting ward. If a laboratory result was abnormal, it was corrected to normal value before the procedure.

- Patients were in supine position during the procedure under local or general anesthesia with monitoring of vital signs and oxygen saturation. Intravenous fluid was given via superficial vein of the left hand.

- Selective angiography was done using 4 or 5 F catheter via common femoral arterial approach. The anatomy of the feeding arteries to the lesions was identified and localized before embolotherapy. Transcatheter embolization was performed via 4 or 5 Fr catheter or coaxial micro- catheter technique in some patients with small-sized feeding arteries. The catheter was advanced as close as possible to the nidus of the AVMs. After that, pre-test embolization was performed by trial injection of contrast agent into the catheter during image acquisition. The volume of contrast material required to fill the nidus and just opacify the draining vein was noted. Embolization was done using a mixture of contrast media and embolic agent. Five to 10 minutes after embolization, an angiogram was performed to determine whether the AVMs had been embolized completely. Meticulous repetition of these techniques was required for complete embolization of at least 1 compartment of the AVM. All patients were followed for immediate or delayed complications.

- Additional embolization was performed if symptoms and signs remained or the AVMs persisted on follow-up imaging studies.

- Non-ionic contrast media used in the procedures included Hexabix 320, Xenetic 350, Ultravist 370 and Omnipaque 370. Dose of contrast media was 1-2 ml/kg.

- The angiogram machines used were Infinic VC DSA; (Toshiba, Japan) from 01 January 2004 to 30 September 2006 and Infinic VC-I flat panel DSA; (Toshiba, Japan) from 01 October 2006 to 31 December 2007.

Evaluation of Angiographic Studies and Clinical Data

Two reviewers independently interpreted the angiographic classification of the peripheral high-flow AVMs, one a board certified interventional radiologist (JT) and the other a second-year body interventional radiology fellow (KH). The interpretation of angiographic classification of the peripheral high-flow AVMs into types I, II, IIIa and IIIb was according to Cho et al.[5]

Data on patient demographics, clinical assessment, imaging studies, treatment, complications, and outcome were obtained from the medical records, as were the results of follow-up consultations, examinations, and imaging. Only the therapeutic and clinical outcomes of embolotherapy were included and not those of combined treatments. The final clinical data were updated by telephone if possible.

Definitions

The angiographic classification of the high-flow peripheral AVMs according to Cho et al.[5] modification are type I, II, IIIa and IIIb. Type I (arteriovenous fistulae) refers to at most 3 separate arterial shunts to a single draining vein. Type II (arteriolovenous fistulae) indicates multiple arterioles shunted into a single draining vein. Type IIIa (arteriolovenulous fistulae with non-dilated fistula) indicates fine multiple shunts between arterioles and venules which appear as a blush or fine striation on angiography. Type IIIb (arteriolovenulous fistulae with

dilated fistula) refers to multiple shunts between arterioles and venules and appear as a complex vascular network on angiography.

The therapeutic outcomes are assessed according to clinical response and degree of devascularization at final angiography. Non-invasive imaging, including color doppler sonogram, CTA or MRA, are additional modalities used to evaluate residual or recurrent lesion. Cure is defined as complete resolution of the clinical symptoms and signs with 100 % devascularization of the AVMs. Partial remission is defined as complete resolution or an improvement in clinical symptoms and signs with 50% to 99% AVM devascularization. No remission is defined as an improvement or no change in clinical symptoms and signs with less than 50% devascularization. Aggravation is defined as a worsening of clinical symptoms and signs regardless of the degree of AVM devascularization. Treatment failure is defined as a procedure that resulted in amputation of the extremity at the lesion site or instances when the nidus of AVM could not be approached. Cure and partial remission are considered to be effective or successful therapeutic outcomes of embolization. Major complications are death, permanent adverse sequelae, need for major therapy or prolonged hospitalization (more than 48 hours). Minor complications are any component adverse sequelae, such as transient nerve injuries, a skin injury that spontaneously heals or pain that spontaneously resolves.

Statistical Analysis

The ordinal data, including age, sex, symptom and location of AVM, was presented as frequency and percentage. The consensus of angiographic classification between the two participants was evaluated using statistical methods (test of agreement, i.e. percent of agreement, Kappa analysis and p-value), and the outcome of embolotherapy was described.

Results

Patient characteristics

16 patients were enrolled, diagnosed with body and/or extremity AVMs by angiogram at the Intervention unit of Department of Radiology, Ramathibodi Hospital from January 2004 to December 2007. There were 6 males and 10 females. The mean age was 29 years (range 10-59 years). 13 patients had presenting symptoms, most common of which was mass (81%). One 10-year-old patient had congestive heart failure. 2 patients had no presenting symptoms, the AVM being an incidental finding from CT or MRI. Most common location of the AVM was the leg (22%). 2 patients had more than one location. One patient had three locations: the pelvic cavity, thigh and leg. Another one had a large AVM involving the forearm, hand and finger. Details of the patient data are shown in Table 1.

Angiographic findings

According to Cho et al[5] classification of high-flow peripheral AVMs, the most common type of AVM in this study was IIIb (n=10, 55.6%) [Table 2, Fig.1 and Fig.2A, 2B]. Type II and type IIIa AVMs were found in three patients (16.7%) [Fig.3 and Fig.2C, 2D]. Two AVMs were categorized as combined type; one type IIIa+IIIb and one type I+IIIb [Fig.4]. In the independent analysis of AVM type by two interventionists, JT and KH, 5 AVMs were classified differently. Two AVMs (II and IIIa) were classified as type IIIb [Fig.3B]. One type IIIb was regarded as type II. One combined type IIIa and IIIb was also

Table 1 Patient characteristic

Patient characteristics	Number (%)
Age (mean 29.5 ± 1.3 yrs, range 10-59 yrs)	
Sex (n=16)	
Male	6 (37.5)
Female	10 (62.5)
Symptom (n=16)	
Mass	13 (81.25)
Ulcer	2 (12.5)
Bleeding	2 (12.5)
Congestive heart failure	1 (6.25)
Pelvic discomfort	1 (6.25)
No symptom	2 (12.5)
Location (n=18)	
Trunk	2 (11.11)
Pelvic cavity	3 (16.67)
Arm	2 (11.11)
Forearm	3 (16.67)
Hand	2 (11.11)
Finger	2 (11.11)
Thigh	1 (5.56)
Leg	4 (22.22)
Foot	1 (5.56)

Table 2 Angiographic classification (n=18)

Angiographic classification	Number of lesion (%)
Type I	-
Type II	3 (16.67)
Type IIIa	3 (16.67)
Type IIIb	10 (55.56)
Type I+IIIb	1 (5.56)
Type IIIa+IIIb	1 (5.56)
Total	**18 (100)**

Type I (arteriovenous fistulae) AVMs: no more than 3 separate arteries shunt to the initial part of a single venous component.

Type II (arteriolovenous fistulae): multiple arterioles shunt to the initial part of a single venous component, in which the arterial components show a plexiform appearance on angiography.

Type IIIa (arteriolovenulous fistulae with non-dilated fistula): fine multiple shunts are present between arterioles and venules and appear as a blush or fine striation on angiography.

Type IIIb (arteriolovenulous fistulae with dilated fistula): multiple shunts are present between arterioles and venules and appear as a complex vascular network on angiography.

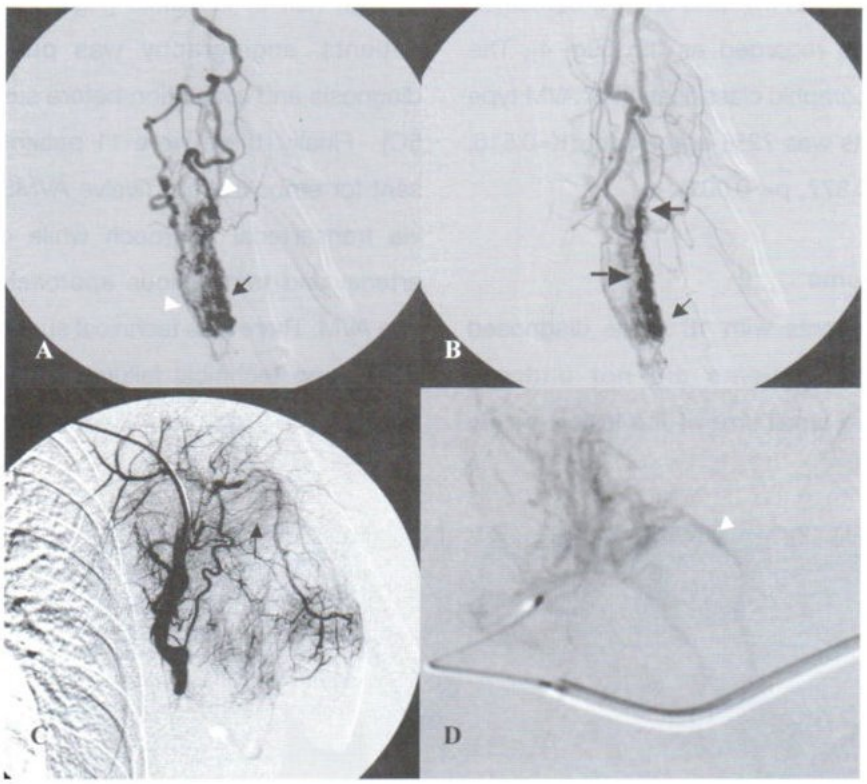

Fig.2 Angiogram of Type III AVM: (A): arterial and (B): venous phases of the type IIIb: complex arteriolar and venulous connection of the nidus (small arrows), arterial feeding (arrowheads) and early draining veins away from the nidus (large arrows). This AVM was not embolized, due to difficult treat safely and high risk for ischemia. The patient was treated by surgical excision. (C and D): two cases of type IIIa: nidus are seen as a blush or fine striation without vascular network (arrow). Note draining vein (arrowhead)

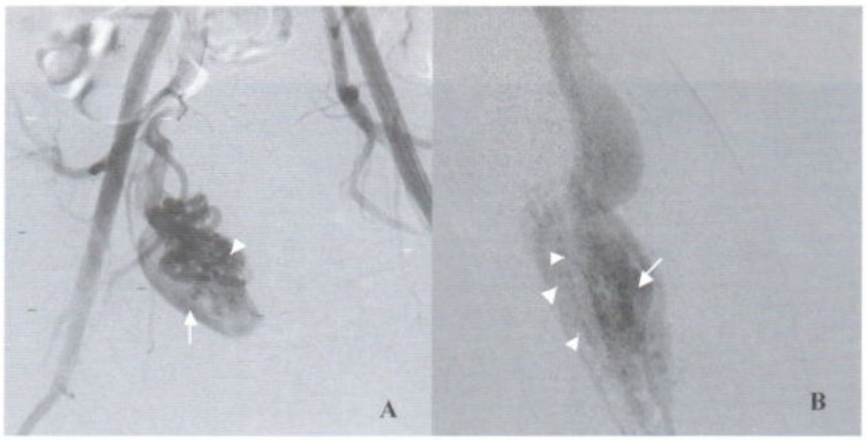

Fig.3 Angiogram of Type II AVM: (A): pelvic and (B): leg AVMs: complex network of arteriolar component and a large venous pouch, nidus (arrowheads) and venous pouch (arrows). The leg AVM (B): this case was classified as type IIIb when independent review because many components of the nidus (arrowhead).

classified as just type IIIa AVM, and another combined type I and IIIb was regarded as IIIb [Fig. 4]. The consensus of angiographic classification of AVM type by 2 interventionists was 72% agreement (K=0.516, 95% CI 0.156 to 0.877, p< 0.001).

Therapeutic outcome

Of the 16 patients with 18 AVMs diagnosed by angiography, 5 patients did not undergo embolization due to small size of the lesion, safety or high risk of ischemia [Fig.2A, 2B, 5A]. In some patients, angiography was performed just for diagnosis and evaluation before surgery [Fig.5B and 5C]. Finally, there were 11 patients with 13 AVMs sent for embolization. Twelve AVMS were accessed via transarterial approach while combined trans-arterial and transvenous approach was used with one AVM. There was technical success with 11 AVMs (85%) and technical failure in 2 patients (patients 10 and 11) [Fig.6 and 7] due to tortuous arterial

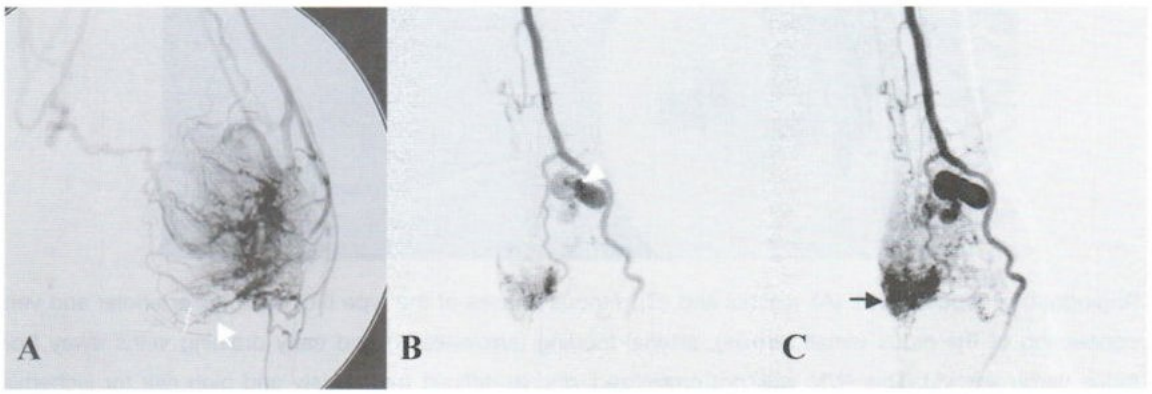

Fig.4 Angiogram of combine AVM type: (A): combine type IIIa and IIIb, which just classified as type IIIa because dominant of blush or fine striation and minimal complex network of nidus (arrow). (B and C): early and late arterial phases of combine type I and IIIb that just classified as type IIIb because dominant complex network of nidus (arrows). Note direct arterovenous fitula: type I AVM (arrowhead).

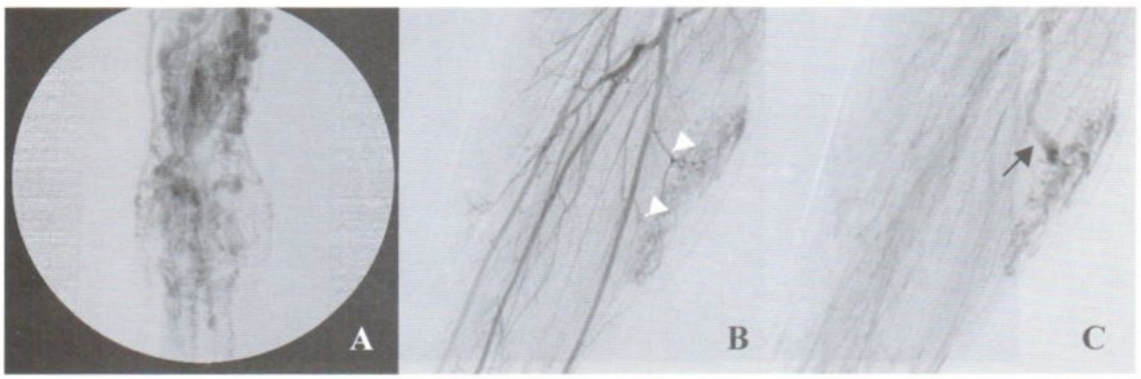

Fig.5 Angiogram of Type IIIb AVM: (A): Infiltrative AVM involving forearm and hand that cannot embolize, due to unsafe to treat. (B): arterial and (C): venous phases of another patient: localize small AVM at the forearm, arterial feeding (arrowheads) and early draining veins away from the nidus (arrow). The initial MRA from other institute showed localize AVM (not show). This AVM was consulted for pre-operative embolization.

feeders hindering superselection into the nidus. Effectiveness of embolotherapeutic outcome in this study was 9 of 12 AVMs (75%)[Table 3], all of which were considered to be in partial remission. No remission was found in 3 AVMs (25%) (patients 9,10 and 11). There was no cure or aggravation of AVM in this study. Embolotherapeutic outcome could not be evaluated in one patient (patient 4) due to consultation for pre-operative embolization 1 day before surgery.

Concerning clinical outcome, symptoms and signs were completely resolved in 1 of 10 AVMs (10%)(patient 1), improved in 7 AVMs (70%) and unchanged in 2 AVMs (20%). Clinical outcome could not be assessed in three patients. Patient 4 presenting with a mass could not be evaluated in an early post-embolization setting. Also two other patients (patients 5 and 6-1) were asymptomatic before embolization [Table 3]. The degree of devascularization was 76-99% in 7 of 13 AVMs (54%), 50-75% in 23% and less than 50% in 23% [Table 3]. Surgery was previously performed on five

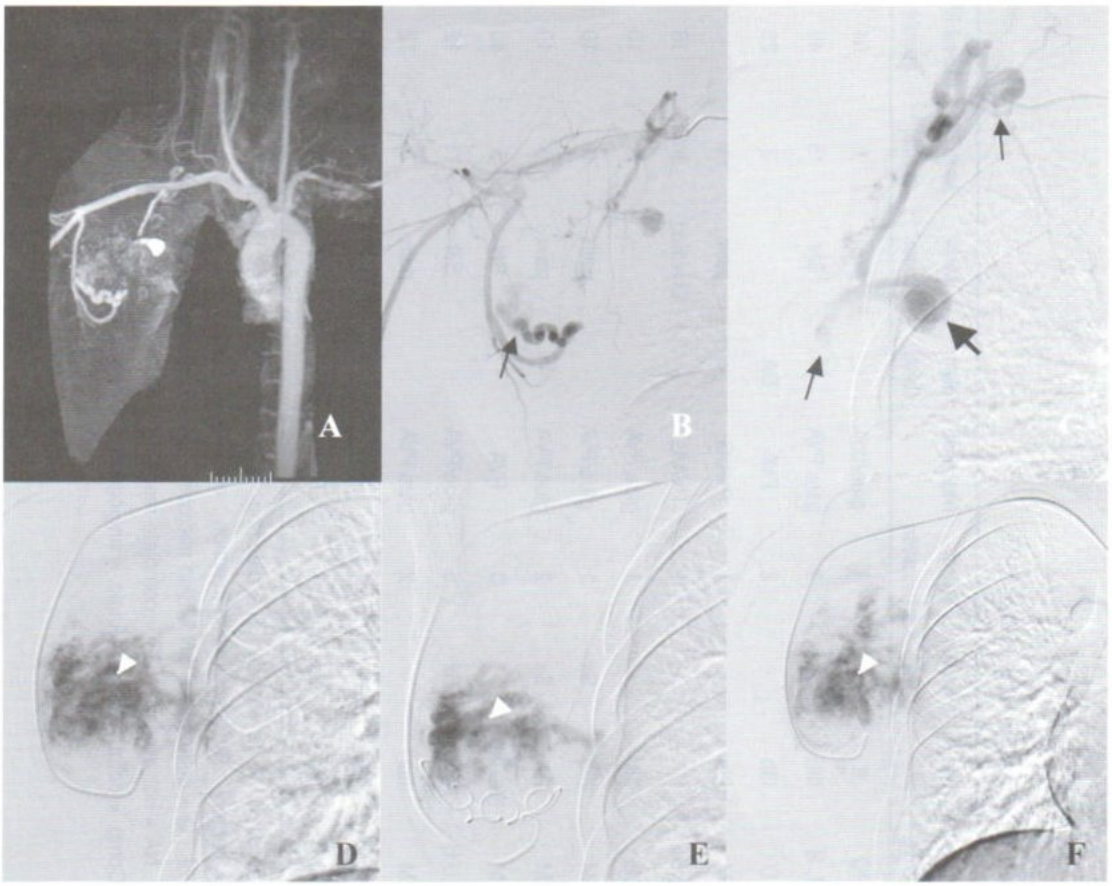

Fig.6 Angiogram of AVM at right-sided back in the patient 10: (A): 3D MRA showed AVM. (B): Early arterial phase showed tortuousity of the arterial feeding (thin arrow). (C): another arterial feeding (thin arrow) and aneurysm (large arrow). (D): late arterial phase showed complex network of the nidus (arrowhead). (E): Embolization using PVA by supperselective technique. (F): Post embolization angiogram showed less than 50% devascularization. Note failure to select the arterial feeding in C.

Table 3 Clinical data and outcome of embolotherapy

Patient No./ Sex/Age (y)	Location of AVMs	Symptoms and Signs[#]	Type	Previous Tx[$]	No. of embolization	Treatment[@]	Major Comp.	Minor Comp.[£]	Angio.F/U (month)[¥]	Clinical F/U (month)	Degree of Devas. (%)	Clinical Outcome[§]	Therapeutic Outcome[§]	Status of Therapy	Tx after em.[$]
1/F/33	pelvis	PD	II	-	3	glue/coil	-	pain	1	64	76-99	CR	PR	complete	-
2/M/24	leg	M, B	IIIb	Sx	3	glue/PVA	-	SN	15	49	76-99	improve	PR	complete	Scl
3/F/21	forearm	U	IIIb	-	2	PVA	DA	-	2	23	76-99	improve	PR	complete	Sx/Scl
4/F/11	back	M	IIIa	-	1	PVA/G	-	pain	Im	-	76-99	NA	NA	loss F/U	Sx
5/M/35	pelvis	No	II	-	1	PVA/G	-	Erection	Im	18	76-99	NA	PR	complete	-
6-1/M/30*	pelvis	No	IIIb	-	1	glue/PVA	-	-	6	10	76-99	NA	PR	complete	-
6-2/M/30*	thigh	M	IIIb	Sx	1	glue/PVA	-	pain	6	10	76-99	improve	PR	complete	-
6-3/M/30*	leg	M	II	Sx	2	glue/PVA	-	pain	6	10	50-75	improve	PR	ongoing	-
7/F/21	hand	M	IIIa+IIIb	-	3	PVA	-	SN	3	40	50-75	improve	PR	complete	Sx/Scl
8/M/55	leg	M,U,B	I+IIIb	Sx	6	glue/PVA	-	SN	11	12	50-75	improve	PR	refuse	-
9/F/10	arm	M	IIIa	-	2	glue/PVA	-	pain	6	12	<50	improve	NR	ongoing	-
10/M/26	back	M	IIIb	-	1	PVA	-	pain	Im	16	<50	no change	NR	ongoing	-
11/F/28	foot	M	IIIb	Sx	1	PVA	-	pain	Im	18	<50	no change	NR	complete	Sx

* Patient 6th has three lesions. # M = mass B = bleeding U = ulcer PD = pelvic discomfort No = no symptom
$ Tx = treatment Sx = surgery Scl = sclerosing injection em. = embolization
@ PVA = polyvinyl alcohol G = gelfoam £ SN = Skin necrosis DA = dissected artery (ulnar artery)
¥ Im = immediate § NA = not assess CR = complete resolving PR = partial remission NR = no remission
Note: No. = number Comp. = complication Angio. = angiogram Devas. = devascularization

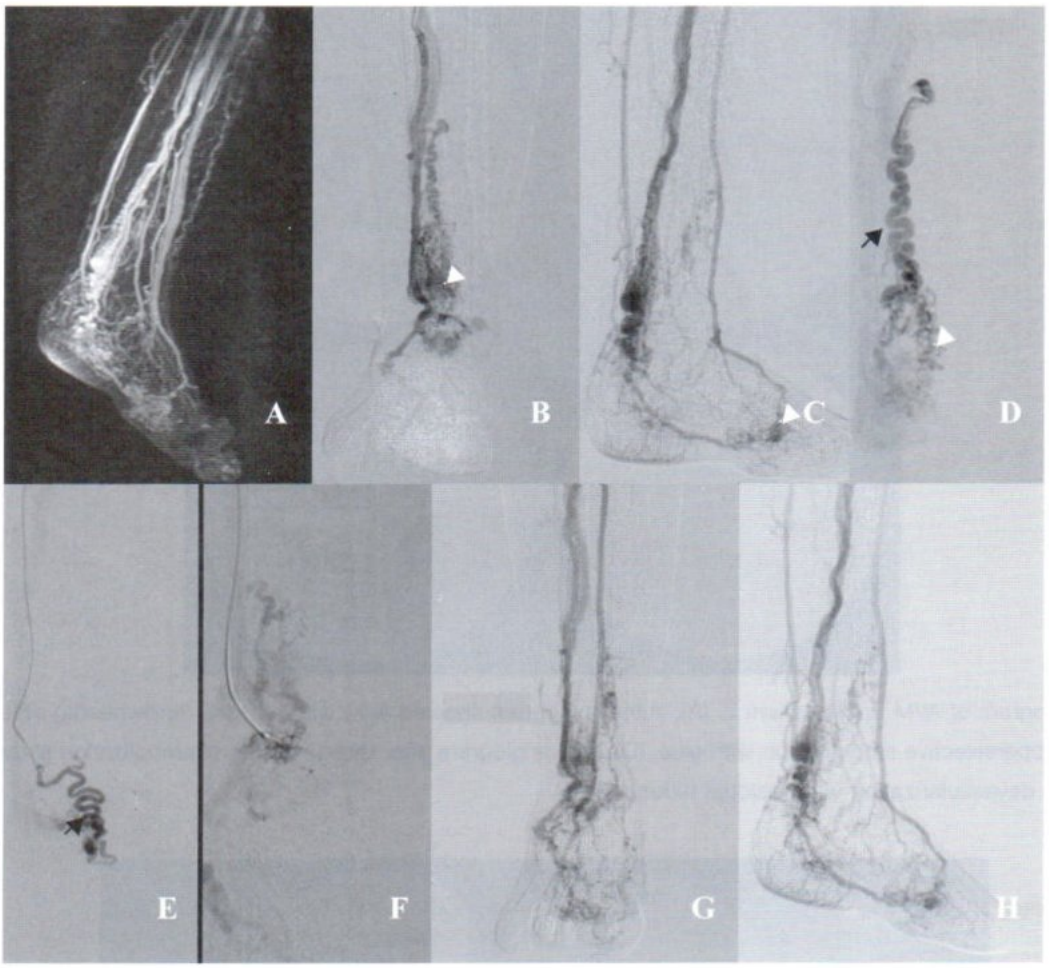

Fig.7 Angiogram of AVM at left foot in the patient 11: (A): 3D MRA and (B, C): arterial phase of PA and lateral angiogram showed infiltrative AVM with nidus (arrowhead). (D, E and F): superselective technique that the microcatheter just located into tortuous arterial feeding (arrows). (G and H): Post embolization angiogram showed less than 50% devascularization.

AVMs (38%). Number of embolizations in this study ranged from 1 to 6 settings (mean = 2.1±1.4 settings). The most number of embolizations was performed in patient 8. The time of follow-up angiography ranged from 0 to 15 months (mean = 4.3±4.7 months), the longest interval found in patient 2. The clinical follow-up time ranged from 10 to 64 months (mean = 23.5±17.8 months). All patients had no symptoms or signs of recurrence. The most used embolic agent was polyvinyl alcohol (PVA) in 12 AVMs. Other embolic agents included glue, coil and gelfoam [Table 3].

In the group of partial remission of therapeutic outcome, the degree of devascularization was 76-99% in 7 AVMs (70%) [Fig.8] and 50-75 % in 3 AVMs (30%)[Fig.9 and 10]. The best outcome of embolization was found in 3 AVMs (patients 1, 5 and 6-1). These AVMs were decreased in degree of

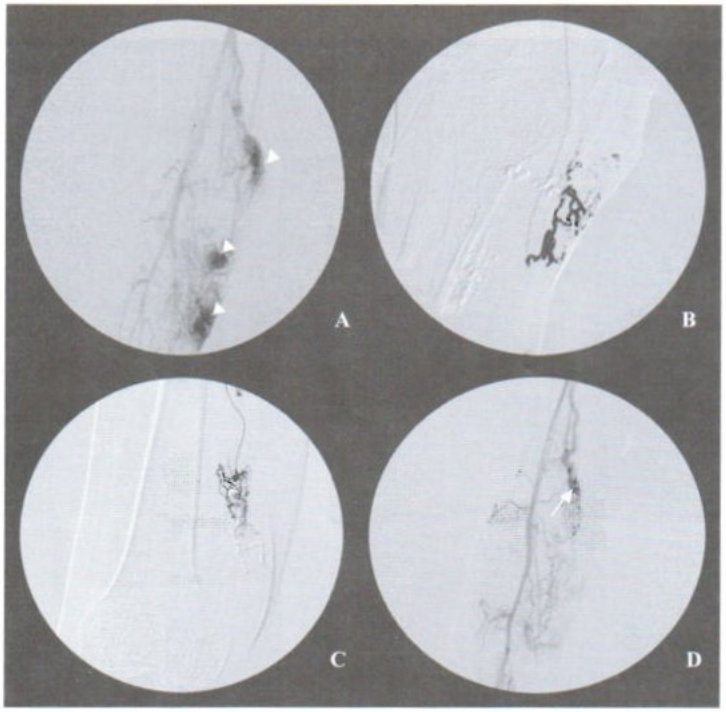

Fig.8 Angiogram of AVM in the patient 2: (A): initial angiogram showed AVM with niduses (arrowheads) at leg. (B and C): superselective embolization with glue. (D): final angiogram after three settings of embolization showed about 80% devascularization with residual nidus (arrow).

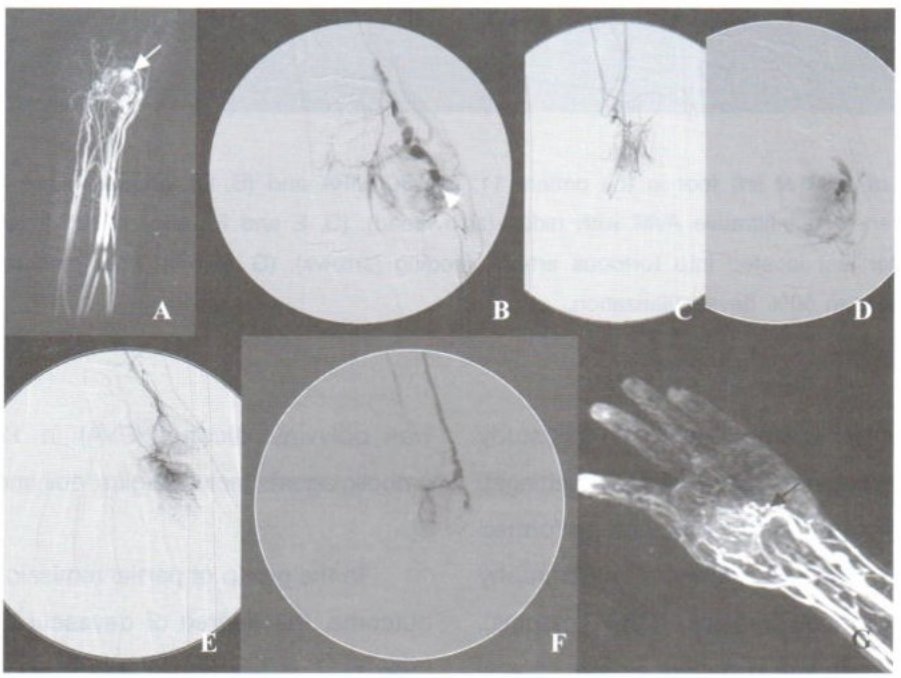

Fig.9 Angiogram of AVM in the patient 7: (A): 3D MRA and (B): late arterial phase of angiogram showed AVM (arrow) and nidus (arrowhead). (C, D and E): superselective technique with PVA embolization. (F): final angiogram after three times of embolization showed about 70% devascularization. (G): 3D MRA after two years of embolization showed small residual AVM (arrow).

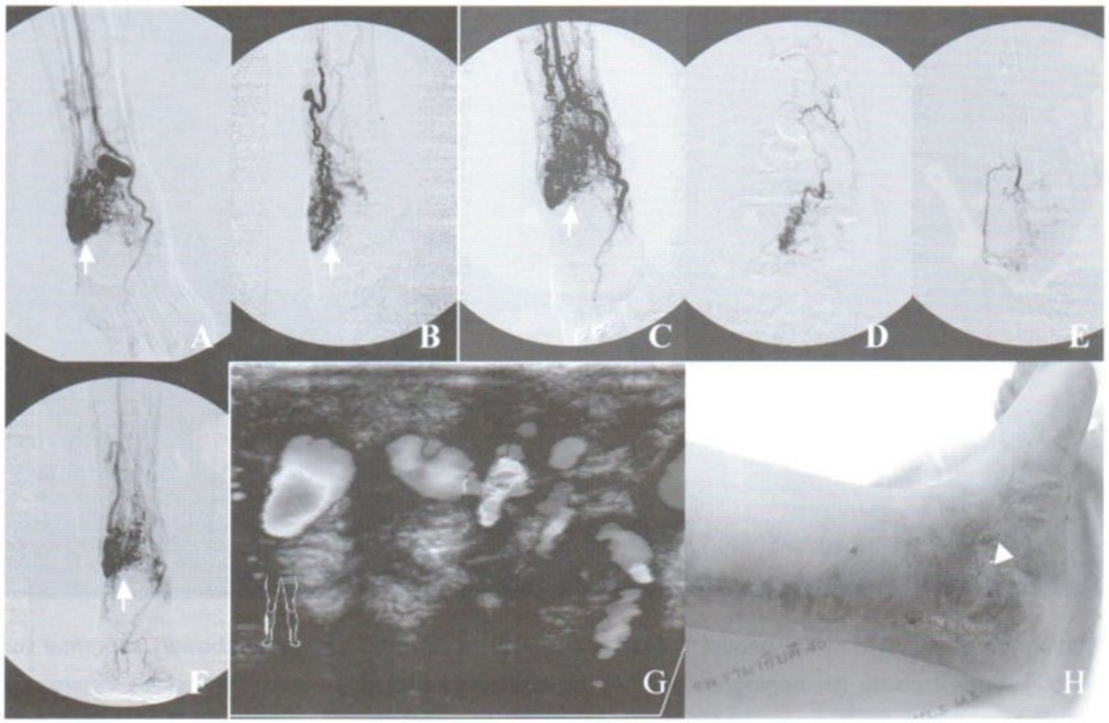

Fig.10 Angiogram of AVM in the patient 8: (A): arterial phase of left foot angiogram showed AVM with nidus. (B): superselective with PVA and glue embolizations. (C): angiogram after three settings of embolization showed 20% devascularization. (D and E): superselective of 4th and 5th embolizations. (F): Post final embolization angiogram showed about 60% devascularization. (G): Doppler US after six years of embolization showed residual AVM. (H): scar after treatment of skin necrosis (arrowhead). Note nidus (arrow).

vascularity more than 90% [Fig.11 and 12] with complete resolution of symptoms in patient 1. Additional treatment was found in three AVMs because of difficult access and high risk of limb ischemia. One AVM (patient 2) was treated by sclerosing agent injection (3% ethoxysclerol), and two other AVMs (patients 3 and 7) were treated by combined excision and sclerosing agent injection after embolization. Seven AVMs underwent complete treatment. One patient (patient 8) refused next embolization or additional treatment after the sixth embolization. Another AVM (patient 6-3) is awaiting further sessions of embolization.

In the group of no remission, all AVMs (patients 9,10 and 11) were less than 50 % devasculralized [Table 3]. One patient (patient 9) was clinically improved and awaits next embolization. There was technical failure in two patients, which did not change clinical outcome after embolization. One patient (patient 10) awaits surgery. Another AVM (patient 11) was excised after failed embolization.

There was one major complication in this study. In one patient (patient 3), ulnar artery dissection occurred during embolization with no symptoms or signs of distal ischemia due to multiple collateral arterial supply from the radial artery and partial recanalization on follow-up imaging[Fig.13]. Five patients (7 AVMs, 53.8%) experienced pain. Skin

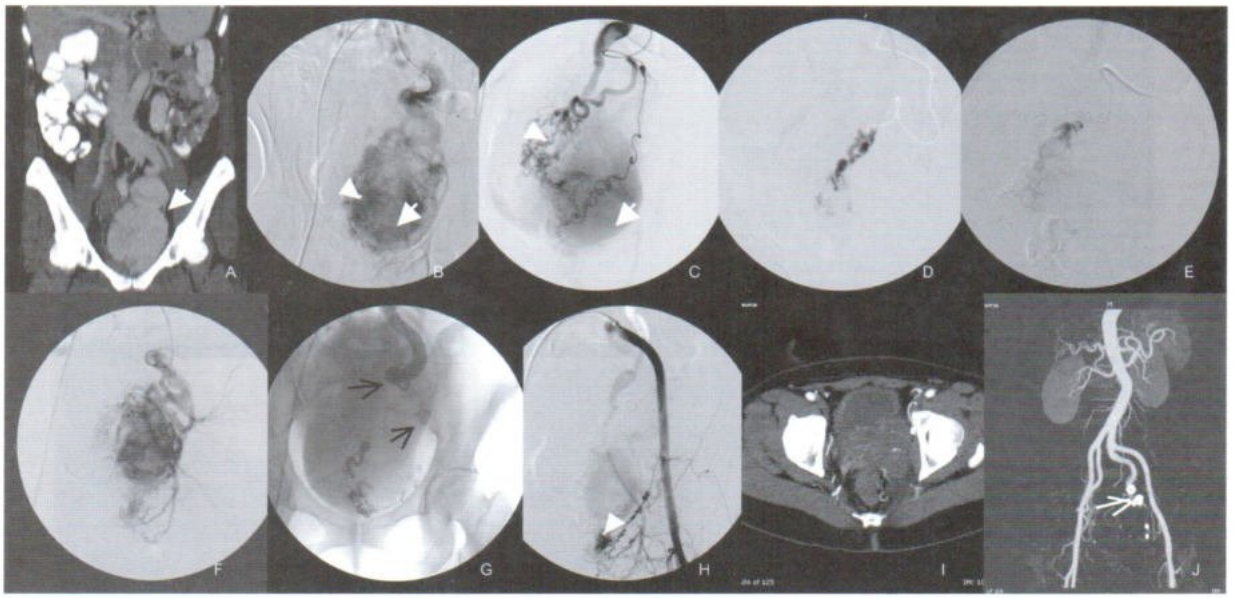

Fig.11 Angiogram of the AVM in the patient 1: (A): coronal MIP of initial CT abdomen showed abnormal venous lake (arrow) in pelvic cavity. (B): angiogram and (C): superselective angiogram of left internal iliac artery showed type AVM with nidus (arrowheads) and large venous pouch (arrows). (D, E): superselective embolization with glue. (F): pre-embolization of final angiogram showed 50% devascularization. (G): multiple coil embolizations with complete occlusion of the left internal iliac (thin arrows). (H): 90 % devascularization with minimal residual nidus (arrowhead) and arterial feeding from branch of left external iliac artery. (I) axial and (J) 3D reformat of the CT angiogram after six years of embolization showed total thrombosis of venous pouch and no recurrence of AVM. Note coils (thin arrow).

necrosis occurred in three patients (23.1%) [Fig.10H]. Another patient (patient 5) had transient frequent erection of the penis. No complications occurred in one lesion (patient 6-1).

Discussion

Congenital AVMs are present at birth, though they may remain clinically silent until later in life. Embryologically, the vascular system evolves through three stages. In the first stage, called the stage of minimal differentiation, blood lakes organize into capillary networks. The second stage is the retiform stage in which capillaries form larger conduits, but no vessel wall differentiation is seen. The final stage of adult maturation begins with the completion of vessel wall maturation. It is felt that the majority of these congenital lesions evolve if a vessel fails to reach the latter stages of differentiation.

According to Cho et al. modified classification[5] of the peripheral AVM type [Fig 1.], the angiographic findings in this study showed that 55.6 % were type IIIb, 16.7% type II, 16.7 % type IIIa, 5.7 % mixed type I and IIIb and 5.7 % mixed type IIIa and IIIb. The original Cho et al. modified classification that reviewed angiographic findings of peripheral AVMs in 66 patients from December 1996-December 2004 showed 45% type IIIb, 20% type II, 18% mixed type IIIa and IIIb, 14 % mixed type II and IIIb and 3% type IIIa. When compared, two studies showed the same results, that is type IIIb [Fig.5,7,8 and 13]

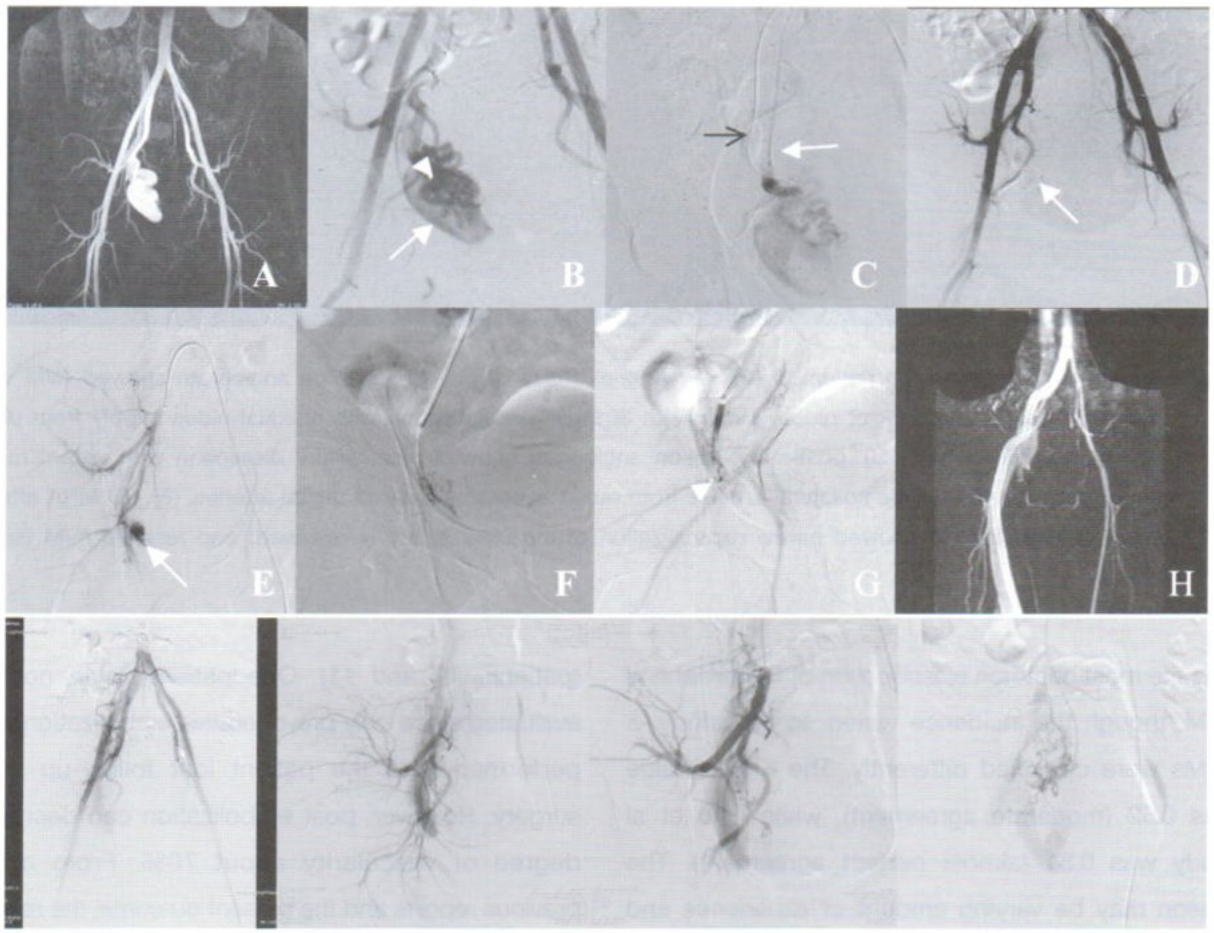

Fig.12 Angiogram of AVM in the patient 5 (A-D): (A): 3D MRA showed AVM in pelvic cavity. (B): late arterial angiogram showed type II AVM with nidus (arrowhead) and venous pouch (large arrow). (C): embolization with PVA by combine transarterial (large arrow) and temporary transvenous balloon occlusion techniques (small arrow). (D): post-embolization angiogram showed nearly complete occlusion of AVM (large arrow). Another angiogram of small AVM in patient 6-1 (E-H): (E): arterial phase angiogram showed small type IVb AVM (large arrow). (F): superselective glue embolization. (G): post-embolization angiogram showed 95% devascularization with retained glue material in arterial feeding (arrowhead). (H): 3D MRA after 1 month of embolization showed no residual or recurrent AVM.

The patent comes back for clinical of recurrent disease, seen from follow up MRA 2 years later. The angiogram (four pictures of the third row of fig.12) showed multiple fine vascular feeding to AVM without demonstrable AVM nidus or significant early draining vein. However, there is still seen large draining vein from the right sided of pelvic cavity. The second partial embolization of the arterial feeding was done with residual some fine feeding artery.

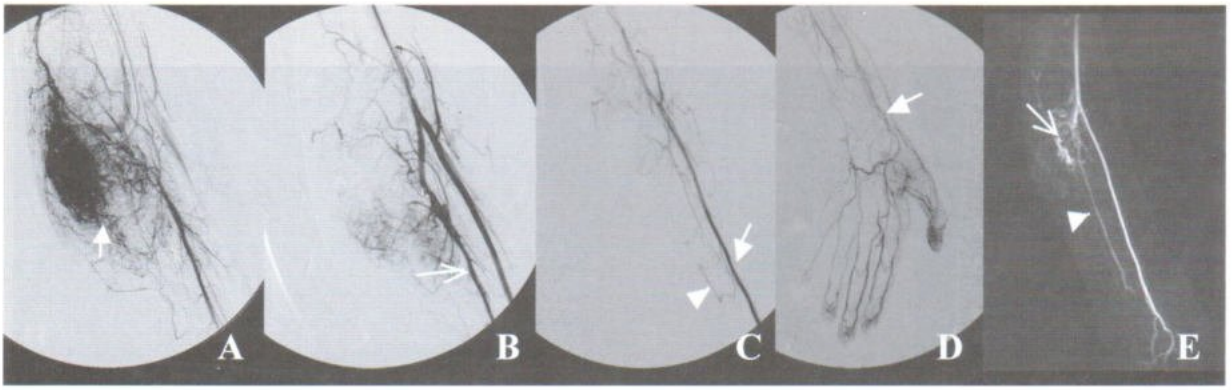

Fig.13 Angiogram of AVM in the patient 3: (A): late arterial phase of pre-embolization angiogram showed AVM with complex vascular network of nidus (arrow). (B): 80% devascularization with residual nidus supply from ulnar artery (small arrow). (C, D): post-embolization angiogram showed ulnar artery dissection with patent radial artery (arrow) and multiple collateral arteries from radial artery to supply all digital arteries. (E): 3D MRA after 3 years of embolization showed partial recanalization of the ulnar artery (arrowhead) and residual AVM (small arrow).

was the most common classification of the peripheral AVM, though the incidence varied. In this study, 5 AVMs were classified differently. The Kappa value was 0.52 (moderate agreement), while Cho et al study was 0.81 (almost perfect agreement). The reason may be varying amount of experience and the small number of the AVMs in this study.

In fact, the aim of AVM treatment outcome is to improve clinical signs and symptoms as well as partially decrease degree of vascularization. Complete devascularization is quite difficult; however, it should be done if possible. Of the many previous studies on embolotherapeutic treatment of congenital AVMs, all reported improved clinical outcome (complete and partial improvement).[5,13,14,17] Recently, Do YS et al (2005)[6] reported the therapeutic outcome of AVM embolization in 40 patients using ethanol from 1996-2003. The results showed 40% cure, 27.5% partial remission, 17.5% no remission, 2.5% aggravated and 12.5% failed. This study showed 75% partial remission and 25% no remission (patients 10 and 11). One patient could not be evaluated since only pre-operative embolization was performed, and the patient lost follow-up after surgery. However, post embolization can decrease degree of vascularity about 70%. From many previous reports and the present outcome, the results showed overall improvement of clinical and therapeutic outcomes. Therefore, embolotherapeutic modalities have advantages in the treatment of high-flow peripheral AVMs. In addition the patient's compliance is an important factor because many high-flow AVMs cannot be treated with good outcome during a short period of embolization.

Historically, surgical ligation of the feeding arteries to the AVM was commonly performed to decrease the blood supply to the lesions. However, this treatment was often unsuccessful as a result of AVM nidus revascularization by microscopic shunts that were not apparent before surgical ligation. Moreover, these shunts are often numerous, small, tortuous, and difficult to access, making subsequent

transcatheter treatments more difficult and often impossible.[3] Recently, embolization has been suggested as the primary therapeutic modality for cure, improvement or presurgical intervention to reduce bleeding and maximize successful resection. There were several studies that mentioned unsuccessful surgical treatment.[3,5,6,11,15] In this study, there were 5 AVMs that recurred after surgery [Table 3]. Four AVMs were in partial remission after embolization while there was no remission of one AVM due to difficult access [Fig.7]. However, surgical treatment has a role in small or localized lesions, embolization failure or safety concerns. In this study, there were 5 non-embolized AVMs that were sent for surgery. 4 other AVMs were also sent for surgery after embolization. Further embolization was deemed unsafe in three lesions, and there was technical failure in one lesion (patient 11) [Table 3]. Additional treatment by sclerosing agent injection was also found in three AVMs for the same reasons as surgical treatment.

In general, transarterial embolization has been preferentially used to embolize AVMs. Recently, transvenous or direct puncture embolization has been used as an alternative technique when important normal arterial branches arise in very close proximity to a malformation or when extreme arterial tortuosity or previous treatment (including surgical ligation and embolization of the feeding artery) preclude successful transarterial catheterization.[5,8] These techniques will increase chance of cure. In our institute, the interventionists still prefer transarterial approach with or without coaxial microcatheter technique for embolization [Fig.6E, 11D and 11E] because of their experience. For this reason, the number of embolizations and angiographic follow-up time were quite less than other previous reports (6) [Table 3], and there was technical failure from transarterial approach in two AVMs [Fig.6 and 7]. However, in one AVM, temporary transvenous balloon occlusion technique was used to decrease flow before transaterial embolization by PVA, which resulted in about 95 % devascularization [Fig.12A-D].

From years past to currently, many endovascular occlusive agents have been used including autologous clot, Gelfoam, Polyvinyl alcohol particle (PVA), various metallic coils with or without fibers, tissue adhesives (IBCA/NBCA), detachable balloons, Ethibloc, Sotradecol and ethyl alcohol.[3,13,18-20] The technique can be applied though transarterial, transvenous or direct puncture approaches to permanently occlude the nidus. Gelfoam, PVA, coils, or detachable balloons rarely cure peripheral AVMs.[3,7,13,18] Tissue adhesives (IBCA/NBCA) were initially thought to be permanent occluding agents. However, their use is difficult, and it is now well-documented that recanalization does occur. In this study, combined embolic agents were more commonly used than single embolic agents. The most common embolic agent was PVA (12 from 13 AVMs), [Fig.9C-E] and second most common was glue (7 from 13 AVMs) [Fig.8B and 8C] [Table 3]. In one pelvic AVM (patient 1) receiving arterial supply from the left internal iliac artery, coil and glue was used, resulting in excellent outcome (90% devascularization and complete resolution of symptoms) [Table 3, Fig.11]. In general, proximal embolization of the feeding artery should be avoided because the lesion recruits collateral flow through more complex.[12] However, in the last embolization of patient 1, coil was use to occlude the left internal iliac artery [Fig.11G] because of near complete occlusion of the nidus from two previous procedures

and the clinicians requirement of cure as the outcome. No serious complications occurred. From review of medical records, this patient underwent a normal pregnancy and labor without complications. The last CT follow-up (December 2008) showed no residual, recurrence or aggravation of disease [Fig.11I and J].

Recently, various reports document that the use of ethanol embolization has the potential for cure in management of AVMs of the body and extremities. However, this technique has great risks, including injury to adjacent normal tissues, particularly the mucosal surface, skin and neurologic tissue. Cardiopulmonary collapse may also be caused by ethanol escape to the right-side heart and pulmonary bed so that close monitoring by the interventionist team is required during the procedure.[3,13,20,21] In our opinion, the selection of embolization technique and embolic agent depends on the availability of materials and instruments in that institute. Moreover, the experience of the interventionists is important. However, in the future, we will try and apply alternative techniques for increased effective outcome in our institute.

One major complication, ulnar artery dissection, occurred in this study, but there were no symptoms and signs of distal ischemia due to multiple collateral arteries from the radial artery and partial recanalization on follow-up imaging [Fig.13B-E]. The rest were minor complications [Table 3]. All cases of skin necrosis healed with wound dressing, and no skin graft was needed [Fig.10H]. Transient frequent erection of penis in patient 5 resolved two days after embolization. The cause may have been increased arterial supply to the penis after AVM was occluded. Pain was resolved a few days to weeks after embolization. Other studies reported complications after embolotherapy. Tan KT, et al[3] in 2004 found 2 major complications including tibial plateau fracture and L5 neuropathy. Cho SK, et al[5] in 2006 reported embolism, brain infarction, bladder necrosis, infection, permanent nerve injury and acute renal failure. Occurrence of reported complications might be dependent on technical approach, embolic material used, location and aggressiveness of the AVM. In this study, there were no serious complications, probably due to aim of palliative embolization. Also, lesions that could not be embolized without placing normal tissue at undue risk were not treated.

There are some limitations in this study. First, the number of AVMs is small due to rarity of the disease, which is appropriate with 4 periods of collected data. Second, the evaluation of AVM type is based on angiographic morphology alone without pathologic confirmation. Third, because of varying embolotherapeutic techniques and embolic materials used in many studies, it may be difficult to compare our results. Fourth, due to the invasive nature of angiography, a routine follow-up angiogram cannot be performed. We compared post-embolization images of the last angiogram with the first angiogram before embolization in almost all cases. Non-invasive imaging, including color doppler sonogram and MRI were just indirect modalities for follow-up. Fifth, clinical follow-up time may not have been enough to assess recurrence.

Conclusion

Congenital arteriovenous malformation (AVM) is a rare disease. Type IIIb (arteriolovenulous fistulae with dilated fistula) was found to be the most common type of peripheral AVM. Transcatheter arterial embolization with/without superselection is

the primary therapeutic modality in the management of patients with peripheral AVMs for improvement, possible cure or presurgical intervention to reduce bleeding and maximize successful resection. The morbidity is also less than primitive surgical excision. Further long-term assessment is necessary to evaluate efficacy of this treatment and recurrence.

Acknowledgment

We thanks Dr. Sutipong and Dr. Jesada for give some cases, Dr. Elenor and Dr. Jantarach for editing and Mrs. Piraya for correcting angiographic data.

References

1. Piyachon C. Radiology of peripheral arteriovenous malformations. Australasian Radiology 1977; 21:246-59.
2. Donnelly LF, Adams DM, Bisset GS. Vascular malformation and hemangioma. AJR 2000; 174:597-608.
3. Tan KT, Simons ME, Rajan DK, Terbrugge K. Peripheral high-flow arteriovenous vascular malformation: A single-center experience. JVIR 2004; 15:1071-80.
4. Osuga K, Hori S, Kitayoshi H, Khankan AA, Okada A, Sugiura T, et al. Embolization of the high flow arteriovenous malformations: Experience with use of superabsorbent polymer microspheres. JVIR 2002; 13:1125-33.
5. Cho SK, Do YS, Shin SW, Kim D, Kim YW, Park KB, et al. Arteriovenous malformation of the body and extremities: Analysis of the therapeutic outcomes and approaches according to a modified angiographic classification. J Endovasc Ther 2006;13:527-38.
6. Do YS, Yakes WF, Shin SW, Lee BB, Kim D, Liu WC, et al. Ethanol embolization of arteriovenous malformation: Interim results. Radiology2005;235:674-82.
7. Pollak JS, White RI Jr. The use of Cyanoacrylate adhesives in peripheral embolization. JVIR 2001;12:907-13.
8. Jackson JE, Mansfield AO, Allison DJ. Treatment of high-flow vascular malformation by venous embolization aided by flow occlusion techniques. Cadiovasc Intervent Radiol 1996;19:323-28.
9. Gandini R, Angelopoulos G, Konda D, Messina M, Chiocchi M, Perreta T, et al. Transcatheter embolization of a large symptomatic pelvic arteriovenous malformation with glubran 2 acrylic glue. Cadiovasc Intervent Radiol 2007; 30:350-4.
10. Stanley AC, Menzoian JO. A congenital arteriovenous malformation of the right subclavian artery: A case report. Vasc Endovascular Surg 2000;34:271-5.
11. Yakes WF, Rossi P, Odink H. Arteriovenous malformation management. Cadiovasc Intervent Radiol 1996; 19:65-71.
12. White RI Jr, Pollak J, Persing J, Henderson KJ, Thomson JK, Burdge CM. Long-term outcome of embolotherapy and surgery for high-flow extremity arteriovenous malformations. JVIR 2000;11:1285-95.
13. Bae S, Do SY, Shin SW, Park KB, Kim D, Kim YW, et al. Ethanol embolotherapy of pelvic arteriovenous malformation: An initial experience. Korean J Radiol 2008;9:148-54.
14. Gomes AS, Mali WP, Oppenheim WL. Embolization therapy in the management of congenital arteriovenous malformations. Radiology 1982;144:41-9.
15. Kaufman SL, Kumar AAJ, Roland JMA, Harrington DP, Barth KH, Haller JA, et al. Thanscatheter embolization in the management of congenital arteriovenous malformation. Radiology 1980; 137:21-9.
16. Bartynski WS, O'Reilly GV, Forrest MD. Hight-flow-rate arteriovenous malformation model for simulated therapeutic embolization. Radiology 1988;167:419-21.
17. Widlus DM, Murray RR, White RI Jr, Osterman FA, Schreiber ER, Satre RW, et al. Congenital arteriovenous malformation: Tailored embolotherapy. Radiology 1988;169:511-6.
18. เจียมจิตร ตปนียากร. Introduction to Vascular Interventional Radiology. ใน: โสภณ จิรสิริธรรม, ประเสริฐ ไตรรัตน์วรกุล, ระวี พิมลศานติ์. ศัลยศาสตร์หลอดเลือด Textbook of Vascular Surgery เล่ม 2. กรุงเทพฯ : สำนักพิมพ์กรุงเทพเวชสาร; 2545.82-98.
19. Castaneda F, Goodwin SC, Swischuk JL, Wong GCH, Bonilla SM, Wang MJ, et al. Treatment of pelvic arteriovenous malformations with ethylene vinyl alcohol copolymer (Onyx). JVIR 2002;13:513-6.
20. Mitchell SE, Shah AM, Schwengel D. Pulmonary artery pressure changes during ethanol embolization procedures to treat vascular malormations: Can cardiovascular collapse be predicted?. JVIR 2006;17:253-62.
21. Yakes WF, Luetbke JM, Parker SH, Stavros AT, Rak KM, Hopper KD, et al. Ethanol embolization of vascular malformations. Radiographics 1990;10:787-96.

THE ASEAN JOURNAL OF RADIOLOGY 2010; 16(3): 166-180

Original Article

Accuracy of Transrectal Ultrasonography in Preoperative Staging of Rectal Cancer

Shalothorn Amornnuratkul, MD.[1], Janjira Jatchavala, MD.[1], Sith Pongkitkarun, MD.[1], Pattana Sornmayura, MD.[2], Kanit Sumboonnanon, MD.[3]

[1] *Department of Radiology, Faculty of Medicine Ramathibodi Hospital, Mahidol University*

[2] *Department of Pathology, Faculty of Medicine Ramathibodi Hospital, Mahidol University*

[3] *Department of Surgery, Faculty of Medicine Ramathibodi Hospital, Mahidol University*

Abstract

Objective: To determine the diagnostic accuracy, sensitivity, specificity, positive predictive value and negative predictive value of transrectal ultrasound in the detection of the depth of tumor invasion, perirectal fat invasion and regional lymph node involvement in rectal cancer patients at Ramathibodi Hospital.

Materials and Methods: A total of 17 patients with biopsy proven rectal cancer, who had undergone transrectal ultrasound evaluation of the invasion of the rectal wall and the mesorectal lymph nodes status were retrospectively studied during a period of 5 years and 6 months. We compared the Transrectal Ultrasonography (TRUS) staging with pathology examination of the resected specimens according to TNM classification.

Results: 15 patients had a radical resection (11 abdominoperineal resection and 4 low anterior resection), and two patients had a local transanal excision. Eight among these 17 patients had preoperative chemoradiation. The overall accuracy in assessing the depth of tumor invasion was 47% and 56%, with 41% and 22% of the tumors overstaged and 12% and 22% understaged, in the all patients group and the other group with no neoadjuvant therapy, respectively. In determining the perirectal fat invasion, the diagnostic accuracy of TRUS was 52.9% with sensitivity 83.3% (95% CI 65.6-101.1), specificity 36.4% (95% CI 13.5-59.2), PPV 41.7% (95% CI 18.2-65.1) and NPV 80% (95% CI 60.9-99.0). The accuracy of TRUS in determining the perirectal fat invasion was higher in the group that excluded neoadjuvant therapy patients at 66.7%, with sensitivity of 66.7% (95% CI 35.9-94.5), specificity 66.7% (95% CI 35.9-97.5), PPV 50.0% (95% CI 17.3-82.7) and NPV 80% (95% CI 53.9-106.1). The accuracy in assessing nodal involvement in 15 patients treated with radical surgery was 60%, with sensitivity 33.3% (95% CI 9.48-57.2), specificity 66.7% (95% CI 42.8-90.5), PPV 20% (95% CI -0.24-40.2) and NPV 80% (95% CI 59.8-100.2).

Conclusion: Since the recent standard treatment for T3 and T4 tumors was to undergo preoperative chemoradiation, the lower accuracy occurred due to down-staging of the tumor from the neoadjuvant treatment. In addition, there was only a small number of included patients, which affected the statistical analysis of this study. The accurate results in the future study of transrectal ultrasound in preoperative staging of rectal cancer should be achieved by an increased sample size.

Keywords: Transrectal Ultrasonography, accuracy, rectal cancer

Introduction

The incidence rate of colorectal cancer in Thailand is the third in frequency in males after liver cancer and lung cancer, and the fifth after cancer of cervix, breast, liver and lung for females. The highest incidence for both sexes is in Bangkok. The estimated incidence rate in Thailand is 8.8 for males and 7.6 for females.[1]

Rectal cancer is highly treatable and often a curable disease when localized. Surgery is the primary treatment and results in a cure in approximately 45% of all patients. The prognosis of rectal cancer is clearly related to the degree of penetration of the tumor through the bowel wall and presence or absence of nodal involvement. These 2 characteristics form the basis for all staging systems developed for this disease.[2]

The preoperative evaluation of the rectal cancer is important in planning therapy and assessing prognosis. Precise knowledge of the depth of tumor invasion of a rectal cancer and the mesorectal nodal status is essential for the planning of optimal therapy. Local excision of early rectal cancer seems to be a good alternative to radical operations.[3] In more advanced rectal lesions, neoadjuvant chemoradiation succeeds in increasing sphincter saving operations and improves local control and survival in these patients.[4]

The currently available methods to evaluate the rectal cancer include digital examination, transrectal ultrasonography (TRUS), computed tomography (CT) and magnetic resonance imaging (MRI). TRUS is a diagnostic modality that has become useful in determining the depth of invasion preoperatively and the presence or absence of metastatic lymph nodes. The current literature suggests that staging with TRUS is equally accurate and often even superior to staging with other techniques.[5-9]

The aim of this study was to evaluate the accuracy of TRUS in accessing tumor infiltration depth and nodal involvement of rectal cancer, determine the sensitivity and specificity of any perirectal fat invaded lesion, as well as determine the sensitivity and specificity of any metastatic regional lymph node by using transrectal ultrasound.

Materials and Methods

During a 5 years and 6 months interval from January 1, 2003 to June 30, 2008, 367 patients were diagnosed with rectal cancer. There were 34 out of 367 patients with biopsy proven rectal cancer who underwent pre-operative TRUS examination at the Radiology Department of Ramathibodi Hospital. Only 17 out of the 34 patients underwent open surgery with an available patho-logical report of the same lesion and were retro-spectively studied. The remaining 17 patients were excluded due to no available pathological report or did not perform further surgery. All TRUS examinations were performed and interpreted by the same radiologist, using a transrectal sonographic 7.5-MHz probe with a transversely oriented radial scan plane (Aloka transrectum mechanical radial scanner ASU-67; Tokyo, Japan, connected with a Prosound SSD-5000; Aloka ultrasound; Tokyo, Japan). The transducer produces transverse 360-degree scans in reference to the longitudinal axis of the rectum. The patients were examined in a left lateral decubitus position. The transducer was inserted into the rectum transanally after being coated with sonographic gel. The transducer was covered with a rubber sheath filled with 20 ml of degassed water, providing an optimal acoustic pathway.

The 5 basic layers seen on TRUS of the rectal wall compare directly with the anatomic layers present in the rectal wall. The 5 layers working out from the lumen of the rectum are:

1. Hyperechoic layer is the interface between the water/balloon and mucosal surface.
2. Hypoechoic layer is the combined layer produced by mucosa and muscularis mucosae.
3. Hyperechoic layer is the submucosa.
4. Hypoechoic layer is the muscularis propria.
5. Hyperechoic layer is the interface between the muscularis propria and perirectal fat or the serosa if present.

Ultrasonographic staging for the depth of tumor infiltration was made according to Kumar et al. (Table 1). The preoperative tumor staging was classified as uT1 when the tumor was limited to the mucosa-submucosa (fig 1), uT2 when the tumor invaded the muscularis propria (fig 2), uT3 when the tumor penetrated through the muscularis propria to involve the perirectal fat (fig 3) and uT4 when adjacent organs were invaded. The mesorectal lymph nodes were considered as malignantly invaded if they were hypoechoic with a smooth border[5]. The predicted tumor invasion depth (T) and nodal status (N) were compared with histopathologic findings, according to TNM classification designated by AJCC.[10]

The final diagnostic staging was established by means of operation with low anterior resection, abdominoperineal resection or transanal excision.

The pathological reports were reviewed by the same pathologist and categorized as:

- Depth of tumor invasion (T)
  - o T0: No evidence of primary tumor
  - o T1: Tumor invades submucosa
  - o T2: Tumor invades muscularis propria
  - o T3: Tumor invades through the muscularis propria into the subserosa, or into non-peritonealized pericolic or perirectal tissues
  - o T4: Tumor directly invades other organs or structures, and/or perforates the visceral peritoneum

(Note: Tumor that is adherent to other organs or structures, macroscopically, is classified as T4. However, if no tumor is present in the adhesion, microscopically, the classification should be pT3. The V and L substaging should be used to identify the presence of vascular or lymphatic invasion.)

The regional lymph node was categorized as

- Regional lymph node (N)
  - o N(-): No regional lymph node metastasis
  - o N(+): Presence of metastasis regional lymph nodes

Table 1 Transrectal ultrasonographic staging system

Stage	Tumor features
uT1	Tumor confined to mucosa or submucosa
uT2	Tumor penetrates muscularis propria, but confined to rectal wall
uT3	Tumor invades perirectal fat
uT4	Tumor invades adjacent structures
N(-)	No metastatic lymph node
N(+)	Metastatic lymph node

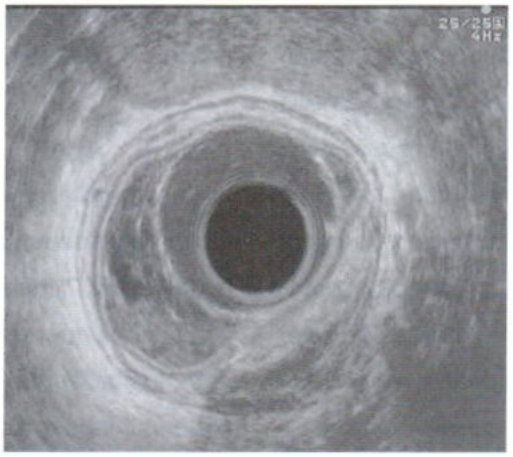

Fig.1 uT1 lesion- confined to mucosa and submucosa

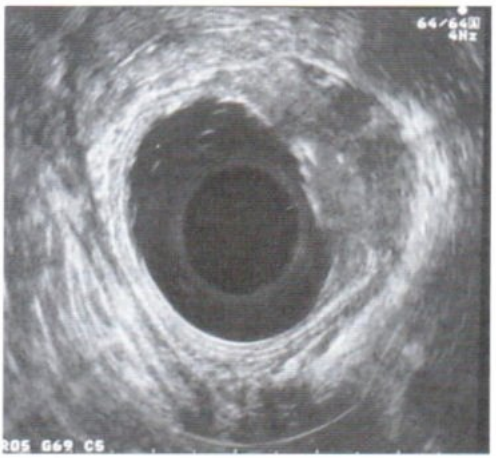

Fig.2 uT2 lesion- penetrates the muscularis propria but confined to the rectal wall

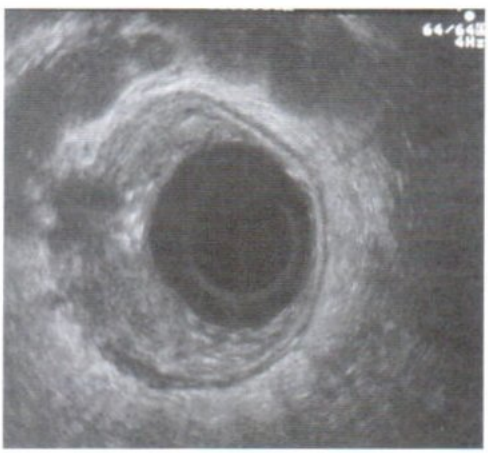

Fig.3 uT3 lesion- penetrates through entire thickness of bowel wall and invades perirectal tissue

Data of all patients were recorded as sex, age at initial TRUS examination, depth of tumor invasion (uT) and presence of regional lymph node metastasis (uN), which is according to the TRUS staging system.

All patients underwent surgery and the time between TRUS examination and surgery, type of surgery, cell type of the tumor, presence of neo-adjuvant therapy before surgery, depth of tumor invasion and presence of regional lymph node metastasis, according to TNM classification were recorded.

The depth of tumor invasion was also divided into two categories as perirectal fat invaded lesion and non-perirectal fat invaded lesion. Perirectal fat invasion was defined as a stage of T3 or T4, while stage T1 or T2 was referred to as non perirectal fat invasion.

Statistical analysis:

Continuous data (age at initial TRUS examination, time between TRUS and surgey) was summarized as mean (SD) and median (range) as appropriate. Categorical data (depth of tumor invasion, presence of regional lymph node metastasis, type of surgery, cell type of tumor) were summarized as counts and percentages. Results of the depth of tumor invasion were presented according to the four categories of tumor staging in a 4x4 contingency table to determine the overall accuracy (total number of correctly staged cases/total number of cases in the study). For each criterion of perirectal fat invaded lesions and presence of metastatic regional lymph node, a 2x2 contingency table was constructed and the sensitivity, specificity, positive and negative predictive value along with their 95% confidence interval (95% CI) were calculated.

All statistical analyses were performed by using STATA v.10 (Stata Corp, College Drive, Texas, USA).

Results

In a total of 34 patients with biopsy proven rectal cancer who underwent TRUS, 17 patients (10 females and 7 males) with a mean age of 55 (15.7) years who underwent tumor resection with available pathological report were enrolled (Table 2). All 17 patients were classified by the transrectal ultra-sonographic staging system. There were 2 cases of uT1 (12%), 3 cases of uT2 (18%), 12 cases of uT3 (70%) and no case of uT4 (0%). No evidence of regional lymph node metastasis (uN(-)) were 12 cases (71%) and presence of lymph node metastasis (uN(+)) in 5 cases (29%). The median time between biopsy and TRUS examination was 12 days (5-53), with a mean of 16.5 days (15.2).

Among 17 patients who were assessed for depth of invasion and regional lymph node metastasis by transrectal ultrasound, 6 patients were treated initially with neoadjuvant therapy (pre-operative chemoradiation) for down staging and underwent surgery later. All patients underwent an operation consisting of abdominoperineal resection (APR) in 11 cases (65%), low anterior resection (LAR) in 4 cases (23%) and transanal excision in 2 cases (12%).

The median time between TRUS and surgery was 60 days (6-577). There were 8 patients (47%) who received neoadjuvant therapy before surgery. All of them were initially treated with concurrent chemoradiation.

The pathological results were adenocarcinoma in 16 cases and 1 case of GIST. There were 2 cases of adenocarcinoma that had no evidence of tumor at the time of surgery due to pre-operative

chemoradiation for down staging (1 case of acute and chronic inflammation, 1 case of granulation tissue and fibrosis). The average size of the tumor was 3.5 (1.4) cm in the greatest diameter.

There were 2 patients who received neo-adjuvant therapy and showed no evidence of tumor at the time of operation. Therefore, the pathologic tumor staging in depth of tumor invasion were 2 cases (12%) of pT0 (no evidence tumor), 3 cases of pT1 (18%), 6 cases of pT2 (35%), 6 cases of pT3 (35%) and no case of pT4 (0%). The studies of regional lymph node metastasis were performed in only 15 patients (88%), because there were 2 patients who were treated with local resection and no information on lymph node status was available. There were 3 cases of pN(+) (20%) and 12 cases of pN(-) (80%). The characteristics and data of all included patients were shown in table 3 and table 4.

The histopathological staging of tumor, concerning the depth of invasion, correctly correlated with ultrasonographic staging in 8 of these 17 patients. Of those who were incorrectly staged, 7 were overstaged and 2 were understaged (Table 5). The overall accuracy in determination of the depth of invasion for all 17 patients was 47%. Overstaging and understaging of tumor appeared in 41% (7/17) and 12% (2/17), respectively (Table 7).

Since 8 (47%) out of 17 patients were treated initially with chemoradiation before surgery, we evaluated the remaining 9 patients (53%), who did not receive initial treatment, separately. There were correctly staged in 5 out of 9 patients, 2 were overstaged and 2 were understaged (Table 6). The overall accuracy of the depth of tumor invasion in this group was 56% (5/9), while the overstaging and understaging of tumor appeared in a similar percentage of 22% (2/9 and 2/9) (Table 7).

The regional lymph node status was correctly assessed by TRUS in 9 out of 15 patients, giving an accuracy of 60% (fig.4). Particularly TRUS diagnosed 8/12 N(-) patients (67%) and 1/3 N(+) patients (33%)

Table 2 TNM classification by AJCC 2002

Primary tumor (T)	
TX	Primary tumor cannot be assessed
T0	No evidence of primary tumor
Tis	Carcinoma in situ: intraepithelial or invasion of the lamina propria
T1	Tumor invades submucosa
T2	Tumor invades muscularis propria
T3	Tumor invades through the muscularis propria into the subserosa, or into nonperitonealized pericolic or perirectal tissues
T4	Tumor directly invades other organs or structures, and/or perforates the visceral peritoneum
Regional lymph nodes (N)	
NX	Regional lymph nodes cannot be assessed
N0	No regional lymph node metastasis
N1	Metastasis in 1 to 3 regional lymph nodes
N2	Metastasis in 4 or more regional lymph nodes

Table 3 Characteristics of all included patients

Characteristics (n=17)	Summary: Number (%)
Age (years)	
Mean (SD)	55.5 (15.8)
Median (Range)	54 (30-85)
Sex	
Male	7 (41.2)
Female	10 (58.8)
Depth of tumor invasion by TRUS (uT)	
uT1	2 (11.8)
uT2	3 (17.6)
uT3	12 (70.6)
uT4	0 (0)
Presence of regional metastatic node (uN): n=15**	10 (66.7)
uN0	5 (33.3)
uN1	
Time between biopsy and TRUS	
Mean	16.5 (15.2)
Median	12 (5-53)
Time between TRUS and surgery (days)	60 (6-577)
Type of surgery	
Transanal excision	2 (11.8)
Low anterior resection (LAR)	4 (23.5)
Abdominoperineal resection (APR)	11 (64.7)
Size of tumor on pathology exam(cm)	
Mean (SD)	3.5 (1.4)
Median (range)	3.5 (1.2-6.5)
Histology of tumor	
Adenocarcinoma	16 (94.1)
GIST	1 (5.9)
Pathological results	
Depth of tumor invasion (pT)	
T0*	2 (11.8)
T1	3 (17.6)
T2	6 (35.3)
T3	6 (35.3)
T4	0 (0)
Regional lymph node metastasis (pN): n=15**	
N0	12 (80)
N1	3 (20)
Neoadjuvant therapy	
Yes	8 (47)
No	9 (53)

* T0 = *Other, compatible with no evidence of malignancy (1 case of acute and chronic inflammation and 1 case of granulation tissue and fibrosis)

** The remaining 2 cases had no data of lymph node pathological report due to transanal excision.

Table 4 The data of all 17 patients

Patient	Sex	Age	Time between biopsy & TRUS (days)	uT	uN	pT	pN	Time between TRUS & surgery (days)	Type of surgery	Neoadjuvant therapy
1	M	30	20	3	(-)	0	(-)	98	APR*	Yes
2	F	61	17	1	(-)	2	No data	21	Transanal excision	No
3	F	38	7	2	(-)	2	(-)	37	APR	No
4	M	63	53	3	(-)	2	(-)	47	APR	Yes
5	F	62	7	3	(-)	1	(-)	173	LAR	No
6	F	85	13	3	(-)	3	(-)	33	APR	No
7	M	54	No data	3	(-)	0	(-)	103	APR	Yes
8	M	53	6	3	(-)	3	(+)	95	APR	Yes
9	M	73	15	3	(-)	3	(-)	577	APR	Yes
10	F	57	5	2	(+)	2	(-)	26	LAR**	No
11	M	72	No data	3	(-)	2	(+)	89	LAR	Yes
12	F	51	12	3	(+)	2	(-)	6	LAR	No
13	F	54	45	3	(+)	3	(-)	60	APR	No
14	F	77	8	1	(-)	1	No data	17	Transanal excision	No
15	F	37	7	2	(-)	3	(-)	33	APR	No
16	F	34	No data	3	(+)	3	(+)	98	APR	Yes
17	M	43	No data	3	(-)	1	(-)	86	APR	Yes

* APR = Abdominoperineal resection

** LAR = Low anterior resection

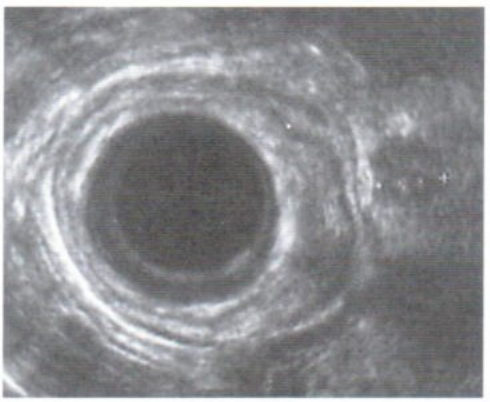

Fig.4 Metastatic node - hypoechoic, varying in size, round rather than oval and have discrete borders

Table 5 Results of transrectal ultrasound and pathologic staging of rectal cancer in determining of depth of invasion

Transrectal ultrasound (uT)		Pathologic findings (pT)				
Category	Number of patients n (%)	pT0	pT1	pT2	pT3	pT4
uT1	2 (11.8)	0(0.0)	1(33.3)	1(16.7)	0(0.0)	0(0.0)
uT2	3 (17.6)	0(0.0)	0(0.0)	2(33.3)	1(16.7)	0(0.0)
uT3	12 (70.6)	2(100)	2(66.7)	3(50.0)	5(83.3)	0(0.0)
uT4	0 (0.0)	0(0.0)	0(0.0)	0(0.0)	0(0.0)	0(0.0)
Total (N)	17 (100.0)	2(100)	3(100)	6(100)	6(100)	0(0.0)

Table 6 Results of transrectal ultrasound and pathological staging of rectal cancer in determining the depth of invasion, which excluded the neoadjuvant therapy group

Transrectal ultrasound (uT)		Pathologic findings (pT)			
Category	Number of patients (n)	pT1	pT2	pT3	pT4
uT1	2 (22.2)	1(50.0)	1(25.0)	0(0.0)	0(0.0)
uT2	3 (33.3)	0(0.0)	2(50.0)	1(33.3)	0(0.0)
uT3	4 (44.4)	1(50.0)	1(25.0)	2(66.7)	0(0.0)
uT4	0 (0.0)	0(0.0)	0(0.0)	0(0.0)	0(0.0)
Total (N)	9 (100.0)	2(100.0)	4(100.0)	3(100.0)	0(0.0)

Table 7 Accuracy in determining depth of invasion by transrectal ultrasound in all patients compared to the neoadjuvant-excluded group.

	All patients	Without neoadjuvant
Accuracy	47% (8/17)	56% (5/9)
Overstaging	41% (7/17)	22% (2/9)
Understaging	12% (2/17)	22% (2/9)

(table 8). Overstaging and understaging in lymph node evaluation occurred in 13% (2/15) and 27% (4/15) of the patients respectively (2 and 4 out of 15 in each group). (Table 9). The sensitivity was 33.3% and specificity was 66.7% with PPV 20% and NPV 80% (Table 8). If we excluded the patients who received preoperative chemoradiation, there were 7 patients left. The TRUS diagnosed 4/7 N(-) patients and 3/4 N(+) patients. No evidence of lymph node metastasis was found in the pathological examination. Therefore, the accuracy and specificity in determining regional lymph node metastasis were similar at 54.2% (Table 10).

When perirectal fat invaded lesion was studied,

transrectal ultrasonographic diagnostic evaluation resulted in an overall accuracy of 52.9%, a sensitivity of 83.3% (95% CI: 65.6 to 101.1%) and a specificity of 36.4% (95% CI: 13.5 to 59.2%) (Table 11). The accuracy was also shown as area under the curve in Graph 1. However, if the neoadjuvant excluded group, were studied the overall accuracy was increased to 66.7% (area under the curve in graph 2), and sensitivity and specificity were similar at 66.7% (95% CI: 35.9% to 97.5%) (Table 12).

Table 8 Correlation of transrectal ultrasound and pathologic staging of rectal cancer in determining regional lymph node involvement

TRUS findings	**Pathologic findings**	
	No lymph node metastasis, n (%)	**Lymph node metastasis, n (%)**
No lymph node metastasis, n (%)	8 (69.2)	2 (66.7)
Lymph node metastasis, n (%)	4 (30.7)	1 (33.3)

TRUS	**Lymph node metastasis**
Sensitivity (%)	33.3% (9.48-57.2)
Specificity (%)	66.7% (42.8-90.5)
Positive predictive value (%)	20% (-0.24-40.2)
Negative predictive value (%)	80% (59.8-100.2)
Accuracy (%)	60%
LR +	1.0
LR -	1.0

Table 9 Accuracy in determining regional lymph node involvement by transrectal ultrasound

	All patients (n=15)
Accuracy	60% (9/15)
Overstaging	13% (2/15)
Understaging	27% (4/15)

Table 10 Correlation of transrectal ultrasound and pathological staging of rectal cancer in determination of regional lymph node involvement (excluded patients who received neoadjuvant therapy)

TRUS findings	**Pathologic findings**	
	Lymph node metastasis, n (%)	**No lymph node metastasis, n (%)**
Lymph node metastasis, n (%)	0	3
No lymph node metastasis, n (%)	0	4

TRUS	**Lymph node metastasis**
Accuracy (%)	57.14%
Specificity (%)	57.14%

Table 11 Correlation of transrectal ultrasound and pathological staging of rectal cancer in determining perirectal fat invasion

TRUS findings	Pathologic findings	
	Perirectal fat invasion (n)	Non-perirectal fat invasion (n)
Perirectal fat invasion (n)	5	7
Non-perirectal fat invasion (n)	1	4

TRUS	Perirectal fat invasion
Sensitivity (%)	83.3% (65.6-101.1)
Specificity (%)	36.4% (13.5-59.2)
Positive predictive value (%)	41.7% (18.2-65.1)
Negative predictive value (%)	80% (60.9-99.0)
Accuracy (%)	52.9%
LR +	1.3
LR -	0.5

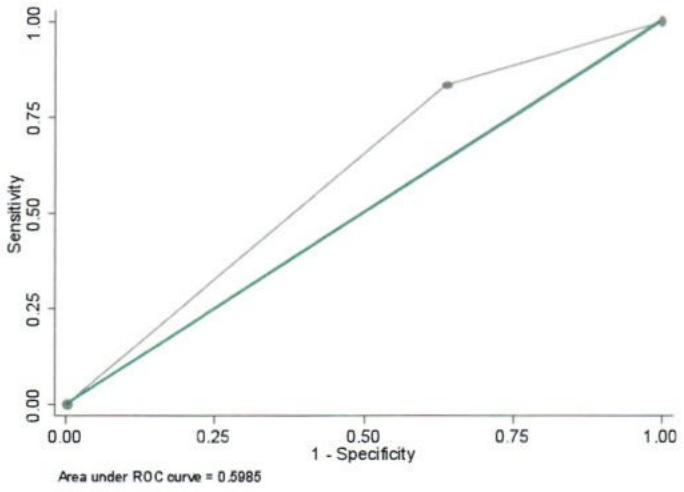

Graph 1. Accuracy of transrectal ultrasound in determining perirectal fat invasion, shown as area under the curve (all patients)

Table 12 Correlation of transrectal ultrasound and pathological staging of rectal cancer in determining perirectal fat invasion, in the neoadjuvant-excluded group

TRUS findings	Pathologic findings	
	Perirectal fat invasion (n)	Non-perirectal fat invasion (n)
Perirectal fat invasion (n)	2	2
Non-perirectal fat invasion (n)	1	4

TRUS	Perirectal fat invasion
Sensitivity (%)	66.7%(35.9-94.5)
Specificity (%)	66.7% (35.9-97.5)
Positive predictive value (%)	50.0% (17.3-82.7)
Negative predictive value (%)	80% (60.9-99.0)
Accuracy (%)	66.7%
LR +	2.0
LR -	0.5

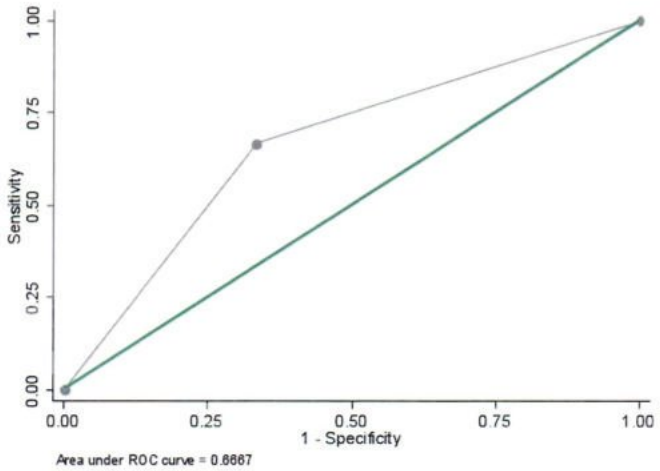

Graph 2. Accuracy of transrectal ultrasound in determining perirectal fat invasion, shown as area under the curve (excluded patients who received neoadjuvant therapy)

Discussion

The preoperative staging of rectal cancer is an important factor in the treatment plan to achieve better prognosis. The precise knowledge of local staging (T, N) is essential for planning of the optimal therapy. Various methods have been used to evaluate the local staging of rectal cancer which include digital rectal examination, computed tomography (CT), and magnetic resonance imaging (MRI). TRUS (Transrectal ultrasound) is considered the diagnostic tool of choice in multicenter studies with a mean accuracy of 79-88%[5,6,8,9,11] in the assessment of depth

of tumor invasion. Metanalysis on the diagnostic accuracy of TRUS compared to CT and MRI found that TRUS provides equal or even superior characterization of the depth of tumor invasion (TRUS, median 89%; CT, median 79%; MRI 82%)[5]. Furthermore, TRUS is easily reproducible, safe, painless and much cheaper.

Findings from our study of TRUS examination in the preoperative staging of rectal cancer showed that the accuracy is 47% in all 17 patients, which was lower than the recent multicenter studies. This was an important factor difference between our study and those in other studies. The patients in our study included the patients that also received pre-operative chemoradiation (8 in 17 patients; 47%) after they underwent TRUS examination, which caused downstaging of the tumor at the time of operation which lowered our accuracy. In another group in which we excluded the patients who received neoadjuvant therapy, we found that the accuracy increased from 47% to 56%, which corresponded with the decrease in overstaging from 41% to 22%. In this group, we correctly staged 56% (5 in 9 patients). Our overstaged and understaged rates for T staging were similar 22% (2 in 9 patients).

Of the understaged cases, there was one case (patient 2) that shown uT1 stage, while the pathological stage was T2 due to microscopically muscularis propria invasion. Another case of understage (patient 15) was staged as uT2, but the pathological report revealed pT3. The time between TRUS and surgery in this case was 33 days. According to the study of Hulsmans et al., they founded that, if patients with a therapy delay of 1 month or more were excluded, all incorrectly staged tumors were overstaged[12]. The explanation of this case could be due to the delayed time between TRUS and surgery (33 day), causing extra time for tumor growth before histopathological staging.

There were two overstaged cases. The first case (patient 12) was interpreted as uT3 but the pathological review show pT2. However, there is some error in this case due to inadequate resection that did not cover all the depth of tumor invasion in some part of the sampling. Therefore, the understaging in this case is still doubtful due to sampling error. Another explanation for overstaging is the time between biopsy and the TRUS study performed. Recent studies demonstrated the relation between the degree of inflammatory cell infiltration and the frequency of overstaging. Recently, it has been suggested that the inflammatory reaction responsible for the overstaging might be caused because the biopsy performed 1 week before TRUS examination[13,14]. In our two overstaged cases (patient 5 and patient 12), the time between biopsy and TRUS were 7 days and 12 days, respectively. Therefore, the inflammatory reaction from biopsy could be the reason for overstaging in our cases.

Although the accuracy was increased when we excluded the neoadjuvant group patient, the overall accuracy was still much lower than the other studies. We believe that the small number of examinations performed was the main reason for poor results.

The most important aim of the pre-therapeutic staging is the discrimination of tumor growth limited to the rectal wall (T1 & T2) and that invaded through this wall (T3 & T4). Related to this, TRUS examination in our study provided a sensitivity and specificity of 83.3% and 36.4%, respectively, with the accuracy of 52.9%. Similar to the above, the perirectal fat invasion detection in the non-neoadjuvant group was better with the accuracy of 66.7% and similar in

sensitivity and specificity of 66.7%, respectively. Data on these parameters from the other literature for the discrimination of T1-T2 VS T3-T4 were higher (accuracy 81-91%, sensitivity 90-94%, specificity 67-87%[6,15]. The reason for our lower results could be due to the small number of the enrolled patients. However, the high rate of prediction of growth beyond the rectal wall in the recent studies indicated that ultrasound can be of importance in the identification of those tumors with perirectal growth for which chemoradiation therapy could be suitable.

In the assessment of mesorectal nodes, the accuracy was 60%, which was lower than that reported in other studies, ranging from 70-86%[5,6,9,16]. Overstaging and understaging can occur during assessment of lymph node involvement[17]. Overstaging in node status is caused mostly by reactive lymph node swelling and understaging by the presence of small involved nodes and metastasis in extramesorectal nodes. The important factor that lowered the results in assessment of nodal involvement in our study was due to the small number of examinations performed.

Conclusion

The overall lower accuracy, sensitivity as well as specificity in this study as compared to the previous studies are probably due to the inclusion of the neoadjuvant therapy-patients group. However, when the neoadjuvant therapy group were excluded, the accuracy was improved, but still lower than others. The small number of included patients was believed to be the reason for the statistical analysis effect. As the recent standard treatment for T3 and T4 tumor was to undergo neoadjuvant therapy, therefore, there were only a small number of included patients left in this study. The accurate results in the future study of transrectal ultrasound in preoperative staging of rectal cancer should be achieved by increased sample size.

References

1. Khuhaprema T, Srivatanakul P, Srilung H, Wiangnon S, Sumitsawan Y, Attasara P. Colon and rectum. Bangkok: Ministry of Public Health, Ministry of Education 1998-2000.
2. Snady H, Merrick MA, eds. Improving the treatment of colorectal cancer: the role of EUS 1998.
3. Varma MG, Rogers SJ, Schrock TR, Welton ML. Local excision of rectal carcinoma 1999.
4. Improved survival with preoperative radiotherapy in resectable rectal cancer. Swedish Rectal Cancer Trial. N Engl J Med 1997;336(14):980-7.
5. Kwok H, Bissett IP, Hill GL. Preoperative staging of rectal cancer. Int J Colorectal Dis 2000;15(1):9-20.
6. Goldman S, Arvidsson H, Norming U, Lagerstedt U, Magnusson I, Frisell J. Transrectal ultrasound and computed tomography in preoperative staging of lower rectal adenocarcinoma. Gastrointest Radiol 1991;16(3):259-63.
7. Heriot AG, Grundy A, Kumar D. Preoperative staging of rectal carcinoma. Br J Surg 1999;86(1):17-28.
8. Bali C, Nousias V, Fatouros M, Stefanou D, Kappas AM. Assessment of local stage in rectal cancer using endorectal ultrasonography (EUS). Tech Coloproctol 2004;8 Suppl 1:s170-3.
9. Kim NK, Choi JS, Sohn SK, Min JS. Transrectal ultrasonography in preoperative staging of rectal cancer. Yonsei Med J 1994;35(4):396-403.
10. AJCC Cancer Staging Manual, Colon and rectum. 6 ed: Newyork 2002.
11. Milsom JW, Graffner H. Intrarectal ultrasonography in rectal cancer staging and in the evaluation of pelvic disease. Clinical uses of intrarectal ultrasound. Ann Surg 1990;212(5):602-6.
12. Hulsmans FJ, Tio TL, Fockens P, Bosma A, Tytgat GN. Assessment of tumor infiltration depth in rectal cancer with transrectal sonography: caution is necessary. Radiology 1994;190(3):715-20.

13. Yamashita Y, Machi J, Shirouzu K, Morotomi T, Isomoto H, Kakegawa T. Evaluation of endorectal ultrasound for the assessment of wall invasion of rectal cancer. Report of a case. Dis Colon Rectum 1988;31(8):617-23.
14. Derksen EJ, Cuesta MA, Meijer S. Intraluminal ultrasound of rectal tumours: a prerequisite in decision making. Surg Oncol 1992;1(3):193-8.
15. Beynon J, Mortensen NJ, Foy DM, Channer JL, Virjee J, Goddard P. Pre-operative assessment of local invasion in rectal cancer: digital examination, endoluminal sonography or computed tomography? Br J Surg 1986; 73(12):1015-7.
16. Kumar A, Scholefield JH. Endosonography of the anal canal and rectum. World J Surg 2000;24(2):208-15.
17. Akasu T, Sugihara K, Moriya Y, Fujita S. Limitations and pitfalls of transrectal ultrasonography for staging of rectal cancer. Dis Colon Rectum 1997;40(10 Suppl):S10-5.

THE ASEAN JOURNAL OF RADIOLOGY 2010; 16(3): 181-194 181

Original Article

Brain Arteriovenous Malformations: Experience in the Interventional Neuroradiology Unit, Ramathibodi Hospital

Ekachat Chanthanaphak, MD., Sirintara Pongpech, MD.
Pakorn Jiarakongmun, MD., Sasikhan Geibprasert, MD.

Department of Radiology, Faculty of Medicine, Ramathibodi Hospital, Mahidol University, Bangkok, Thailand

Abstract

Objective: To review patient demographics, clinical symptoms, presentation, imaging characteristics and embolization results as well as its complications of patients with brain AVMs seen in the Interventional Neuroradiology unit at Ramathibodi Hospital.

Materials and Methods: Retrospective review of all patients diagnosed with brain AVMs from cerebral angiography during January 2001 to December 2005 at the Interventional Neuroradiology Unit, Radiology Department, Ramathibodi hospital.

Results: There were a total of 189 patients. 44 patients were excluded due to incomplete medical records or loss of imaging data. Of the remaining 145 patients, 87 (60%) underwent partial-targeted embolization, 9 (6.2%) underwent curative embolization, 29 (20%) radiosurgery alone, 11 (7.6%) surgical resection alone, 1 (0.7%) spontaneously thrombosed, 2 (1.4%) received conservative treatment without any further treatment and 6 (4.1%) loss to follow up. 84 (57.9%) were male patients and 61 (42.1%) were female. The mean age at the time of angiographic diagnosis was 27.2 years +/- 15.1. The initial presentations included intracranial hemorrhage in 88 (60.7%), seizures in 29 (20%), headaches in 18 (12.4%), 2 (1.4%) with focal neurological deficit, incidental finding in 1 (0.7%) and 7 (4.8%) with other presentations. Ruptured AVM were mainly of small size (65.9%, P=0.03), single deep vein (27.3%, P<0.05) with locations in the deep gray nuclei, midline structures and corpus callosum (31.8%, P=0.001). Only 18 of 27 intranidal aneurysms were found in patient with ruptured AVMs, two times higher compared to patients with non-ruptured AVMs however without statistical significance (P=0.72). In 87 patients with goals of partial targeted embolization,

the majority of the AVMs (55 of 80) had more than 50% reduced flow, which were related to small and medium sized AVMs ($P<0.05$). AVMs with single arterial feeder ($P=0.001$) and single draining vein ($P<0.05$). There was failure of partial targeted embolization in 3 of 87 patients. Success rate of curative embolization is 89% (8 of 9 patients). Clinically significant complications after embolization (ischemia or hemorrhage) were seen in 7 of 96 patients (7.3%).

Conclusion: In our experience, the presentation of brain AVMs and risk factors of hemorrhage were similar to the previous studies. The total success rate of curative embolization was 8.3%, while partial targeted embolization was able to reduce the AVM flow more than 50% in the majority of patients with less significant clinical complications.

Keywords: Brain arteriovenous malformations, cerebral arteriovenous malformations

Background

Brain arteriovenous malformations (AVMs) represent an uncommon but important source of neurological morbidity in young adults.[1] The basic morphology is of a vascular mass, called the nidus, which directly shunts blood between the arterial and venous circulations without a true capillary bed. There is usually high flow through the feeding arteries, nidus and draining veins.

Clinical presentations of brain AVMs are variable. Intracranial hemorrhage is the most common clinical presentation of AVMs, with a reported frequency ranging from 30-82%.[2,3] Others include epileptic seizures, headaches and neurological deficits with only few appearing to be asymptomatic.[4]

The risk of hemorrhage from brain AVMs is approximately 1-3% per year[27-29] and persists until the lesion is completely obliterated. Therefore, the goal of treatment is to achieve complete obliteration with the minimal neurological risk and complications.[5] There are three established treatment modalities for brain AVMs, i.e. microsurgery, endovascular embolization and radiosurgery.[6] All play a role for specific patients. The most appropriate plan for any given patient, of course, would take many factors into account, including clinical risk factors, angiographic features, age, and neurological status.

Endovascular treatment of brain AVMs aims to be either curative or partial targeted to reduce the size, weak points or flow of the AVMs, however the complications are serious with a wide range of morbidity and mortality risk (10-50% neurological deficit, 1-4% mortality) in previous reports.[7]

The purpose of this study is to review patient demographics, clinical symptoms, presentation, imaging characteristics and embolization results as well as its complications of patients with brain AVMs seen in the Interventional Neuroradiology Unit at Ramathibodi hospital.

Materials and Methods

Patients

All patients diagnosed with brain AVMs from by cerebral angiography during January 2001 to December 2005 at Interventional Neuroradiology Unit at Ramathibodi Hospital were included in this study. Medical records and imaging data were retrospectively reviewed.

The patient lists are searched from the registration records and the hospital electronic database (ICD-10 code Q28.2). Patients with incomplete medical records or radiographic studies were excluded.

Imaging analysis:

CT, MRI and angiographic images were retrospectively reviewed by board certified interventional neuroradiologists.

AVM characteristics

The cerebral angiograms were analyzed for the AVM morphological characteristics, including size, anatomic location, arterial feeder (pattern and distribution of supply), venous drainage (either into the superficial cortical veins or the deep venous system), and the presence of associated prenidal, nidal and postnidal aneurysms. The AVM size was determined from CT, MRI and cerebral angiograms.

Cerebral angiography and endovascular embolization

The purpose of cerebral angiography and embolization was classified into three groups: 1) diagnostic cerebral angiography without endovascular treatment, 2) partial-targeted embolization

(i.e. pre-surgical or pre-radiosurgical procedure) and 3) curative embolization. The criteria for the last group includes small AVM size, single or two arterial feeders and probability to reach the nidus with a microcather.

Diagnostic cerebral angiography was performed via a transfemoral arterial route under local anesthesia. After placement of a 5-6-Fr Terumo sheath, a 4-5-Fr vertebral catheter was routinely used for young patients while a 5-Fr JB or Sim-2 catheter was used for older patients with tortuous aortic arches to select the carotid and vertebral arteries. Digital subtraction angiographic in antero-posterior and lateral views were performed with iodinated contrast injections of carotid or vertebral arteries, depending on AVM location.

In contrast, endovascular embolization procedures were performed with the patients under general anesthesia. Selective angiography was used in pre-embolization planning, and standard techniques of digital subtraction angiography with road mapping were used during endovascular procedures.

Flow- and wire-guided microcatheters of various sizes were used to advance the microcatheter tip as close as possible to the AVM nidus. Once in optimal position (i.e., wedged in the nidus or placed in the terminal arterial feeder proximal to the nidus), permanent vessel occlusion was obtained with injection of n-butyl cyanoacrylate (NBCA) into the target vessels. The degree of nidal penetration and target vessels varied, depending on the embolization treatment goals. If embolization was used as an adjunct to surgical resection, the specific goals of embolization were to facilitate surgical excision by 1) nidus size and flow reduction, 2) the occlusion of deep, surgically inaccessible or deep feeding arteries 3) and the occlusion of intranidal arteriovenous fistulas.[6,8] If embolization was performed before radiosurgery, then AVM compartment penetration was attempted to achieve also greater size & reduction and make the AVM more amenable to radiation therapy.[9] The flow reduction was evaluated and classified into 4 ranges depend on percentage of reduced flow after the embolization (Figure 1). If embolization was used alone, the goal of embolization was complete obliteration of the AVM nidus. All treated patients underwent both radiographic (magnetic resonance imaging, computered tomography or cerebral angiography) and clinical follow-up after embolization.

Statistical analysis

All patient data were analyses by statistical software (SPSS, version 13.0 for Windows). The continuous data such as patient's age and total number of embolization procedures were calculated for mean, SD and median (range) values. Other frequency data i.e. sex, clinical symptoms, presentation, imaging characteristics, embolization results, technical complications and clinically significant complications are described by number of cases and percentage.

Chi-square tests (X2) were done for statistical significance with a confidence interval of 95% ($P<0.05$).

Results

Patients and AVM characteristics

In a 5 year period from January 2001 to December 2005, there were 189 brain AVM patients were seen in our unit. 44 patients were excluded due to incomplete medical records in 16 patients, loss of imaging data in 25 patients and unknown causes of death in 3 patients. Remaining 145 patients

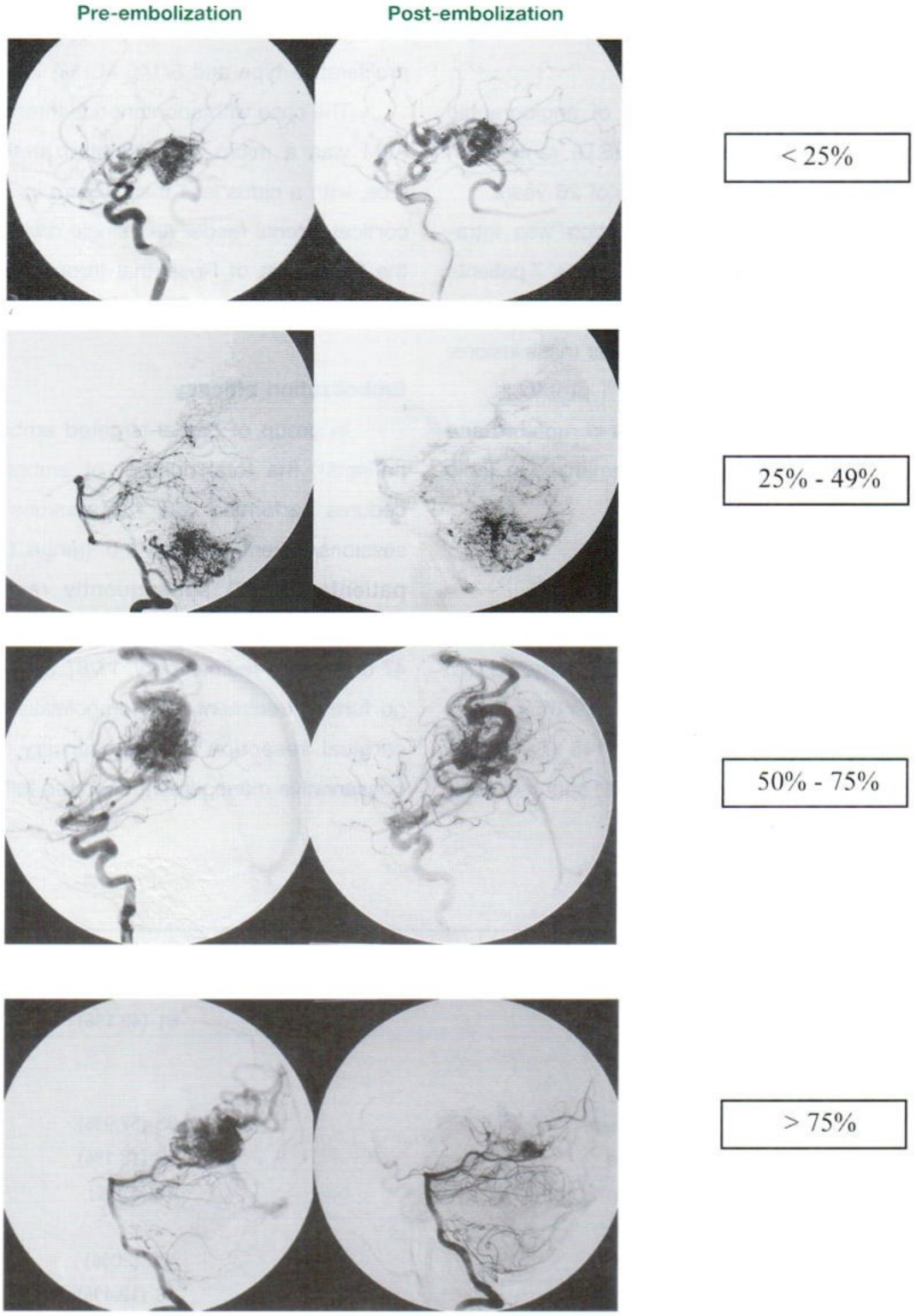

Fig.1 Percentage of flow reduction compared between pre- and post embolization

were enrolled in this study. Patient demographics and clinical presentations are summarized in Table 1.

The mean age at the time of angiographic diagnosis was 27.2 years +/- 15.1 (S.D), range from 0.8 to 16 years and a median age of 26 years.

The most common presentation was intracranial hemorrhage in 88 (60.7%) patients. 7 patients presented with other symptoms including 2 visual problems, 1 facial neuralgia, 2 vascular mass lesions, 1 alteration of consciousness and 1 proptosis.

Morphological characteristics in ruptured and non-ruptured AVM groups are summarized in Table 2.

AVM treatments

96 in 145 of the patients (66.2%) underwent endovascular treatment with a partial-targeted aim in 87 (60%) and curative in 9 (6.2%). 29/145 patients (20%) had radiosurgery alone, 11/145 (7.6%) had surgical resection alone. 1/145 (0.7%) spontaneously thrombosed. 2/145 (1.4%) received conservative management without any further treatment due to proliferative type and 6/145 (4.1%) loss follow up.

The case with spontaneous thrombosis of the AVM was a micro AVM, located at the temporal lobe, with a nidus less than 0.5 cm in size, a single cortical arterial feeder and single draining vein into the basal vein of Rosenthal thrombosed after the first episode of hemorrhage.

Embolization efficacy

In group of partial-targeted embolization (87 patients), the total number of embolization procedures performed was 133 sessions (mean =1.5 sessions/patient, median 1.0 (range 0-4)). Most patients (63/87) subsequently received other treatment; of which 16 underwent surgical resection, 47 underwent radiosurgery. 17/87 patients received no further treatment after embolization - 2 denied surgical resection or radiosurgery, 3 received conservative management and loss follow up in 12

Table 1 Patient characteristics (n=145)

Sex, n (%)	
Male	84 (57.9%)
Female	61 (42.1%)
Initial presentation, n (%)	
Rupture	
Intraparenchymal hemorrhage	63 (57.9%)
Intraventricular hemorrhage	19 (13.1%)
Subarachnoid hemorrhage	6 (4.1%)
Non-rupture	
Seizure	29 (20%)
Headache	18 (12.4%)
Focal neurological deficit	2 (1.4%)
Incidental (in patient with subdural hematoma)	1 (0.7%)
Others	7 (4.8%)

Table 2 Arteriovenous malformation characteristics

	Total AVMs (n=145)	Ruptured AVMs (n = 88)	Non-ruptured AVMs (n = 57)	P value
AVM size (Spetzler-Martin criteria), n (%)				*P=0.03*
Small (<3 cm)	73 (50.3%)	58 (65.9%)	15 (26.3%)	
Medium (3-6 cm)	44 (30.3%)	21 (23.9%)	23 (30.4%)	
Large (> 6 cm)	28 (19.3%)	9 (10.2%)	19 (33.3%)	
AVM location, n (%)				*P=0.001*
Lobar location	110 (75.9%)	60 (68.2%)	50 (87.7%)	
Frontal lobe	38 (26.2%)	18 (20.5%)	20 (35.1%)	
Parietal lobe	26 (17.9%)	15 (17%)	11 (19.3%)	
Temporal lobe	29 (20.0%)	18 (20.5%)	11 (19.3%)	
Occipital lobe	4 (2.8%)	1 (1.1%)	3 (5.3%)	
Cerebellar lobe	13 (9.0%)	8 (9.1%)	5 (8.8%)	
Deep gray nuclei and midline structures	23 (15.9%)	19 (21.6%)	4 (7.0%)	
Basal ganglia	6 (4.1%)	3 (3.4%)	3 (5.3%)	
Thalamus	13 (9.0%)	13 (14.8%)	0	
Brain stem	4 (2.8%)	3 (3.4%)	1 (1.8%)	
Others	12 (8.3%)	0	0	
Corpus callosum	11 (7.6%)	9 (10.2%)	2 (3.5%)	
Optic chiasm	1 (0.7%)	0	1 (1.8%)	
Arterial feeders, n (%)				*P=0.35*
Single	21 (14.5%)	18 (20.5%)	3 (5.3%)	
Cortical branch	13 (8.9%)	11 (12.5%)	2 (3.5%)	
Choroidal branch	6 (4.1%)	5 (5.7%)	1 (1.8%)	
Perforator branch	2 (1.4%)	2 (2.3%)	0	
Multiple	124 (85.5%)	70 (79.5%)	54 (94.7%)	
Cortical branches	78 (53.8%)	40 (45.5%)	38 (66.7%)	
Choroidal branches	3 (2.1%)	3 (3.4%)	0	
Perforator branches	6 (4.1%)	5 (5.7%)	1 (1.8%)	
Combined	37 (25.6%)	22 (25%)	15 (26.3%)	
Associated aneurysm, n (%)				
Prenidal	21 (14.5%)	10 (11.4%)	11 (19.3%)	*P=0.41*
Nidal	27 (18.6%)	18 (20.5%)	9 (15.8%)	*P=0.72*
Postnidal	18 (12.4%)	10 (11.4%)	8 (14%)	*P=0.98*
Venous drainage, n (%)				*P<0.05*
Single	54 (37.3%)	46 (52.3%)	8 (14%)	
Superficial vein	19 (13.1%)	16 (18.2%)	3 (5.3%)	
Deep vein	28 (5.5%)	24 (27.3%)	4 (7%)	
Cavernous sinus	1 (0.7%)	1 (1.1%)	0	
Posterior fossa vein	6 (4.1%)	5 (5.7%)	1 (1.8%)	

Table 2 (continue) Arteriovenous malformation characteristics

	Total AVMs (n=145)	Ruptured AVMs (n = 88)	Non-ruptured AVMs (n = 57)	P value
Venous drainage, n (%)				*P<0.05*
Multiple	91 (62.3 %)	42 (47.7%)	49 (86%)	
Presence of deep vein +/- cavernous sinus	45 (31%)	20 (22.7%)	25 (43.9%)	
Absence of deep vein or cavernous sinus	46 (31.7%)	22 (25%)	24 (42.1%)	
Spetzler-Martin grade, n (%)				*P=0.29*
I	27 (18.6%)	21 (23.9%)	6 (10.5%)	
II	43 (29.7%)	25 (28.4%)	18 (31.6%)	
III	43 (29.7%)	32 (36.4%)	11 (19.3%)	
IV	19 (13.1%)	6 (6.8%)	13 (22.8%)	
V	13 (9.0%)	4 (4.5%)	9 (15.8%)	
Presence of venous obstruction, n (%)	12 (8.3%)	6 (6.8%)	6 (10.5%)	*P=0.89*
Intranidal fistula, n (%)	12 (8.3%)	6 (6.8%)	6 (10.5%)	*P=0.34*

Table 3 Angiographic features and totally reduced flow of AVMs (n=80)

	Percentage of totally reduced flow				
	< 25% (n=5)	25-49% (n=20)	50-75% (n=33)	>75% (n=22)	P value
AVM size (Spetzler-Martin criteria), n (%)					*P<0.05*
Small (<3 cm)	0	5 (25%)	9 (27.3%)	14 (63.6%)	
Medium (3-6 cm)	3 (60%)	9 (45%)	18 (54.5%)	5 (22.7%)	
Large (> 6 cm)	2 (40%)	6 (30%)	6 (18.2%)	3 (13.6%)	
AVM location, n (%)					*P=0.59*
Lobar location	5 (100%)	16 (80%)	29 (87.8%)	16 (7.7%)	
Deep gray nuclei and midline structures	0	3 (15%)	2 (6.1%)	2 (9.1%)	
Others:					
Corpus callosum	0	0	2 (6.1%)	4 (18.2%)	
Optic chiasm	0	1 (5%)	0	0	
Arterial feeders, n (%)					*P=0.001*
Single	0	0	0	7 (31.8%)	
Multiple	5 (100%)	20 (100%)	33 (100%)	15 (68.2%)	
Venous drainage, n (%)					*P<0.05*
Single	1 (20%)	2 (10%)	7 (21.2%)	16 (72.7%)	
Multiple	4 (80%)	18 (90%)	26 (78.8%)	6 (27.3%)	

Table 3 (continue) Angiographic features and totally reduced flow of AVMs (n=80)

	Percentage of totally reduced flow				
	< 25% (n=5)	25-49% (n=20)	50-75% (n=33)	>75% (n=22)	P value
Spetzler-Martin grade, n (%)					*P=0.18*
I	0	3 (15%)	3 (15%)	4 (18.2%)	
II	2 (40%)	5 (25%)	10 (30.3%)	11 (50%)	
III	2 (40%)	4 (20%)	11 (33.3%)	3 (13.6%)	
IV	1 (20%)	6 (30%)	4 (12.1%)	3 (13.6%)	
V	0	2 (10%)	5 (15.2%)	1 (4.5%)	
Obliteration of intranidal fistula, n (%)	0	4 (20%)	4 (12.1%)	1 (22%)	*P=0.037*
Subsequently treatments, n (%)					
Radiosurgery	2 (40%)	14 (70%)	20 (60.6%)	11 (50%)	*P=0.378*
Surgical resection	1 (20%)	2 (10%)	7 (21.2%)	6 (27.3%)	*P=0.673*
No further treatment	0	0	0	3 (13.6%)	*P=0.009*
Loss follow up	1 (20%)	3 (15%)	6 (18.2%)	2 (9.1%)	*P=0.632*
Denied further treatment	1 (20%)	1 (5%)	0	0	*P=0.003*

Table 4 Patient characteristics and angiographic features of 8 completed obliterated AVM patients in curative embolization

Patient ID	Sex	Age (yrs)	Clinical presentation	AVM location	No. and type of arterial feeders	Aneurysms	No. and type of venous drainage	Emboliza-tions (n)
4	M	17	ICH*	Corpus callosum	Single, cortical br.	Intranidal	Single, cortical v.	2
77	M	32	ICH	Frontal	Single, cortical br.	-	Single, deep v.	1
99	F	22	IVH**	Cerebellar	Two, cortical br.	Intranidal	Single, deep v.	1
109	F	13	ICH	Midbrain	Single, PchA***	-	Single, deep v.	2
112	F	13	ICH	Frontal	Single, cortical br.	-	Two, cortical v.	1
114	M	20	ICH	Cerebellar	Single, cortical br.	-	Single,posterior fossa v.	1
115	F	6	ICH	Temporal	Single, cortical br.	-	Single, deep v.	1
135	F	26	ICH	Parietal	Single, cortical br.	-	Single, deep v.	1

* = Intracerebral hemorrhage

** = Intraventricular hemorrhage

*** = Posterior choroidal artery

Table 5 Technical complications and clinically significant complications

Technical Complications, n (%)	
Microperforation	7 (43.8%)
Glued vein	5 (31.2%)
Microcatheter fracture	1 (6.3%)
Dissection	2 (12.5%)
Reflux of glue into parent artery	1 (6.3%)
Clinically significant complications, n (%)	
Intraparenchymal hemorrhage	2 (28.6%)
Intraventricular hemorrhage	1 (14.3%)
Subarachnoid hemorrhage	2 (28.6%)
Arterial infarction	2 (28.6%)

patients. 3/87 patients had complete obliteration of the nidus after follow up by MRI or diagnostic angiography without further treatment. 4/87 patients in which we failed embolization - 2 patients had radiosurgery, no further management in 1 patient (large proliferative type of AVM) and loss follow up in 1 patient. Angiographic features and totally reduced flow of 80 patients are summarized in Table 3. Evaluation of the totally reduced flow after the last embolization showed: 5 patients had <25% decreased flow, 20 patients had 25 to 49% decreased flow, 33 patients had 50 to 75% and 22 patients had >75% decreased flow.

All 9 intranidal fistulas, 12 of 14 (86%) intranidal aneurysms and 6 of 8 (75%) postnidal aneurysms were successfully treated with glue.

9 patients which we aimed for curative embolization, 8 were completely obliterated within the first or second time of embolization. The details of each patient are detailed in Table 4. 1 patient lost to follow-up after diagnostic angiography.

Complications

A total of 16 technical complications occurred during embolization. There were clinically significant complications in 7/16, the most frequent being intracerebral hemorrhage. No deaths related to these complications were encountered. The technical and clinically significant complications are summarized in Table 5.

Discussion

In previously reported series,[4,10,11] the mean age of patients with brain AVM varies from 33 to 35 years with female predominance. In our study, the mean patient age is lower, about 27.2 +/- 15.2 years with slightly more male patients (52.9%).

The most common presentations of brain AVMs are intracranial hemorrhage (60.6%) and seizure (20%), which are similar to other series.[4,10,11] Other presenting symptoms include headaches, focal neurological deficits, visual disturbance, facial neuralgia and vascular mass lesion. Only 1 patient

had an incidentally found brain AVM during investigation of a contralateral subdural hematoma.

Ruptured and non-ruptured AVMs had statistically significant differences in angiographic features (Table 2), which were the AVM size, localization in deep gray nuclei, midline structures and corpus callosum, including number and type of venous drainage. The small size and presence of deep vein drainage were associated with a high incidence of hemorrhagic presentations.[12,13] In our study, ruptured AVMs were mainly of small size (65.9%, P=0.03) with single deep vein drainage (27.3%, P<0.05). This observation contradicts with the previously reported study[30] since small sized AVMs tend to have no other symptoms and therefore, will only present after bleeding. No statistical difference between the two groups was found in cases with multiple draining veins. Moreover, AVMs locating in the deep gray nuclei, midline structures and corpus callosum (P=0.001) were also associated with high incidence of rupture. The presence of an intranidal aneurysm with association of intracranial hemorrhage is still controversial.[14] Mansmann U, et al15 reported factors associated with intracranial hemorrhage in brain AVM. His study demonstrated no any association of intranidal aneurysm and intracranial hemorrhage. In our study, only 18 of 27 intranidal aneurysms were found in patients with ruptured AVMs, two times higher as compared to patient with non-ruptured AVM however without any statistical significance (P=0.72). The lobar AVM location, number & type of arterial feeder, Spetzler-Martin grade, presence of venous obstruction and intranidal fistula were also not statistically significant.

In many studies,[9,16-18] the aim of partial targeted embolization was to reduce the AVM size and close the intranidal aneurysm to prevent of re-rupture of the AVM, which was then followed by radiosurgery or surgical resection for further treatment. In addition, in our personal experience, that reduction of the flow through the AVM and closing of intranidal fistula are helpful to promote epithelialization of AVM, facilitating complete obliteration after radiosurgery. Pre-operative embolization before surgical resection of the AVM has been shown to improved postsurgical outcome.[19]

The factors related to percentage of total flow reduction are shown in Table 3. The AVM size, number of arterial feeder and venous drainage were statistically significant. Most of the small and medium sized AVMs had more than 50% (55 of 80) reduced flow from embolization (P<0.005). AVMs with single arterial feeder (P=0.001) and single draining vein (P<0.05) were also found to have a higher percentage of decreased flow from the embolization. There was no statistical difference in the large sized AVMs and the AVMs with intranidal fistulas. All patients which received no further treatment after the embolization (n=3) until the time of this study had >75% reduced flow (P=0.009). 2 patients are children (11 and 14 age years) with residual small AVMs, whom we decided to follow up with possible further radiosurgery, 1 patient had CAMS with a large proliferative AVM. The AVM location and Spetzler-Martin grade were not statistically significant.

The prior study[20] revealed success rate of curative embolization was 60% with no recurrence in follow up angiography. In our study, we succeeded in complete obliteration of the AVM in 8 of 9 patients (89%) whom we aimed for curative embolization. The total success rate of curative embolization was 8.3%. All of these AVMs have a small size, one or

two arterial feeders and required one or two sessions of embolization, similar to the other study[20] with varying locations. However, this high success rate is probably due to a large number of patients who were excluded from the study.

The major risk of embolization is ischemic or hemorrhagic complications during and after treatment. The complication rate is influenced primarily by the technical aspects of the procedure, including vascular damage, which is related to operator skill, catheter features.[21,22] characteristics of the embolic material including hemodynamic changes after embolization[23] and inflammatory reaction of vessels.[24] Complication rates vary among studies. Guo WY, et al[25] reported 19% morbidity and Sorimachi T, et al[26] reported 14% morbidity and death in 3%. In our series, permanent deficits were seen in 7of 96 patients with embolization (7.3%).

Our study has some limitations. Due to retrospective study, first, a large number of patients were excluded from loss of medical or angiographic data. Second, evaluation of total flow reduction is subjective data, which may lead to misinterpretion.

In the future, comparison of non-embolization and partial targeted embolization with complete obliteration of AVM after radiosurgery should be studied, in order to confirm our hypothesis regarding the usefulness of decreased flow after embolization.

Conclusion

The most common presentation of brain AVMs is intracranial hemorrhage, being more frequent in AVMs localized in the deep gray nuclei, midline structures and corpus callosum with single deep vein drainage. Small sized AVM were also found to have higher hemorrhagic presentations. The presence of intranidal aneurysms were two times higher in the ruptured AVMs compared to the non-ruptured ones and may be one risk factor. In our experience, partial targeted embolization was able to reduce the AVM flow more than 50% in the majority of patients with less significant clinical complications than the previous studies.

References

1. Arteriovenous Malformation Study Group. Current concepts: arteriovenous malformations of the brain in adults. N Engl J Med. 1999 June;340:1812-18.
2. Al-Shahi R, Warlow C. A systematic review of the frequency and prognosis of arteriovenous malformations of the brain in adults. Brain. 2001 Oct;124:1900-26.
3. Fleetwood IG, Steinberg GK. Arteriovenous malformations. Lancet. 2002 Mar 9;359(9309):863-73.
4. Stapf C, Khaw AV, Sciacca RR, Hofmeister C, Schumacher HC, Pile-Spellman J, et al. Effect of age on clinical and morphological characteristics in patients with brain arteriovenous malformation. Stroke. 2003 Nov;34(11): 2664-9.
5. Lee CZ, Young WL. Management of brain arteriovenous malformations. Curr Opin Anaesthesiol. 2005 Oct;18(5): 484-9.
6. Ogilvy CS, Stieg PE, Awad I, Brown RD Jr, Kondziolka D, Rosenwasser R, et al. Recommendations for the management of intracranial arteriovenous malformations: a statement for healthcare professionals from a special writing group of the Stroke Council, American Stroke Association. Circulation. 2001 May 29;103(21):2644-57.
7. Ledezma CJ, Hoh BL, Carter BS, Pryor JC, Putman CM, Ogilvy CS. Complications of cerebral arteriovenous malformation embolization: multivariate analysis of predictive factors. Neurosurgery. 2006 Apr;58(4):602-11.
8. Vinuela F, Dion JE, Duckwiler G, Martin NA, Lylyk P, Fox A, et al. Combined endovascular embolization and surgery in the management of cerebral arteriovenous malformations: experience with 101 cases. J Neurosurg. 1991 Dec; 75:856-64.

9. Gobin YP, Laurent A, Merienne L, Schlienger M, Aymard A, Houdart E, et al. Treatment of brain arteriovenous malformations by embolization and radiosurgery. J Neurosurg. 1996 Jul;85(1):19-28.
10. Halim AX, Singh V, Johnston SC, Higashida RT, Dowd CF, Halback VV, et al. Characteristics of brain arteriovenous malformations with coexisting aneuryms: a comparison of two referal centers. Stroke. 2002 Mar;33(3):675-9.
11. Hartmann A, Stapf C, Hofmeister C, Mohr JP, Sciacca RR, Stein BM, et al. Determinants of neurological outcome after surgery for brain arteriovenous malformation. Stroke. 2000 Oct;31(10):2361-4.
12. Watimo O. The relationship of size, density and localization of intracranial arteriovenous malformations to the type of initial symptom. J Neurol Sci. 1973 May;19(1):13-9.
13. Itoyoma Y, Uemura S, Ushio Y, Kuratsu J, Nonaka N, Wada H, et al. Natural course of unoperated intracranial arteriovenous malformations: study of 50 cases. J Neurosurg. 1989 Dec;71(6):805-9.
14. Kader A, Young WL, Pile-Spellman J, Mast H, Sciacca RR, Mohr JP, et al. The influence of hemodynamic and anatomic factors on hemorrhage from cerebral arteriovenous malformations. Neurosurgery. 1994 May;34(5):801-7; discussion 807-8.
15. Mansmann U, Meisel J, Brock M, Rodesch G, Alverez H, Lasjaunias P. Factors associated with intracranial hemorrhage in cases of cerebral arteriovenous malformation. Neurosurgery. 2000 Feb;46(2):272-9; discussion 279-81.
16. Liu HM, Huang YC, Wang YH. Embolization of cerebral arteriovenous malformations with n-butyl-2-cyanoacrylate. J Formos Medl Assoc. 2000 Dec;99(12):906-13.
17. Mounayer C, Hammami N, Piotin M, Spelle L, Benndorf G, Kessler I, et al. Nidal embolization of brain arteriovenous malformations using Onyx in 94 patients. AJNR Am J Neuroradiol. 2007 Mar;28(3):518-23.
18. van Rooij WJ, Sluzewski M, Beute GN. Brain AVM embolization with Onyx. AJNR Am J Neuroradiol. 2007 Jan;28(1):172-7. discussion 178.
19. DeMeritt JS, Pile-Spellman J, Mast H, Moohan N, Lu DC, Young WL, et al. Outcome analysis of preoperative embolization with N-Butyl cyanoacrylate in cerebral arteriovenous malformations. AJNR Am J Neuroradiol. 1995 Oct;16(9):1801-7.
20. Yu SC, Chan MS, Lam JM, Tam PH, Poon WS. Complete obliteration of intracranial arteriovenous malformation with endovascular cyanoacrylate embolization: initial success and rate of permanent cure. AJNR Am J Neuroradiol. 2004 Aug;25(7):1139-43.
21. Wikholm G, Lundqvist C, Svendsen P. Transarterial embolization of cerebral arteriovenous malformations: improvement of results with experience. AJNR Am J Neuroradiol. 1995 Oct;16(9):1811-7.
22. Frizzel RT, Fisher WS. Cure, morbidity, and mortality associated with embolization of brain arteriovenous malformations: a review of 1246 patients in 32 series over a 35-year period. Neurosurgery. 1995 Dec;37(6):1031-40.
23. Takeuchi S, Abe H, Nishimaki K, Minakawa T, Koike T, Kameyama S, et al. Cerebral haemodynamic changes after endovascular treatment of arteriovenous malformations: evaluation by single-photon emission CT. Acta Neurochir (Wien). 1994;127(3-4):142-50.
24. Deveikis JP, Manz HJ, Luessenhop AJ, Caputy AJ, Kobrine AI, Schellinger D, et al. A clinical and neuropathologic study of silk suture as an embolic agent for brain arteriovenous malformations. AJNR Am J Neuroradiol. 1994 Feb;15(2): 263-71.
25. Guo WY, Wikholm G, Karlsson B, Lindquist C, Snendsen P, Ericson K. Combined embolization and gamma knife radiosurgery for cerebral arteriovenous malformations. Acta Radiol. 1993 Nov;34(6):600-6.
26. Sorimachi T, Koike T, Takeuchi S, Minakawa T, Abe H, Nishimaki K, et al. Embolization of cerebral arteriovenous malformations achieved with polyvinyl alcohol particles: angiographic reappearance and complications. AJNR Am J Neuroradiol. 1999 Aug;20(7):1323-8.
27. Karlsson B, Lindquist C, Johansson A, Steiner L: Annual risk for the first hemorrhage from untreated arteriovenous malformations. Minim Invasive Neurosurg. 1997 Jun; 40(2):40-6.
28. Brown RD Jr, Wiebers DO, Forbes G, O'Fallan WM, Peipgras DG, Marsh WR, et al. The natural history of unruptured intracranial arteriovenous malformations. J Neurosurg. 1988 Mar;68(3):352-7.

29. Graf CJ, Perret GE, Torner JC. Bleeding from cerebral arteriovenous malformations as part of their natural history. J Neurosurg. 1983 Mar;58(3):331-7.

30. Stefani MA, Porter PJ, terBrugge KG, Montanera W, Willinsky RA, Wallace MC. Large and deep brain arteriovenous malformations are associated with risk of future hemorrhage. Stroke. 2002 May;33(5):1220-4.

THE ASEAN JOURNAL OF RADIOLOGY 2010: 16(3): 195-199 195

Original Article

The Outcome of Craniospinal Irradiation in Supine Position at Siriraj Hospital: Preliminary Results

Nan Suntorrnpong, MD., Piyanan Liammookda M.Sc. (Medical physics), Lalida Tuntipumiamorn M.Sc. (Radiological science), Kullathorn Thephamongkol, MD.

Department of Radiology, Faculty of Medicine Siriraj Hospital, Mahidol University, Bangkok10700, Thailand

Abstract

Objective: To study the outcome of craniospinal irradiation (CSI) in supine position in aspect of treatment control and acute treatment toxicity.

Materials and Methods: The medical records of all patients treated with CSI in supine position between July 2007 and December 2008 at Division of Radiation Oncology, Department of Radiology, Siriraj Hospital were retrospectively reviewed.

Results: Twenty patients were identified with 13 (65%) showed complete response at median follow-up 23.5 months. No one developed intracranial, spinal or distant failure. No disease failure occurred at craniospina or spinalspinal junction from CSI in supine position. Grade 3-4 leucopenia and neutropenia were found in 13 (65%) and 11 (55%) patients respectively.

Conclusion: Supine position can be an alternative technique for CSI. Disease control is acceptable with some Grade 3-4 hematologic toxicity.

Keywords: Craniospinal irradiation, supine position

Introduction

The entire craniospinal axis is the standard volume for radiation therapy (RT) in tumors with risk of leptomeningeal involvement. These tumors are found in pediatric patients who require anesthesia during treatment. Craniospinal irradiation (CSI) need to encompass whole brain and whole length of spinal axis with covering meninges. This technique has traditionally been administered to patients in prone position using lateral opposed cranial fields and posterior spinal fields down to the end of thecal sac. This position allows direct visualization of junction for craniospinal field and spinalspinal fields. Disadvantages of prone position are patient uncomfort, difficulty to tolerate especially in children and risk to access airway for anesthesia.

To minimize these disadvantages, CSI in supine position should be an alternative technique. This study reported our preliminary outcome with this technique in aspect of disease control and acute treatment toxicity.

Materials and Methods

The medical records of all patients treated with CSI in supine position between July 2007 and December 2008 at Division of Radiation Oncology, Department of Radiology, Siriraj Hospital were retrospectively reviewed. This study was approved by Siriraj Ethical Committee (Si202/2010)

Radiation Therapy

For simulation, all patients were in supine position with neck extended to avoid radiation to mandible. Patients were immobilized by customized thermoplastic mask for head and styrofoam pad for trunk. Axial computed tomography images were obtained with a 5-mm slice thickness for entire craniospinal axis by Philips CT simulator. All data then were tranfered to treatment planning system (Eclipe version 8.1, Varian Medical Systems, Palo Alto, CA) for 3 -dimensional technique using lateral opposed cranial fields and posterior spinal fileds. Half beam block technique of cranial field with isocenter setting on midline and midplane at level of C3-C5 based on anatomy of patients were introduced. Collimators of cranial fields were rotated until completely matched with the divergence of posterior spinal field. For patients with spinal length more than 40 cm, the spinal field was split into 2 fields using 2 isocenters technique. The upper field still was asymmetric field with isocenter at 20 cm fixed distance from isocenter of cranial field. For the lower field, moving gap junction technique using asymmetric field was proposed to reduce overdose at field junction. Location of lower isocenter was determined at 10-15 cm from upper isocenter for the acceptable dose distribution at gap junction.The gap junction were moved 4 times at every 3 cm during whole course of RT as shown in Figure 1.

Chemotherapy

All patients with medulloblastoma received CSI followed by chemotherapy. Only weekly vincristine was given concurrent with RT. For patients with intracranial germ cell tumor and acute leukemia, chemotherapy was given before CSI.

Treatment response and toxicity

Treatment response were evaluated as complete remission (CR) or partial remission (PR) at 1 month after complete CSI. Acute treatment-related toxicity were evaluated according to Common Toxicity Criteria Adverse Event V.3.0 during CSI to 1 month after complete CSI. The guidelines

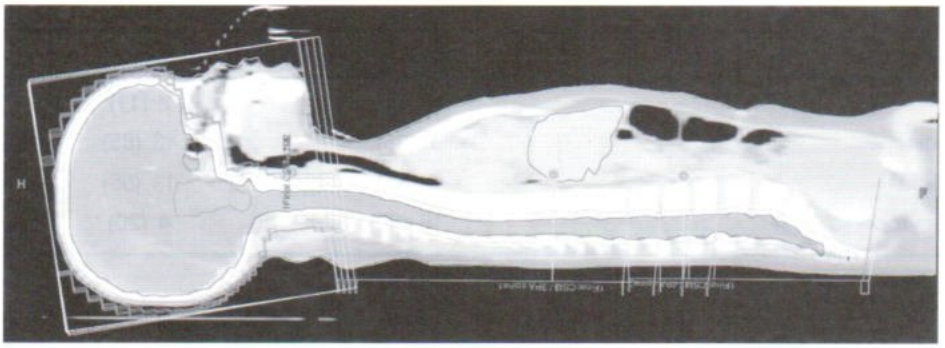

Fig.1 Mid-saggittal plane of patient treated with CSI in supine position. The gap junction were moved 4 times at every 3 cm during RT.

for interruption of RT were absolute neutrophil count <1.0x10 /L or platelet count <50x10/L.

Results

Total of 20 patients were identified in this study. Patient characteristics were shown in Table 1.

At a median follow-up 23.5 (range 3-35) months, 13 (65%) patients with CR and 7 (35%) patients with PR were documented respectively. Neither intracranial nor spinal failure developed in any patient. No distant failure was found. One patient with acute lymphoblastic leukemia and one patient with mixed germ cell tumor died from septicemia at 2 and 8 months after complete CSI respectively.

The pattern of acute hematologic toxicity were shown in Table 2.

Treatment interruption due to hematologic toxicity during CSI lasting 1-3 days were developed in 3 patients. Two patients were interrupted for more than 3 days. Skin toxicity showed no Grade 3-4.

Discussion

CSI in supine position have been investigated in many institutions due to practical advantages over

Table 1 Patient characteristics

Characteristics		No. of patients
Median age (year)		10 (range 2-46)
Gender	- Male	12
	- Female	8
Histology	- Medulloblastoma	9
	- Intracranial germ cell tumor	4
	- Acute leukemia	7
Median dose for CSI (Gy)		36 (range 21.6-39.6)
Median dose for primary tumor (Gy)	- Medulloblastoma	55.8
	- Intracranial germ cell tumor	54

Table 2 Acute hematologic toxicity

Toxicity	Gr1-2 (%)	Gr3-4 (%)
Anemia	18 (89)	2 (11)
Leucopenia	7 (35)	13 (65)
Neutropenia	9 (45)	11 (55)
Thrombocytopenia	16 (80)	4 (20)

traditional prone position[1-4]. Thses included patient comfort,high reproducibility and low risk for anesthesia. Matching technique for craniospinal and spinal spinal junction in CSI is important part of this complicated RT technique to prevent under or overdosage.Collimator rotation of lateral opposed cranial fields to match the divergence of posterior spinal fields is commonly used method. However, supine position does not permit direct observation for craniospinal and spinal spinal junctions so CT-based technique has to be used. With a median follow-up 23.5 months, no disease failure occurred at craniospinal or spinal spinal junctions from CSI in this study.

Some lliterature using supine position for CSI have been published. Huang et al reported on 14 medulloblastoma patients using CT-based technique. Two patients recurred in brain but no one recurred at craniospinal or spinal spinal junctions with median follow-up 32.4 months.Lymphopenia grade 3-4 was found in all[5]. South et al reported on 23 patients receiving supine CSI using intrafractional junction shift and field in field dose shaping.With median follow-up time 20.2 months, 5 failures occurred but not in junctions[6]. Alternative delivery methods for CSI have been used such as helical tomotherapy or proton-based technique[7-9].

Acute hematologic toxicity in this study were higher than those from CSI in prone position.Chang et al showed 32, 22 and 4 % leucopenia,neutropenia and thrombocytopenia respectively from mean dose photon 32 Gy for CSI in pediatric patients.[10]

Longer follow -up is needed for late treatment-related toxicity .Spinal intensity modulated RT have been investigated to improve target homogeneity by Panandiker et al. No neurotoxicity attributable to matching of craniospinal or spinalspinal junctions occurred.[11]

Conclusion

CSI in supine position is an alternative technique for RT in tumor with risk of leptomeningeal involvement. No disease failure occurred at craniospinal and spinal spinal junctions in this study but some Grade 3-4 hematologic toxicity were found.

References

1. Parker WA, Freeman CR. A simple technique for craniospinal radiotherapy in the supine position. Radiother Oncol. 2006 Feb;78(2):217-22.
2. Chang EL, Wong PF, Forster K, Petru A, Kowalski A, Maor M. Verification techniques and dose distribution for computed tomographci planned supine craniospinal radiaiton therapy.Med Dosimetry 2003,28,127-31.

3. Rades D,Baumann R,bremer M,Leuwer M,KarstenJ. Application of a new verification technique allowing craniospinal irradiation in supine position. Rad Oncol 2001;2:215-7.
4. Bauman G, Wong E, Trenka K, Scott D.A simple technique for craniospinal radiotherapy in the supine position Radiother Oncol. 2006 Sep;80(3):394. Epub 2006
5. Huang F, Parker W, Freeman CR. Feasibility and early outcomes of supine-position craniospinal irradiationPediatr Blood Cancer. 2010;54(2):322-5.
6. South M, Chiu JK, Teh BS, Bloch C, Schroeder TM, Paulino AC. Supine craniospinal irradiation using intrafractional junction shifts and field-in-field dose shaping: early experience at Methodist HospitalInt J Radiat Oncol Biol Phys. 2008;71(2):477-83.
7. Parker W, Brodeur M, Roberge D, Freeman C. Standard and nonstandard craniospinal radiotherapy using helical TomoTherapy.Int J Radiat Oncol Biol Phys. 2010;77(3): 926-31.
8. Sharma DS, Gupta T, Jalali R, Master Z, Phurailatpam RD, Sarin R.High-precision radiotherapy for craniospinal irradiation: evaluation of three-dimensional conformal radiotherapy, intensity-modulated radiation therapy and helical tomotherapy. Br J Radiol. 2009;82(984):1000-9.
9. Peñagarícano J, Moros E, Corry P, Saylors R, Ratanatharathorn V. Pediatric craniospinal axis irradiation with helical tomotherapy: patient outcome and lack of acute pulmonary toxicity. Int J Radiat Oncol Biol Phys. 2009; 75(4):1155-61.
10. Chang EL, Allen P, Wu C, Ater J, Kuttesch J, Maor MH. Acute toxicity and treatment interruption related to electron and photon craniospinal irradiation in pediatric patients treated at the University of Texas M. D. Anderson Cancer Center.Int J Radiat Oncol Biol Phys. 2002;52(4):1008-16.
11. Pai Panandiker A, Ning H, Likhacheva A, Ullman K, Arora B, Ondos J, Craniospinal irradiation with spinal IMRT to improve target homogeneity. Int J Radiat Oncol Biol Phys. 2007;68(5):1402-9.

THE ASEAN JOURNAL OF RADIOLOGY 2010; 16(3): 200-205

Original Article

Outcome of Radioiodine Treatment by Using 4-Hour I-131 Uptake Value for Dose Calculation in Graves' Disease

Kanaungnit Kingpetch, MD.

Division of Nuclear Medicine, Department of Radiology, Faculty of Medicine, Chulalongkorn University, Bangkok, Thailand.

Abstract

Objective: To evaluate outcome of radioiodine treatment by using 4-hour I-131 uptake value for calculation therapeutic dose for patients with Graves'disease.

Materials and Methods: We studied 122 Graves' disease patients with hyperthyroidism. The 4-hour ^{131}I uptake was done in each patient, the 24- hour ^{131}I uptake was estimated from the equation: *predicted 24 hr ^{131}I uptake = 36.7764 + 0.518 (4 hr ^{131}I uptake)*. The RAI treatment dose was calculated using the formula based on estimated thyroid size and predicted 24-hour ^{131}I uptake. We determined thyroid status of these patients at 1 year after the treatment.

Results: Ninety - five patients (77.9%) were euthyroidism or hypothyroidism at 1 year after treatment, and Twenty-seven patients (21.1%) had persistent hyperthyroidism. The patients who had persistent hyperthyroidism had larger thyroid gland ($P < 0.001$) and higher 4- hr ^{131}I uptake value ($P = 0.003$). We found the outcome of treatment of our study were similar to the outcome of other studies that used other regimens in the treatment of Graves' disease patients with ^{131}I.

Conclusion: Radioiodine treatment (^{131}I) based on 4- hour ^{131}I uptake is an effective treatment for patients with Graves' disease. This approach is safe, simple and convenience for the patients.

Keyword: Hyperthyroidism, Early I-131 uptake

Introduction

Radioactive iodine (^{131}I) has been used for treatment of hyperthyroidism more than 60 years.[1] Currently, it is the most common treatment for Graves' disease.[2] Radioiodine therapy is generally safe, with only harmless side - effects and having a high cost/benefit ratio.[3] A number of therapeutic dosing regimens have been proposed ranging from those based on high precision dosimetry, to a large or fixed doses of ^{131}I intended to cause euthyroidism or hypothyroidism after ^{131}I treatment.[4] Regarding the dose calculation, the most widely used is to calculate the radioiodine dose in microcuries (μCi) per gram of thyroid tissue. The calculation requires an estimated thyroid weight, the dose to be delivered per gram and 24-hour radioactive iodine uptake (RAIU). This method requires the patient has to come for measurement of RAIU for two days. The inconvenience and expense associated with 2 - day test had led many hospitals to use early uptake (3 to 6 hours) of ^{131}I for calculated therapeutic dose.[5-8] This would permit same day uptake measurement and therapy, thus reducing the cost and inconvenience of 2 - days examination.

The purpose of this prospective study was to assess the outcome of treatment by using 4- hour ^{131}I uptake value in the calculation of the treatment dose of radioactive iodine in Graves' disease patients.

Materials and Methods

Patients

One hundred and twenty - nine patients with Graves' disease were recruited in this study. All patients were diagnosed with Graves' disease based on their clinical findings, including the present of hyperthyroidism and a diffuse goiter without nodule and high level of serum thyroid hormones.

Recorded information included : age at the time of therapy , gender ,thyroid weight by palpitation, radioiodine (^{131}I) uptake at 4 -hour, administered ^{131}I treatment dose. Antithyroid drug was discontinued for at least 7 days before ^{131}I administration.

Methods

All patients (n = 129) were given an oral dose of ^{131}I approximately 20 μCi each orally. Radioactive iodine uptake was then performed after 4 hours using a single probe counting system consisting of sodium iodine crystal and single channel analyzer (Quadra 605, Macintosh Corp.). Then we used an equation : **predicted 24 hr ^{131}I uptake = 36.7764 + 0.518 (4 hr ^{131}I uptake)**, to estimated 24- hour ^{131}I uptake based on measured 4-hour ^{131}I uptake[8]. These predicted 24-hour ^{131}I uptake was then used to calculate the therapeutic doses of ^{131}I to be given to the patient. The therapeutic doses were calculated using the following formula; **^{131}I therapeutic dose (mCi) = 100 μCi/gm X thyroid gland weight (gm) X 1000 / (predicted 24 hr ^{131}I uptake) X 100.** In some patients ,antithyroid medications (PTU, MMI) were restarted at least 5 days following the ^{131}I therapy. No patient had thyroid tenderness or thyroid storm in the first 3 months after the therapy.

Follow up after ^{131}I therapy

The patient treatment outcome was patient's thyroid status within 1 year after ^{131}I therapy. A satisfactory outcome is either stable euthyroidism or permanent hypothyroidism. A euthyroid outcome was defined as normal serum FT_3 or FT_4 and TSH concentrations without any medication at 1 yr. A hypothyroid outcome was defined as biochemical evidence of inadequate thyroid hormone production (elevated serum TSH) requiring long - term thyroid

hormone replacement. Hyperthyroidism was defined as elevated serum FT_3 and suppressed TSH, with or without the patient continued to require antithyroid medication or further ^{131}I treatment.

Statistical analysis

Descriptive statistic data for dermographics were presented as the mean ± SD. Univariable analysis for continuous data used Unpair t tests and for category data used Fisher's exact test. Multivariable analysis used binary logistic regression for predict failure rate outcome. Significance was accepted when P value < 0.05.

Ethic

This study protocol was approved by Ethic Committee of the Faculty of Medicine, Chulalongkorn University, Bangkok, Thailand.

Result

Of the 129 patients, we were able to obtain follow - up data for 122 patients (94.57%). Their baseline characteristics were shown in Table 1. The average age was 37.5 yr and the female to male ratio was 5 : 1. Thyroid gland weight average approximately 53 gm, the average 4-hr ^{131}I uptake was 56% and the average predicted 24-hr ^{131}I uptake was 66%. The average therapeutic dose of ^{131}I was 8.1 mCi (300 MBq).

Table 2 shows outcomes of ^{131}I treatment at 1 yr. Ninety - five patients (77.9%) were successfully treated (hypothyroidism or euthyroidism), and 27 (22.1%) remained hyperthyroid at 1 year. Of those successfully treated, over 90% responed to ^{131}I therapy within the first 6 months, as judged by biochemical analysis, symptom improvement and/or no requirements for antithryoid medication; the remainder responded within the first year.

The three factors (gender, thyroid weight and 4-hr ^{131}I uptake) were identified by binary logistic regression as effective factors for the outcome of ^{131}I therapy in these hyperthyroid patients. The adjusted odd ratio for gender was 3.57 (CI = 1.054-12.095), thyroid weight was 1.06 (CI = 1.032-1.090) and 4-hr ^{131}I uptake was 1.031 (CI = 1.001-1.063).

Two patients had transient hypothyroidism followed by recurrent hyperthyroidism (Table 3). These patients had low serum FT_4 and elevated

Table 1 Characteristics of 122 patients

Age (years)	37.5 ± 12.3
Sex	
Males	20 (19.6%)
Females	102 (80.4%)
Thyroid weight (gm) *	53.6 ± 29.7
4 hr ^{131}I uptake (%)	56 ± 18.3
Predicted 24 hr ^{131}I uptake (%) **	66 ± 13.4
Dose ^{131}I treatment (mCi) ***	8.1 ± 3.9

* Evaluated thyroid weight by palpation

** Calculated from an equation : predicted 24 hr ^{131}I uptake = 36.7764 + 0.518 (4 hr ^{131}I uptake)

*** Calcualted using the formula : Dose ^{131}I treatment (mCi) = 100 μCi/gm X thyroid weight (gm) X 1.000 / (predicted 24 hr ^{131}I uptake) X 100

serum TSH concentration at 3 months after the ^{131}I therapy in the absence of antithyroid drug. Then they had a spontaneous recurrent thyrotoxicosis at 6 months after the ^{131}I therapy.

Characteristics of patients with persistent hyperthyroidism:

Compared with the patients treated successfully, the patients who has persistent hyperthyroidism were male, had larger thyroid size, higher 4-hr and predicted 24-hr ^{131}I uptake value and higher dose of ^{131}I treatment. The age was the same in both groups.

Discussion

The effectiveness of ^{131}I treatment depends on multiple factors including iodine uptake, effective half - life of the iodine in the gland, distribution of radioactivity within tissue and radio - sensitivity of follicular cells. Five approaches for therapeutic dose calculation for patients with Graves' disease have been employed.[9]

Table 2 Outcome of ^{131}I treatment at 1 yr (n = 122 patients)

	Successful treatment n=95 (77.9%)	Treatment failure n=27 (22.1%)	P value
Age (years)	37.3 ± 11.9	38.2 ± 13.6	0.747
Gender (female/male)	7.6/1	1/1	0.015
Thyroid weight (gm) *	45.4 ± 16.5	82.7 ± 44.7	<0.001
4 hr. ^{131}I uptake (%)	53 .5 ± 17.5	65.3 ± 18.8	0.003
Predicted 24 hr ^{131}I uptake (%) **	64.7 ± 9.2	70.6 ± 9.8	0.005
Dose ^{131}I treatment (mCi) ***	7.1 ± 2.2	11.8 ± 6.0	0.001

* Evaluated thyroid weight by palpation

** Calculated from an equation: predicted 24 hr ^{131}I uptake = 36.7764 + 0.518 (4 hr ^{131}I uptake)

*** Calcualted using the formula: Dose ^{131}I treatment (mCi) = 100 μCi/gm X thyroid weight (gm) X 1000 / (predicted 24 hr ^{131}I uptake) X 100

Table 3 Baseline characteristics, ^{131}I uptake ,treatment dose and serum thyroid hormones after ^{131}I treatment in two patients who had transient hypothyroidism

	Patient No.1	Patient No.2
Gender (female or male)	female	male
Age at treatment (yr)	32	54
Thyroid weight (gm)	70	85
4 hr ^{131}I uptake (%)	54	71
Predicted 24 hr ^{131}I uptake (%)	65	74
Dose ^{131}I treatment (mCi)	10	12
Serum TSH at 3 months after ^{131}I treatment	24	70
Serum FT4 at 3 months after ^{131}I treatment	0.7	0.1

1. small doses repeated as necessary;
2. a large ablative dose;
3. a "sliding scale" based on thyroid size;
4. a standard formula for administered dose based on estimated thyroid size;
5. precise dosimetry for the administered dose.

The most common method in dose determination employs a formula based on estimated thyroid size and 24 -hour RAIU as used in this study.

Hayes AA et al.[6] studied a group of 27 hyperthyroid patients with Graves' disease using a logarithmic regression equation which was developed to predict 24- hour ^{131}I uptake from the 4-hour ^{131}I uptake[5]. They obtained a high correlation between the predicted 24-hour ^{131}I uptake (PUp) and the actual 24-hour ^{131}I uptake ($r = 0.94$). Hennessy JV et al. also studied a group of 51 hyperthyroid patients with Graves' disease using early ^{131}I uptake and reported that the predicted 24-hour ^{131}I uptake correlated well with the actual 24-hour ^{131}I uptake ($r = 0.73$) and the correlation of calculated doses obtaining from the predicted and the actual 24-hour ^{131}I uptake were highly significant ($r = 0.91$).

According to our former study conducted in a group of 160 Graves' disease patients[8], we found high correlation between the predicted 24- hour ^{131}I uptake and the actual 24-hour ^{131}I uptake ($r = 0.73$); the correlation between therapeutic doses based on the predicted 24-hour ^{131}I uptake and the actual 24- hour ^{131}I uptake is 0.92.

In this study, we established the outcome of ^{131}I treatment by using 4-hour ^{131}I uptake value in the calculation of the treatment dose. We concluded that the goal of therapy is euthyroidism or hypothyroidism within 1 year of therapy. Our results show the efficacy of this protocol, at 1 year after treatment we found 77.9% of Graves' disease patients have successful treatment. These results were similar to the other studies that were performed to evaluate the effectiveness of ^{131}I therapy by used the actual 24-hr ^{131}I uptake to calculate the treatment dose.[10-12]

We found that patients with persisted hyperthyroidism had a larger thyroid gland, higher 4-hor and predicted 24-hour ^{131}I uptake value, compared to those who became hypothyroidism or euthyroidism. Two patients (1.6%) had transient hypothyroidism followed by recurrent hyperthyroidism. Other studies have reported similar findings in 1-6% of patients treated with radioactive iodine had transient hypothyroidism.[13-15]

In summary, ^{131}I therapy based on 4-hour radioiodine uptake is an effective treatment for patients with Graves' hyperthyroidism. The advantage of this method is that the uptake and ^{131}I therapy can be performed within the same day; therefore, it is convenience, simple and safe for the patients.

Acknowledgments

We are indebted to Prof. Dr. Makumkroung Poshyachinda for helpful comments and assistance in the review of this manuscript.

This work was supported by the Ratchadapiseksompotch Fund, Faculty of Medicine, Chulalongkorn University.

References

1. Sawin CT, Becker DV. Radioiodine and the treatment of hyperthyroidism: the early history. Thyroid 1997;7: 163-76.
2. Soloman B, Glinoer D, Lagasse R, Wartofsky LN. Current trends on the management of Graves' disease. J Clin Endocrinal Metab 1990;70:1518-24.

3. Dietlein M, Lauterbach KW, Schicha H. Treatment of toxic nodular goiters: comparative costing of radioiodine therapy and surgery. Exp Clin Endocrinol Diabetes 1998;106 (Suppl 4):S66-S70.
4. Franklyn JA, Daykin J, Drole Z, Farmer M, Sheppard MLN. Long term follow up of treatment of thyrotoxicosis by three different methods. Clin Endocrind (Qxf) 1991;34:71-6.
5. Hayes AA, Akre CM, Garman CA . Iodine - 131 treatment of Graves' disease using modified early iodine-131 uptake measurement in therapy dose calculation. J Nucl Med 1990;31:519-22.
6. Hennessey JV, Berg LA, Ibrahim MA, et al . Evaluation of early (5 to 6 hours) Iodine - 123 uptake for diagnosis and treatment planning in Graves' disease. Arch Intern Med 1995;155:621-24.
7. Usha SV, Francis BA, Harvey AZ. Therapy dose calculation in Graves' disease using early I-123 uptake measurements. Clin Nucl Med 1996;21:102-05.
8. Kingpetch K, Poshyachinda M. Dose calculation using 4-hour I-131 uptake for retreatment radioiodine therapy of patients with Graves' disease .Asean J Radio 2003;9: 63-8.
9. Shapiro B. Optimization of radioiodine therapy of thyrotoxicosis: what have we learned after 50 years?. J Nucl Med 1993;34:1638-41.
10. Alexander EK, Larsen PR. High dose ^{131}I therapy for the treatment of hyperthyroidism caused by Graves' disease. J Clin Endocrinal Metab 2002;87:1073-77.
11. Leslie WD, Peterdy AE , Dupont JO. Radioiodine treatment outcomes in thyroid glands previously irradiated for Graves' hyperthyroidism. J Nucl Med 1998;39:712-6.
12. Solomon B, Glinoer D, Lagasse R, Wartofsky L. Current trends in the management of Graves' disease. J Clin Endocrinol Metab 1989;70:1518-22.
13. Sawers JS, Toft AD, Irvine WJ, Brown NS, Seth JN . Transient hypothyroidism after iodine - 131 treatment of thyrotoxicosis. J Clin Endocrinal Metab 1980;50:226-9.
14. Aizawa Y, Yoshida K, Kaise N, Fukazawa H, Kiso Y, Sayama N, Hori H, Abe K. The development of transient hypothyroidism after iodine - 131 treatment in hyperthyroid patients with Graves' disease: prevalence, mechanism and prognosis. Clin Endocrinal (Oxf) 1997;46:1-5.
15. Gomez N, Gomez JM, Orti A, Gavalda L, Villabona C, Leyes P, Soler J. Transient hyothyroidism after iodine - 131 therapy for Graves' disease. J Nucl Med 1995;36: 1539-42.

THE ASEAN JOURNAL OF RADIOLOGY 2010; 16(3): 206-221

Original Article

Safety and Efficacy of Percutaneous Fiducial Marker Implantation for Image-guided Radiation Therapy; Initial experience in Ramathibodi Hospital

Tanapong Panpikoon, MD., Banjongsak Wedsart, MD.
Jiemjit Tapaneeyakorn, MD., Thanipa Inman, MD.

Division of Body Interventional Radiology, Department of Radiology, Ramathibodi Hospital

Abstract

Purpose: To evaluate the safety and technical success rate of percutaneous fiducial marker implantation in preparation for image-guided radiation therapy.

Materials and Methods: From January 2009 to September 2009, we retrospectively reviewed 21 percutaneous fiducial marker implantations by interventional radiologist in 20 patients. Of the 21 implantations, 3 were in the lung, 9 were in the prostate gland, 8 were in the liver and one was in the pancreas. Procedure-related major and minor complications were documented. Technical success was defined as implantation enabling adequate treatment planning and computed tomographic simulation.

Results: The major and minor complication rates were 4.8% and 19.1%, respectively. Pneumothorax after lung implantation was the most common complication. Pneumothoraces were seen in 2 of the 3 lung implantations (66.6%); a chest tube was required in one of three the lung transplantations. Of the 21 implantations, 17 were successful (80.9%); in 1 implantation at the lung the fiducial markers migrated. However, it not required additional procedures or more implantation.

Conclusions: Percutaneous implantation of fiducial marker at the liver, pancreas and prostate gland is a safe and effective procedure with risks that are similar to those of conventional percutaneous organ biopsy. However, lung implantation is high risk to the pneumothorax that may require chest tube.

Introduction

The advance technology of tumor localization radioation therapy has enabled the use of stereotactic radiation therapy in the treatment of extracranial and extraspinal tumor. The CyberKnife (Accuray, Sunnyvale, California) is one such technology that delivers frameless precision radiation therapy. To track tumor position throughout the respiratory cycle, radiopaque gold markers called "fiducial" markers must be implanted in around the tumor. The fiducial markers act as internal radiological landmarks and move with a constant relationship to the targeted tumor during therapy for the precise delivery of radiation (Figure 1A, 1B & 2). The purpose of this retrospective study was to describe the safety and technical success rate of percutaneous fiducial marker implantation in extracranial locations such as the lung, liver, pancreas and the prostate gland, which performed by interventional radiologist.

Materials and Methods

This retrospective study was granted by the institutional review board. Data were collected from January 2009 to December 2009. 20 patients (mean age, 69.4 years; age range, 49-87 years) underwent 21 procedures

One patient underwent implantations on two separate occasions for anatomically distinct tumors

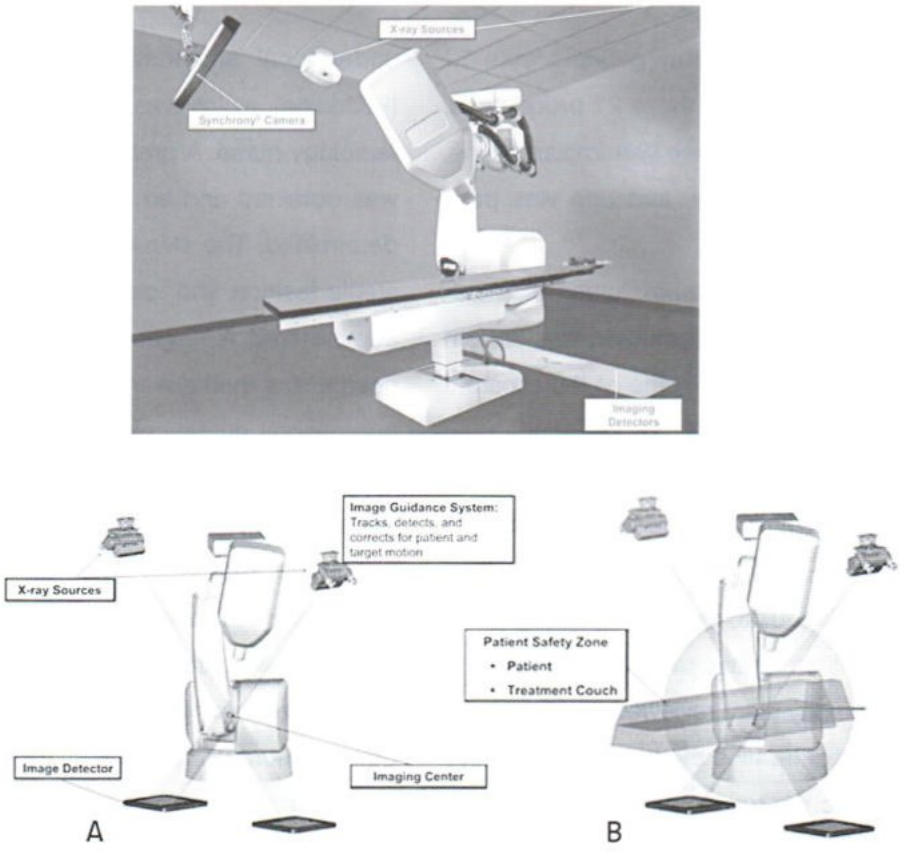

Fig.1 (A&B) CyberKnife and image guidance system

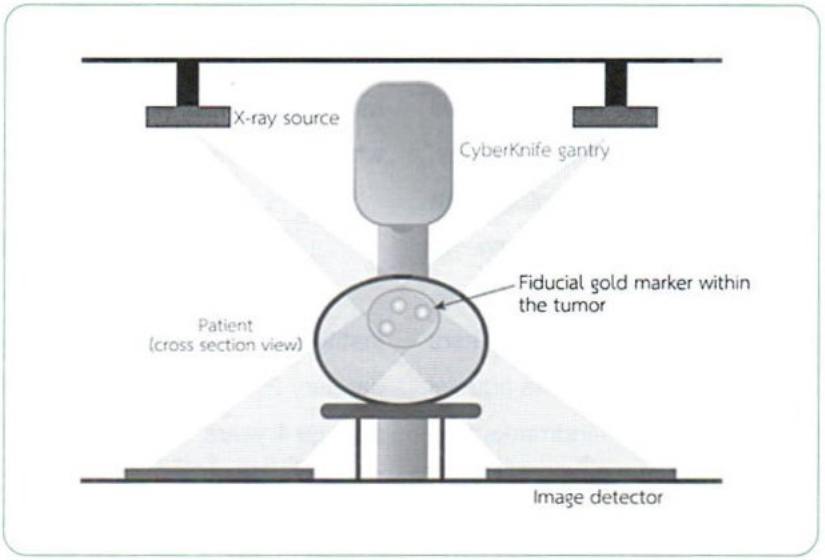

Fig.2 Cross-sectional illustration of the CyberKnife system and demonstrated fiducial gold maker implantation or targeted treatment.

at the liver and pancreas. Twenty patients were 19 men and one was women. Of these 21 procedures, 3 were lung implantations, 8 were liver implantations, 9 were prostatic implantations and one was pancreatic implantation.

The mean overall maximum tumor diameter with exclude the prostatic implantation was 2.9 cm (range 1-5.9 cm). The mean volume of the prostate glands were 67.1 cc (range 24-126 cc).

All cases were discussed at their respective tumor boards and were deemed unresectable or failure for other modality. The patients were then evaluated by the diagnostic radiologist to determine their suitability for stereotactic radiation therapy. The interventional radiology team reviewed the diagnostic imaging studies to determine the best percutaneous needle approach to the tumor. All procedures were performed by using computed tomography (CT) and ultrasound (US) with additional fluoroscopy.

Procedures were performed with the patient under local anesthesia with pain reduced drug (Pethidine), which was administered by a registered radiology nurse. A preliminary unenhanced CT scan was obtained and an appropriate needle trajectory determined. The skin entry site was prepared in a sterile fashion and local anesthesia (lidocaine 1%) administered. A 19-gauge thin-wall coaxial introducer needle was then advanced into the lesion under CT fluoroscopy guidance.

The prostatic implantation was performed under transrectal approach (Figure 7A). A rapid absorbed antibiotic such as ciprofloxacin was administrated in one dose just before and in several doses following the procedure. The cleansing enemas before performing fiducial implantation were also done. Patient on anticoagulatory agents (Aspirin or Warfarin) were no undergo procedure until these drugs had been discontinues. Local anesthesia was used during procedure. This was injected into the neurovascular bundles at base of the prostate gland.

After anesthetic procedure, three to four cylindrical fiducial markers measuring 0.8 mm in diameter and 5 mm in length were deposited via the 19-gauge coaxial introducer needle. The fiducials were introduced into the coaxial needle by using a curved hemostat and advanced into the lesion by using the trochar of the introducer needle.

Because the CyberKnife uses orthogonal x-rays at 45° to vertical to track the tumor and fiducial markers, the markers must be placed in a noncollinear array in different sectors of the tumor to define a three dimensional space enclosing the tumor. Unenhanced CT was performed at the end of procedure to evaluate for immediate complications and confirmed position of these fiducials. In case of implantation with US guidance was performed. The plan radiographic with AP, both obliques (45°) and lateral views was also done for determine the proper position of the fiducial markers.

Patients without any complications were monitored for 12-24 hours and then discharged from the hospital. Patients with complications were admitted for observation and appropriate treatment planning with CT simulation was done a minimum of 7 days after implantation to allow for the resolution of tissue inflammation and fiducial marker migration (Figure 7B &7C).

A custom-made immobilization and proper position of devices were prescribed. The criteria for proper position of the fiducial marker were described as follow (Figure 3 & 4).

1. Minimum 3 fiducial required
2. Minimal distance between fiducial more than 20 mm.
3. Set the minimal angle between three fiducial more than 15 degree for each angles (not colinear placement) (Figure 4).
4. Distance between fiducial marker and target not more than 50-60 mm.

The CT simulation images were transferred to the CyberKnife treatment planning system. The tumor volume and adjacent crucial structures were outlined, and an appropriate radiation dose was prescribed by radiation oncologist.

The fiducial markers were identified on the images, allowing the guidance system to calculate the exact location of the tumor in relation to the fiducial markers and surrounding structures. A treatment plan was formed on the basis of this information, which was then translated to robotic control for the precise delivery of the therapeutic dose.

Complications were documented by using the SIR clinical practice guidelines[1].

A major complication was defined as that requiring therapy with hospitalization for less than 48 hours, major additional therapy, or an unplanned increase in the level of care or hospitalization for more than 48 hours and that causing permanent adverse sequelae or death.

A minor complication was defined as that requiring no or nominal therapy, including overnight hospitalization for observation with no permanent consequence[1].

Technical success was defined as implantation that enabled adequate tracking of the tumor during all phases of respiration for treatment planning and CT simulation. For this, at least three non-collinear fiducials had to be present and adequately visualized on the digitally reconstructed radiographs obtained by the two orthogonal x-ray sources.

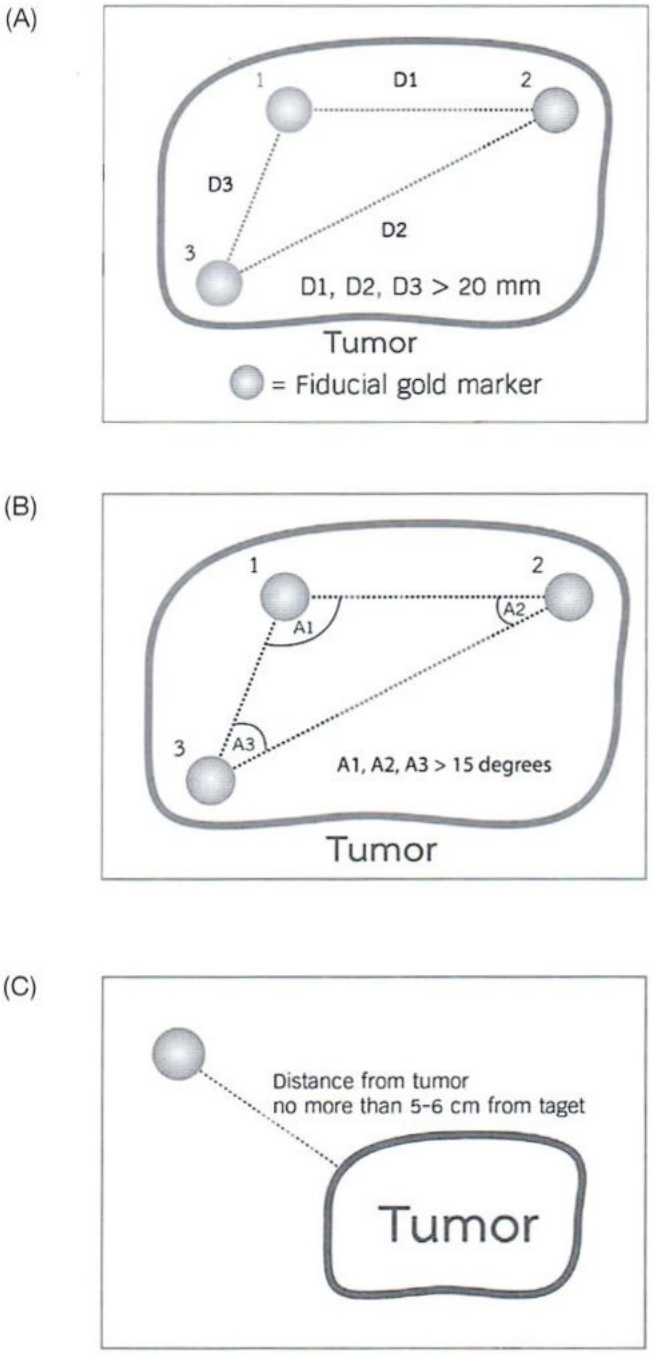

Fig.3 The criteria for proper position of the fiducial marker

A. Minimal distance between fiducial more than 20 mm.

B. Set the minimal angle between three fiducial more than 15 degree for each angles (not colinear placement)

C. Distance between fiducial marker and target not more than 50-60 mm.

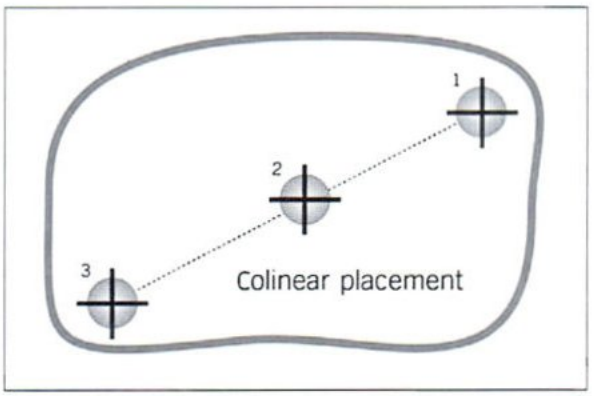

Fig.4 Three fiducial placement with not proper position (Colinear placement)

Results

Safety and Technical Success

The median number of fiducial markers implanted for each tumor was three (range, 2-4). There were no procedure-related deaths. Major complications occurred in one of the 21 implantations (4.76%).

Minor complications occurred in four patients (19.04%). Of the 21 implantations, 17 were technically successful; in one lung implantation (4.76%), the fiducial markers migrated into the pleural space. Three implantations in the prostate gland were too closed than 2 cm in distance, resulting difficult to radiation therapy. The results are summarized in table 1 & 2.

Lung Implantation

A total of three patients underwent lung implantation procedures. Major complications were seen in one of the three lung implantations (33.3%). The most common complications were pneumothorax. One patient (33.3%) was symptomatic and required placement of a chest tube. Localized pulmonary hemorrhage was observed in two patients (Figure 5). Two of three patients had a small amount of hemoptysis. However, none of the patients required additional treatment or transfusion. In one patient (33.3%), the one fiducial marker migrated into the pleural space and cannot ongoing the radiation therapy with cyberknife, which implanted under fluoroscopic guidance (Figure 6).

Liver Implantation

A total of 8 patients underwent liver implantation procedures. There were no major complications. No fiducial marker migration is observed. The entire fiducial markers located in the proper position with criteria as described above.

Pancreas Implantation

One patient underwent two separate procedures for two distinct tumors. He had history of

Table 1 Summary of Patient Demographics

Parameter	Value
Total fiducial marker implantation (n=20)	
Mean patien age	69.4 (49-87)
Sex	
No. of men	19 (95%)
No. of women	1 (5%)
Mean tumor size	2.9 cm (1-5.9)
Lung (n=3)	
Mean tumor size (cm)	3.1 (2.6-3.5)
Liver (n= 8)	
Mean tumor size (cm)	4.1 (2-5.9)
Pancreas (n= 1)	
Tumor size (cm)	4.5
Prostate gland (n=9)	
Mean prostate volume (cc)	67.1 (24-126)

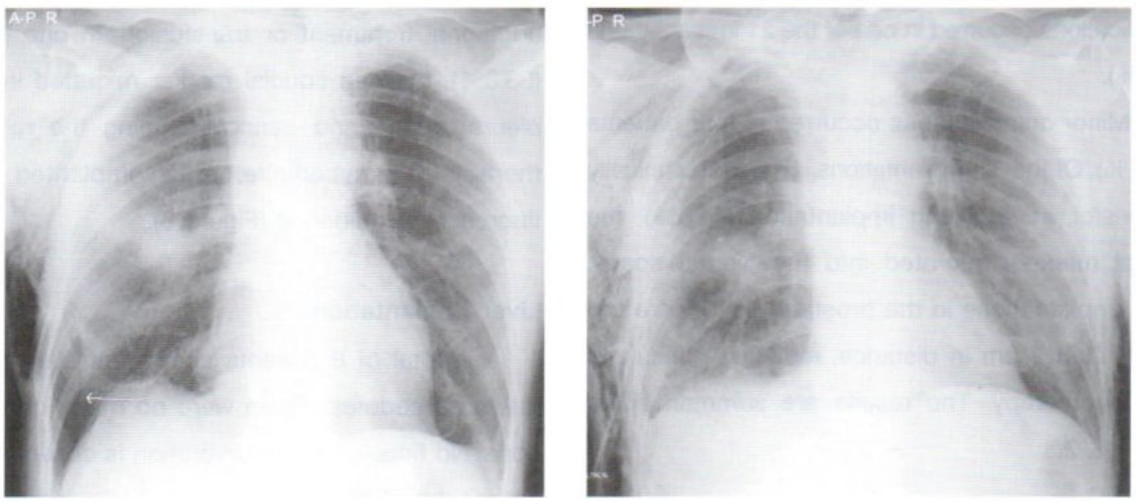

Fig.5 A 66-year-old male with history of recurrent CA lung, presented with severe pneumothorax after fiducial placement. ICD insertion was required for treatment.

Table 2 Summary of Complication and Outcome

Parameter	Value
Total procedure (n = 21)	
Complications	1 (4.8%)
Major	4 (19.1%)
Minor	17 (80.9%)
Technical success	
Lung procedure (n = 3)	
Complications	
Major	
Pneumothorax requiring chest tube	1 (33.3%)
Minor	
Pneumothorax not requiring chest tube	1 (33.3%)
Hemoptysis (not requiring blood transfusion)	3 (100%)
Pulmonary hemorrhage (not requiring blood transfusion)	1 (33.3%)
Technical success	2 (66.7%)
Liver procedure (n = 8)	
Complications	
Major	-
Minor	-
Technical success	8 (100%)
Pancreatic procedure (n = 1)	
Complications	
Major	-
Minor	-
Technical success	1 (100%)
Prostatic procedure (n = 9)	
Complications	
Major	-
Minor (minimal hemorrhage per rectum)	3 (33.3%)
Technical success	6 (66.7%)

colon cancer with liver and pancreatic metastasis. Two separate implantation procedures were performed, using three fiducials for each liver and pancreas. There is no major or minor complication for pancreatic implantation. No migration was detected.

Prostate Implantation

Nine patients with a mean age of 74.9 years (range 67-87 years) participated in this study. Fiducial placement under transrectal guidance was successful in all patients. A total of 34 fiducials were deployed in a four-quadrant manner outlining the prostate

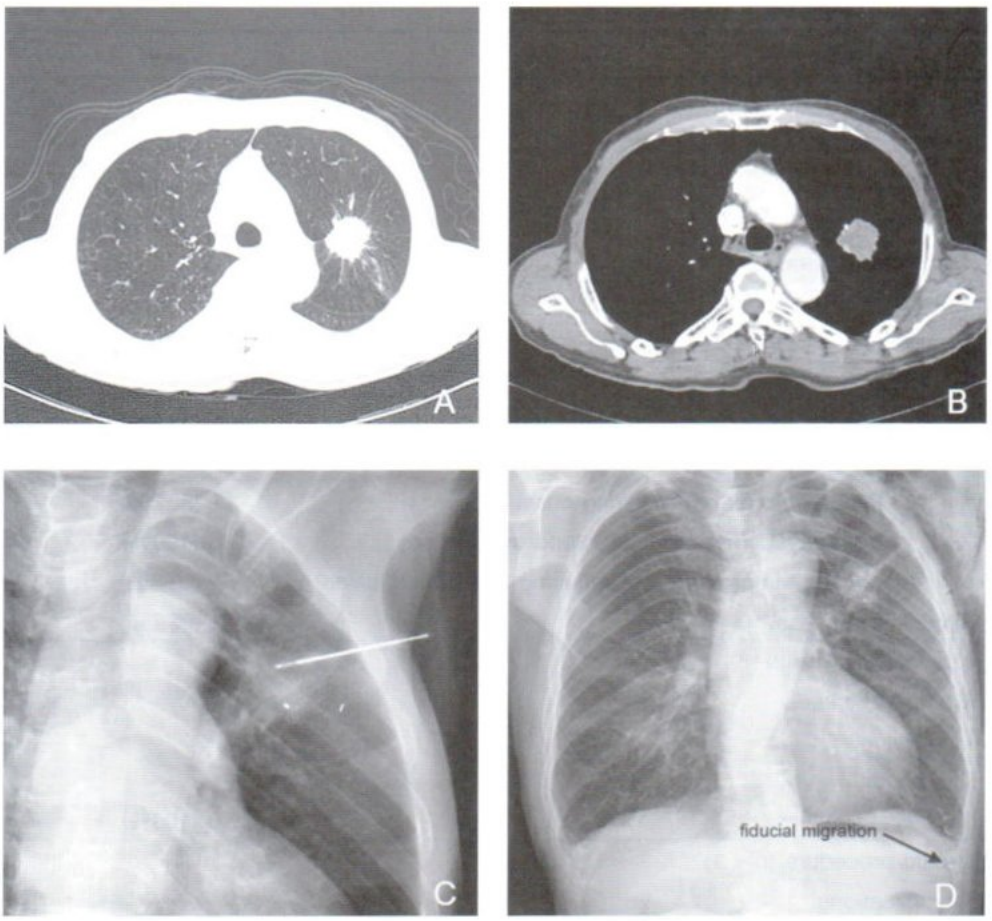

Fig.6 A 78-year-old male, known case of CA lung at LUL, was sent for fiducial placement (A&B). Successful implantation of four fiducial gold markers was performed (C). There was migration of one fiducial into pleural space after 1 week of follow up (D).

gland. There was no evidence of fiducial migration. However, there patients had minimal distance between fiducial less than 20 mm that not appropriate for the radiation therapy.

All patients tolerated the procedure well with minimal discomfort. No major complications occurred during the recovery period at 24 hours after the procedure. Three patients had minimal bleeding per rectum with spontaneous stop after procedures. No evidence of hematuria, dysurea or UTI was observed. There was no reported fiducial migration throughout the course of therapy because this was monitored daily through the comparison of the images acquired on each day of therapy with the initial planning CT.

Discussion

For more than half a century, principles of stereotaxy have been used in radiation therapy. Traditional stereotaxy requires rigid immobilization to establish spatial coordinates for precise guidance.

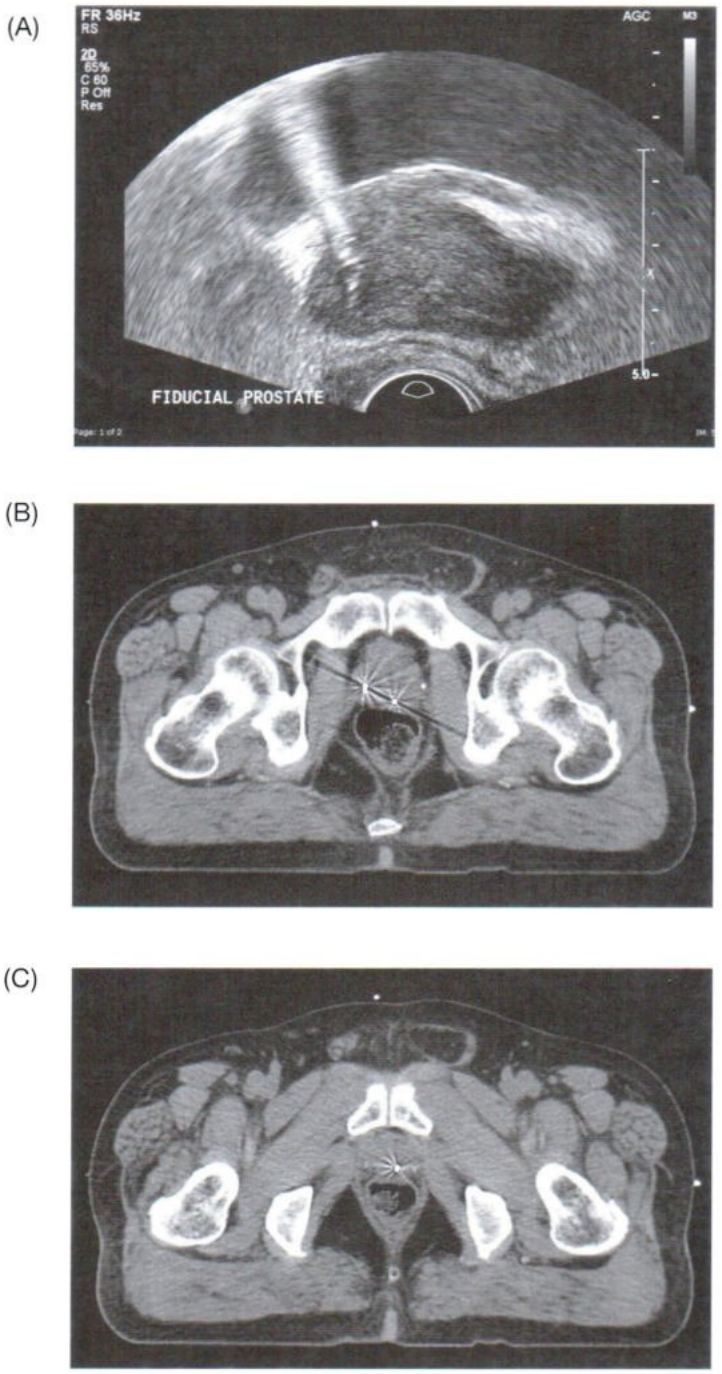

Fig.7 (A) Transrectal US image demonstrates fiducial deployment in the prostate gland. The fiducial marker appears as a hyperechoic, linear structure with an associated hyperechoic shadow. (B&C) Treatment planning with CT simulation was done a minimum of 7 days after implantation.

Table 3 Individual patient characteristic and demographic summary

Case No.	Sex	Age	Underlying/Pathology	Location	Tumor size*	Number of fiducial	Techinique	Major/ Minor complication	Fiducial migration	Fiducial position
1	M	71	CA sigmoid colon with liver & lung metastasis	LUL	2.6	4	CT guidance	-	No	Good
2	M	66	Recurrent CA lung S/P RUL & RML lobectomy	Right hilar region	3.1	3	CT guidance	Pneumothorax with ICD/ Lung hemorrhage	No	Good
3	M	78	Unresected CA lung	LUL	3.5	4	Fluoroscopic guidance	Minimal pneumothorax	Yes	Good for the rest fiducials
4	M	71	HCC	Segment IVa	2.0	4	US guidance	-	No	Good
5	M	76	Recurrent HCC S/P left hepatectomy	Segment VIII	3.7	4	US guidance	-	No	Good
6	M	75	HCC with failure TOCE	Segment II	4.0	3	US guidance	-	No	Good
7	M	56	Metastatic leiomyosarcoma	Segment VII	4.2	3	US guidance	-	No	Good
8	F	60	Liver metatasis	Segment VI	4.4	3	US guidance	-	No	Good
9	M	49	CA colon with liver & pancreatic metastases	Hepatic segment IVa & pancreatic head	4.0 & 5.2	6	US guidance	-	No	Good
10	M	54	HCC S/P TOCE & RFA	Segment VI	5.9	3	US guidance	-	No	Good
11	M	58	HCC S/P TOCE	Segment VII	3.4	3	US guidance	-	No	Good
12	M	82	CA prostate	Prostate gland	4.0x4.2x4.8	4	Transrectal US	-	No	Good
13	M	87	CA prostate	Prostate gland	3.5x4.2x3.9	4	Transrectal US	-	No	Good
14	M	67	CA prostate	Prostate gland	3.8x3.6x3.4	4	Transrectal US	minor localized hemorrhage	No	Good
15	M	76	CA prostate	Prostate gland	3.9x4.2x4.8	4	Transrectal US	-	No	Good
16	M	77	CA prostate	Prostate gland	3.4x1.5x1.8	4	Transrectal US	minor localized hemorrhage	No	Too close
17	M	70	CA prostate	Prostate gland	3x4.5x3.7	3	Transrectal US	-	No	Too close
18	M	72	CA prostate	Prostate gland	2.6x3.9x4.4	3	Transrectal US	-	No	Good
19	M	70	CA prostate with bony metatasis	Prostate gland	3.0x3.2x3.6	4	Transrectal US	-	No	Good
20	M	73	CA prostate	Prostate gland	4.6x3.8x3.6	4	Transrectal US	minor localized hemorrhage	No	Too close

Table 4 Specific Major Complication for Image-guided Percutaneous Biopsy (SIR recommendation)

Major Complications	Reported Rate (%)	Suggested Threshold (%)
Bleeding (requiring transfusion or intervention)		
Large needle (18-gauge or larger)	5-10	10
Small needle (19-gauge or smaller)	3	6
Fine needle (21-gauge or smaller)	0.1-2.0	2
Infection (requiring hospitalization or specific therapy)		
All biposy (sterile)	1	2
Prostatic biopsy (nonsterile)	2.5-3.0	6
Peritonitis (requiring hospitalization or specific therapy)		
Abdominal biopsies	1.5	2
Hemoptysis (requiring hospitalization or specific therapy)		
Lung biopsies	0.5	1
Pneumothorax (requiring chest tube)		
All biopsies (other than lung)	0.5	1
Lung biopsies	5	10

This can be achieved for intracranial and spinal targets with rigid frames but is limited for extracranial sites. The limitations of applying conventional systems to extracranial targets include respiratory and musculoskeletal motion due to patient discomfort. Image-guided radiation therapy systems have been developed that address the task of localization by tracking the target in real time without rigid immobilization.

CyberKnife is one such commercially available system. The CyberKnife combines tracking technology and robotics to offer frameless precision stereotactic radiation therapy. It consists of a lightweight linear accelerator (LINAC) specifically designed for radiation therapy. The second component of this system is real-time image guidance that eliminates the need for external fixation and immobilization. High-resolution digital images are acquired by a pair of orthogonally arranged x-ray radiography systems. The images are electronically registered to the digitally reconstructed radiographs derived from the treatment-planning CT scans. Difference in the anatomic translation and rotation in the three axes are measured by using computer algorithms. The complete process of image acquisition, registration, and compensation is automated and fast enough to provide real-time localization for extracranial applications[2,3]. Respiratory motion, however, is a challenge even for sophisticated robotics such as the CyberKnife. Several previous studies have demonstrated that thoracic and abdominal tumors move by several centimeters

during various phases of the respiratory cycle.

Tumors at the lung base in close proximity to the diaphragm can move up to 25 mm[4]. Pancreatic lesions can move up to 35 mm during respiratory cycles and liver lesions, especially those at the dome, can move similar distances[5]. Respiratory tracking for extracranial applications is essential to ensure that the entire tumor is treated without requiring a substantial increase in the volume of tissue treated. To track the tumor and allow the delivery of radiation throughout the respiratory cycle, a continuous respiratory tracking system called the Synchrony is used along with the standard components of Cyber-Knife for the treatment of thoracic and abdominal lesions.

The fiducial markers act as internal radiologic landmarks, maintaining a fixed relationship with the tumor and with each other. The relative movements of the chest wall and fiducial markers are used to calculate a predictive model that is continuously updated. With the ability to compensate for respiratory motion, stereotactic radiation therapy is rapidly gaining extracranial applications.

Image-guided radiation therapy has also been used in the treatment of primary and secondary liver tumors that are not fully amenable to interventions, such as transarterial chemoembolization and radiofrequency ablation; however, data about image-guided radiation therapy are limited. As the experience with extracranial image-guided radiation therapy grows, a greater number of radiology practices with interventional radiologist will be involved in fiducial marker implantation. Because of interventional radiologist has experience and familiar with technique of image-guided procedure.

In this study, we report our rate of technical success as well as the complication rate for percutaneous fiducial marker implantation.

Few reports exist on this; hence, comparisons are drawn from reported standards for percutaneous biopsies. Our overall major complication rate was 5%, which is within the reported range for percutaneous biopsies[6].

Most complications occurred in patients undergoing fiducial marker placement in a lung tumor. Of the 3 lung implantations, 33.3% developed a pneumothorax that required the placement of a thoracostomy tube. This rate is higher than that reported in the literature (5%) and is above the suggested threshold of 10%[6]. However, other studies that detail complications associated specifically with fiducial marker implantation for thoracic tumors have had pneumothorax and thoracostomy tube insertion rates similar to ours[7]. Previous studies have reported an incidence of pneumothorax as high as 49% in patients with chronic obstructive pulmonary disease after percutaneous biopsy[8]. Because most patients undergoing image-guided radiation therapy are poor surgical candidates due to their underlying poor lung function and general condition, the higher incidence of pneumothorax is not unusual.

Minimal localized pulmonary hemorrhage was seen in 66.6% of the cases; however, none of these patients required any additional therapy such as blood transfusion and the complication rate was well within the suggested SIR threshold (table 4)[6]. Technical challenges in fiducial marker implantation are also responsible for the higher frequency of pneumothoraces and local hemorrhage. For the orthogonal x-ray beams to identify the individual fiducial markers, the fiducial markers must be placed in three or four distinct quadrants. This requires manipulation of the needle within the lung parenchyma, which, in theory, could increase the risk of

local hemorrhage. Migration of the fiducial maker into the pleural space was observed in one patient who implanted under fluoroscopic guidance. Therefore one fiducial was implanted near the pleural space and consequence migration of the fiducial was observed in 7 days later. However, the radiation therapy planning was still processed because three fiducial markers with appropriated position were placed.

External skin markers and bony landmarks were traditionally used as surrogates for prostate position during the radiotherapeutic management of prostate cancer. It has been shown that the treatment margins used to compensate for daily organ motion and setup uncertainties could be as large as 1.5-2 cm if these surrogates were used[9]. These large margins are not compatible with the delivery of high radiation doses above 70 Gy that are used in current routine practice.

During recent years, imaging and localized techniques prior to and during the daily treatment delivery have allowed better localization of the prostate and tighter margins[10]. Implantation of fiducial markers into the prostate gland with image-based radiographic methods is technique that is increasingly being used for targeting. In this study, there were only minor complications with minimal bleeding per rectum in three patients (33.3%). No other complication was observed. To our knowledge, there was only one study in the literature reporting in detail marker-induced toxicity in a large patient group. In that study, Langenhuijsen et al[11] reported their experience with fiducial markers in 209 patients. After transrectal implantation of four gold markers, the side effects in a mean time of 90 weeks were recorded. Haematuria lasting 3 days and rectal bleeding occurred in 3.8% and 9.1% of the patients, respectively.

Compared with diagnostic biopsy data, where multiple biopsy cores are taken, our complication rates seem to be acceptable. Two large European screening programs noted haematuria in 23-63% of men after biopsy, rectal bleeding in 2.1-21.7% and urinary tract infection in 3.5-10.9%[12,13].

There of nine patients had minimal distance between fiducial less than 20 mm that too close for discriminated length of CyberKnife therapy. In our experience, the fiducial plantation of the prostate gland under transrectal US guidance had limited angles and filed of view of implanted needles.

We could not demonstrate any detrimental effects of advanced tumor stage or shorter duration of hormonal treatment on bleeding complications, as shown by Langenhuijsen et al[11]. A possible explanation could be that our longer median time on hormonal treatment (12 weeks VS 7 weeks) at the time of implantation allowed maximal shrinkage in tumor volume and decreased vascularization.

Our study had only one case for pancreatic implantation without major or minor complication. Alternate approaches such as endoscopic ultrasonography have been successful for certain abdominal and thoracic tumors[14] that are difficult or unsafe targets for a percutaneous approach and should be considered for any tumor adjacent to a hollow viscus.

Overall, technical success was high, with successful four-quadrant fiducial marker implantation in 80.9% of cases. Fiducial marker migration has been evaluated in the lungs as well as in abdominal and prostatic tumors[15,16]; however, most of these reports have used other modalities of implantation, such as bronchoscopic or endoscopic placement. Irrespective of that, fiducial marker migration or

"settling" is a known phenomenon and can occur up to 7 days after implantation. Hence, most centers advocate waiting at least 7 days after implantation before performing CyberKnife planning CT. In our study, substantial migrations were seen predominantly in the lungs (33.3%). This migration may be related to the incidence of pneumothorax.

Given this, alternate fiducial marker agents (eg. platinum coils) or alternate modalities (eg. bronchoscopic implantation)[17] should be further evaluated to revolve this problem.

In conclusion, the percutaneous implantation of fiducial markers can be achieved with a relatively low rate of major complications and high technical successful rate in liver and prostate implantation. However, fiducial marker migration and major complication (severe pneumothorax) may occur in lung implantations. This may necessitate additional procedures or the implantation of alternate agents (eg. coils) or bronchoscopic or endoscopic placement.

Limitations of this study include the small number of patients and single-center experience, particularly in the pancreatic and lung implantations.

References

1. Sacks D, McClenny TE, Cardella JF, Lewis CA. Society of Interventional Radiology clinical practice guidelines. J Vasc Interv Radiol. 2003 Sep;14(9 Pt 2):S199-202.
2. Chang SD, Adler JR. Robotics and radiosurgery--the cyberknife. Stereotactic and functional neurosurgery. 2001;76(3-4):204-8.
3. Adler JR, Jr., Murphy MJ, Chang SD, Hancock SL. Image-guided robotic radiosurgery. Neurosurgery. 1999 Jun;44(6):1299-306; discussion 306-7.
4. Ohara K, Okumura T, Akisada M, Inada T, Mori T, Yokota H, et al. Irradiation synchronized with respiration gate. International journal of radiation oncology, biology, physics. 1989 Oct;17(4):853-7.
5. Bryan PJ, Custar S, Haaga JR, Balsara V. Respiratory movement of the pancreas: an ultrasonic study. J Ultrasound Med. 1984 Jul;3(7):317-20.
6. Cardella JF, Bakal CW, Bertino RE, Burke DR, Drooz A, Haskal Z, et al. Quality improvement guidelines for image-guided percutaneous biopsy in adults. J Vasc Interv Radiol. 2003 Sep;14(9 Pt 2):S227-30.
7. Yousefi S, Collins BT, Reichner CA, Anderson ED, Jamis-Dow C, Gagnon G, et al. Complications of thoracic computed tomography-guided fiducial placement for the purpose of stereotactic body radiation therapy. Clinical lung cancer. 2007 Jan;8(4):252-6.
8. Cox JE, Chiles C, McManus CM, Aquino SL, Choplin RH. Transthoracic needle aspiration biopsy: variables that affect risk of pneumothorax. Radiology. 1999 Jul;212(1):165-8.
9. Poli ME, Parker W, Patrocinio H, Souhami L, Shenouda G, Campos LL, et al. An assessment of PTV margin definitions for patients undergoing conformal 3D external beam radiation therapy for prostate cancer based on an analysis of 10,327 pretreatment daily ultrasound localizations. International journal of radiation oncology, biology, physics. 2007 Apr 1;67(5):1430-7.
10. Langenhuijsen JF, van Lin EN, Kiemeney LA, van der Vight LP, McColl GM, Visser AG, et al. Ultrasound-guided transrectal implantation of gold markers for prostate localization during external beam radiotherapy: complication rate and risk factors. International journal of radiation oncology, biology, physics. 2007 Nov 1;69(3):671-6.
11. Langenhuijsen JF, van Lin EN, Kiemeney LA, van der Vight LP, McColl GM, Visser AG, et al. Ultrasound-guided transrectal implantation of gold markers for prostate localization during external beam radiotherapy: complication rate and risk factors. International journal of radiation oncology, biology, physics. 2007 Nov 1;69(3):671-6.
12. Raaijmakers R, Kirkels WJ, Roobol MJ, Wildhagen MF, Schrder FH. Complication rates and risk factors of 5802 transrectal ultrasound-guided sextant
13. Djavan B, Waldert M, Zlotta A, Dobronski P, Seitz C, Remzi M, et al. Safety and morbidity of first and repeat transrectal ultrasound guided prostate needle biopsies: results of a prospective European prostate cancer detection study. The Journal of urology. 2001 Sep;166(3):856-60.

14. Pishvaian AC, Collins B, Gagnon G, Ahlawat S, Haddad NG. EUS-guided fiducial placement for CyberKnife radiotherapy of mediastinal and abdominal malignancies. Gastrointestinal endoscopy. 2006 Sep;64(3):412-7.

15. Imura M, Yamazaki K, Shirato H, Onimaru R, Fujino M, Shimizu S, et al. Insertion and fixation of fiducial markers for setup and tracking of lung tumors in radiotherapy. International journal of radiation oncology, biology, physics. 2005 Dec 1;63(5):1442-7.

16. Kitamura K, Shirato H, Shimizu S, Shinohara N, Harabayashi T, Shimizu T, et al. Registration accuracy and possible migration of internal fiducial gold marker implanted in prostate and liver treated with real-time tumor-tracking radiation therapy (RTRT). Radiother Oncol. 2002 Mar;62(3):275-81.

17. Anantham D, Feller-Kopman D, Shanmugham LN, Berman SM, DeCamp MM, Gangadharan SP, et al. Electromagnetic navigation bronchoscopy-guided fiducial placement for robotic stereotactic radiosurgery of lung tumors: a feasibility study. Chest. 2007 Sep;132(3):930-5.

THE ASEAN JOURNAL OF RADIOLOGY 2010; 16(3): 222-229

Case Report

Megalencephalic Leukodystrophy with Subcortical Cysts: A Case Report

Chewarat Wirojtananugoon, MD.[1], **Annette Douglas-Akinwande, MD.**[1], **Bhuwan Garg, MD.**[2]

[1] *Department of Radiology, Indiana University School of Medicine, Indianapolis, Indiana, USA*

[2] *Department of Neurology, Indiana University School of Medicine, Indianapolis, Indiana, USA*

Abstract

Megalencephalic leukodystrophy is a rare neurodegenerative disorder which is characterized by macrocephaly in early infancy, slowly progressive neurologic deterioration and epilepsy. It was first described by Van der knaap in 1995. We present evolution of the imaging findings from 11 months to 10 years of age.

Introduction:

Leukodystrophy is a heterogeneous group of inherited metabolic disorders with one common denominator; abnormalities of the white matter of the central nervous system. A progressive mental regression with motor abnormalities is the most frequent clinical finding. In addition to the classic leukodystrophies such as Canavan disease and Alexander disease that have been extensively delineated, almost half of patients with leukodystrophies are of unknown cause. In the past few years, neuroimaging, especially cranial MRI, has played a major role in the identification of a number of new clinico-pathologic entities. Megalencephalic leukodystrophy with subcortical cyst is one of the novel leukodystrophies described by Van der knapp in 1995 by its characteristic clinical and MRI findings. We report a case with characteristic clinical and radiological findings including sequential imaging from infancy to adolescence.

Case Report

The patient is a child of healthy unrelated white parents, delivered normally at term after an uneventful pregnancy. Birth weight was 8-9 lbs. Head circumference at birth was normal. In the course of his 1st year of life, macrocephaly developed. His occipito-frontal circumference (OFC) at the age of 4 years was above the ninety-eight percentile at 58 cm. His development was delayed. He walked at 2 years of age. He spoke only one word ("mom") at 4 years of age. He has history of minor head trauma at the age of 16 months, history of murmur at birth, which spontaneously resolved, and history of asthma also resolved. The patient has 3 healthy unaffected siblings. He was referred for seizure work up at the age of 4 years. The episode consisted of eye blinking, face twitching, and tremor-like activity of the upper extremities, lasting 10 minutes, followed by an extended post-ictal period. Neurological examination revealed generalized hypotonia with normal muscle bulk. Antiepileptic drug treatment was initiated. He was seizure free for 4 years on antiepileptic drugs. He remained seizure free for 2 years off antiepileptic drugs before the focal seizures returned at the age of 10 years. His motor function deteriorated after he had seizures.

At the age of 9 years, he developed generalized spasticity, progressive dysphagia, ataxia of the limbs; particularly of the left upper extremity. Clonus and Babinski's signs were positive. By 10 years of age, he was unable to walk.

Laboratory investigations, including CBC, BUN/Cr, Electrolytes, blood glucose, liver function test, urine biochemical profile analysis, ammonium level were normal. Metabolic screening of a 24-hr sample of urine for amino acids, organic acids, oligosaccharides, mucopolysaccharides was normal. Assessment of lysosomal enzyme, B12, folate and vitamin E were normal. EMG was normal. Peripheral motor and sensory nerve conduction velocity for left peroneal and left sural nerve were normal. EEG revealed abnormal continuous left temporal slowing and frequent epileptiform discharges over the left temporal region which is indicative of a structural abnormality with epileptogenic potential in that region.

Cranial computed tomographic (CT) examinations were performed in 1994, 1995, 1997 and 2004 at the age of 10 months, 1.5, 4 and 10 years, respectively. The first CT at 10 months of age (Fig.1a) showed diffuse low density with mild expansion of the cerebral white matter bilaterally and symmetrically with a left anterior temporal subcortical cyst. The second CT performed at 18 months of

age was unchanged. The CT, performed at 4 years of age (Fig. 1b) showed the development of volume loss as indicated by increase prominence of the cortical sulci and ventricles with stable left anterior temporal subcortical cyst. The CT performed in 2004 showed (Fig. 1c) slight progression of atrophy but stable left anterior temporal subcortical cyst.

Cranial MRI in 1998, 2002 and 2004 performed at 4, 8 and 10 years of age respectively demonstrated diffuse, symmetric T1 and T2 signal prolongation within the cerebral white matter bilaterally. Subcortical cysts were present in the left frontal and both anterior temporal lobes (Fig. 2-5). These cystic lesions were isointense to CSF on both T1- and T2-weighted

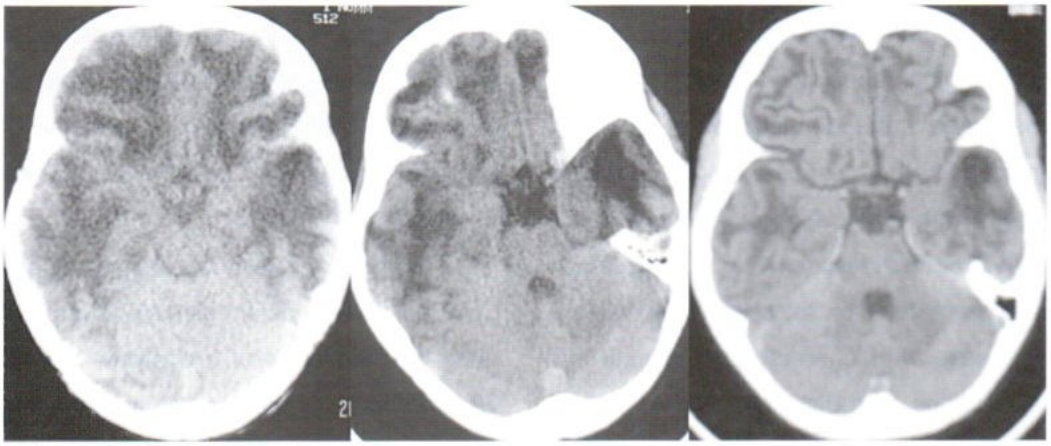

Fig.1 Transaxial CT in 1994 (a), 1997 (b) and 2004(c) (from left to right) shows diffuse cerebral white matter low density with a left anterior temporal subcortical cyst and progression of cerebral atrophy.

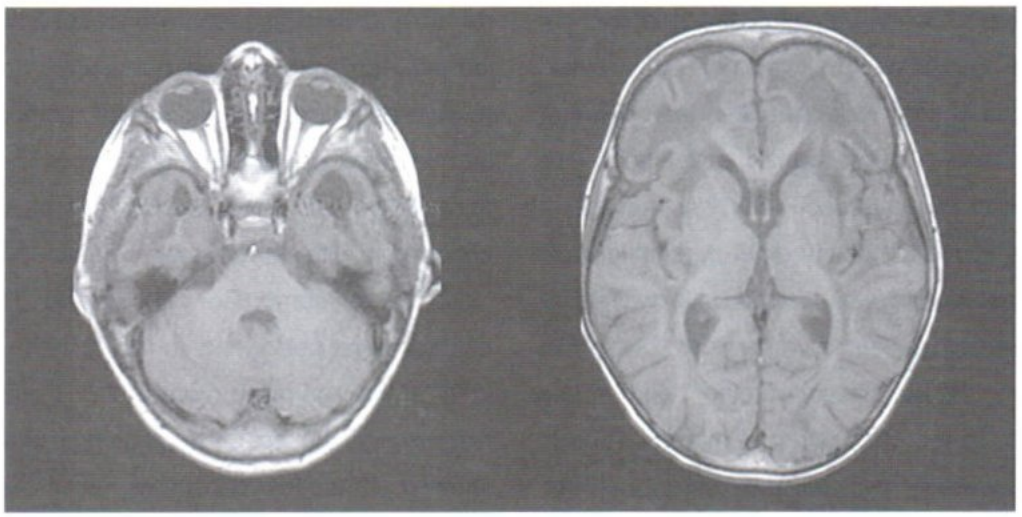

Fig.2 Axial T1-weighted images (TR.450 ms; TE.14 ms) shows diffuse T1 prolongation of the cerebral white matter predominantly at the frontotemporal lobes with anterior temporal subcortical cysts.

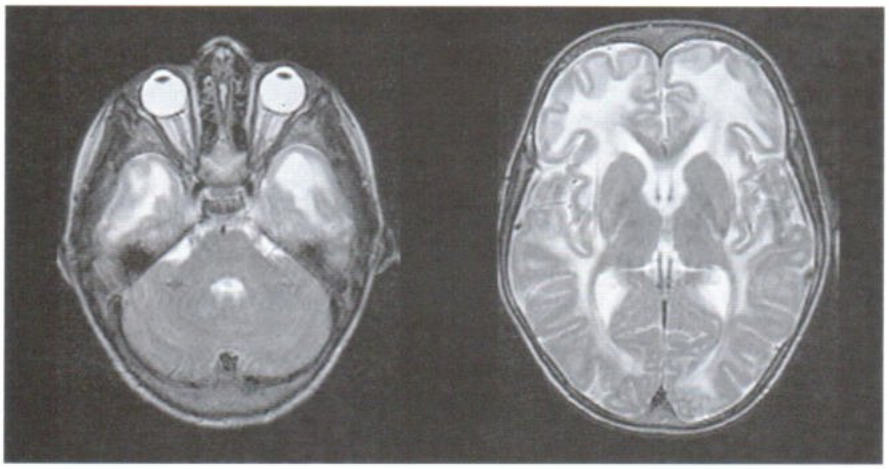

Fig.3 Axial T2-weighted (TR.3000 ms/TE.105 ms) images show diffuse T2 prolongation of the cerebral white matter predominantly at the frontotemporal lobes with anterior temporal subcortical cysts. Note increased T2 prolongation of the dentate nuclei (asterisk) and dorsal pons (black arrow).

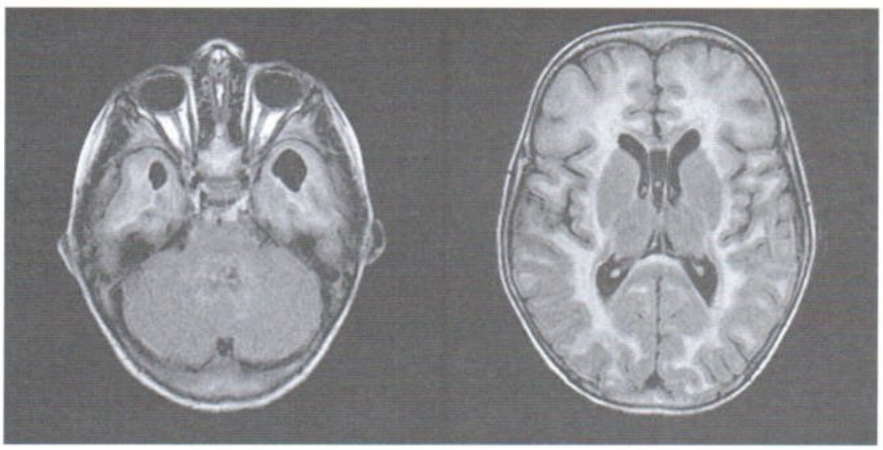

Fig.4 Axial FLAIR images show diffuse abnormal hyperintensity of the cerebral white matter predominantly at the frontotemporal lobes with anterior temporal subcortical cysts. Note increased signal of the dentate nuclei and dorsal pons.

images. There was no swelling of the gyri. The cerebral sulci and ventricular system appeared slightly prominent. There was sparing of central white matter structures, including corpus callosum, anterior limb of the internal capsule, a periventricular rim of the occipital white matter (optic radiation), and some subcortical white matter, especially in the occipital lobes (Fig. 2-4). The cerebellar white matter was spared, but there was increased T2 signal of the dentate nuclei and dorsal pons bilaterally (Figure 3-4). There is no significant difference among these three MRI studies. Proton magnetic resonance spectroscopy (MRS) using PRESS technique with TE 35 and 288, performed at the age of 8 years

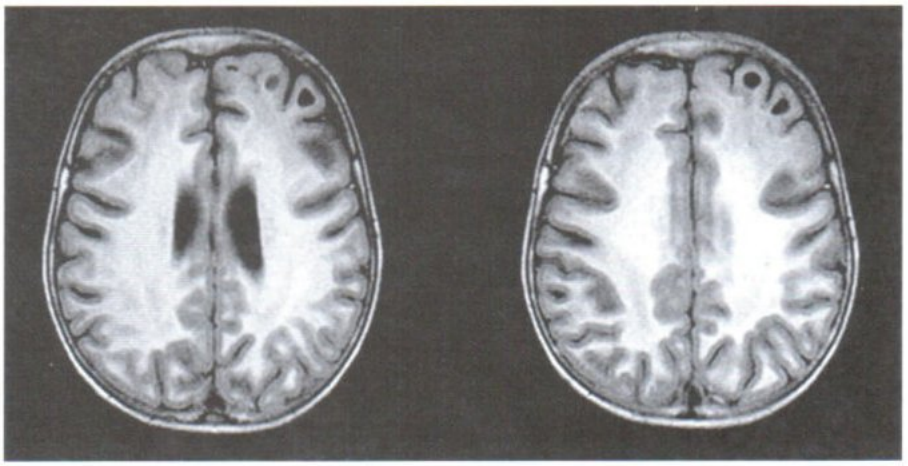

Fig.5 Axial FLAIR images show diffuse abnormal hyperintensity of the cerebral white matter with several left frontal subcortical cysts.

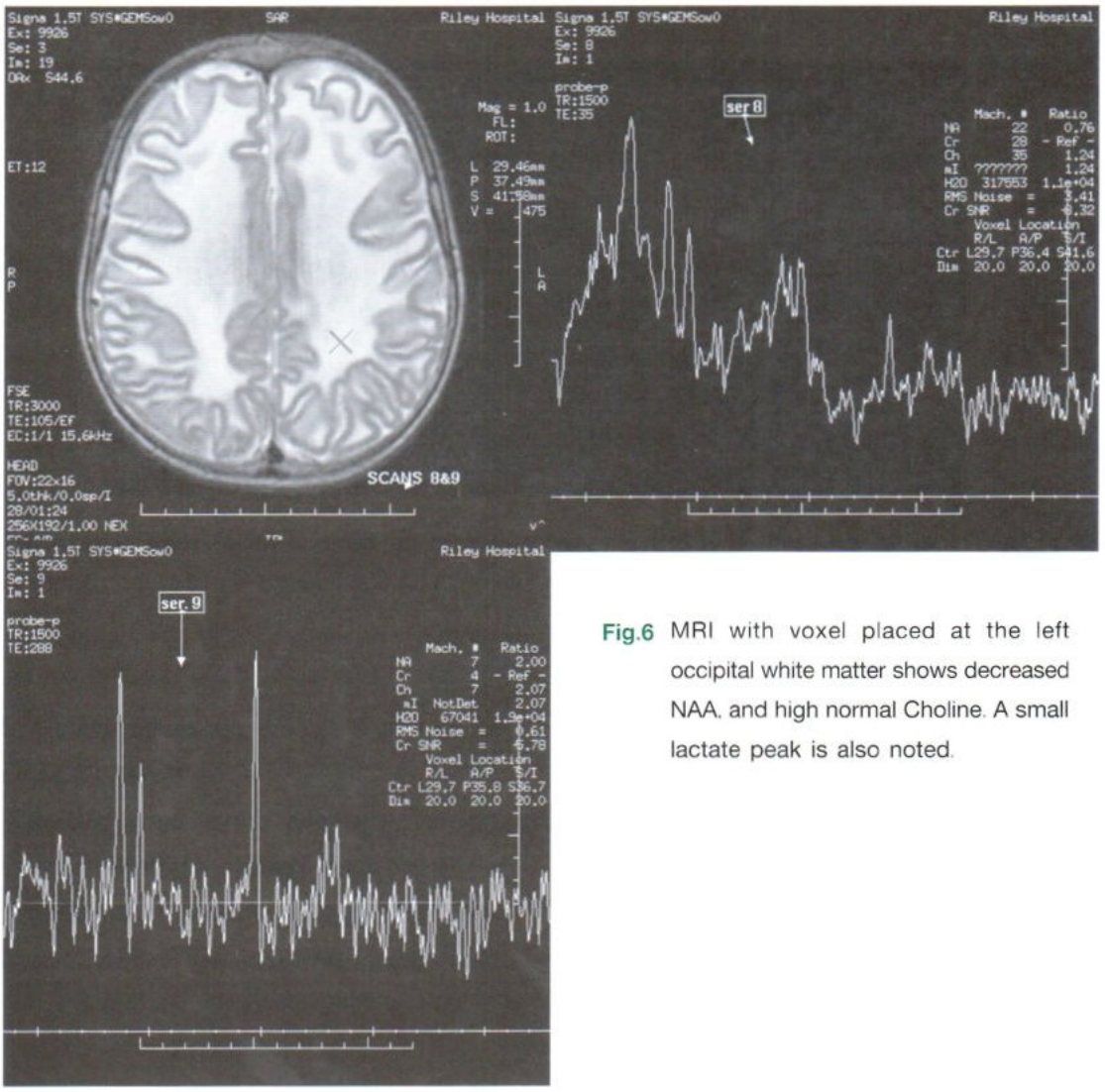

Fig.6 MRI with voxel placed at the left occipital white matter shows decreased NAA, and high normal Choline. A small lactate peak is also noted.

showed decreased NAA. Choline at the upper limits of normal and high Myo-Inositol in the white matter (Fig. 6) with normal spectrum of the basal ganglia.

Discussion and Literature Review

The first two reported cases of infantile onset megalencephaly and leukodystrophy syndrome were reported by Harbord et al. in 1990. There was no mention of subcortical cysts and no MRI study was performed.

In 1995, van der knaap et al. described detailed distinctive clinical and radiological characteristics of this new syndrome based on eight cases. Subsequently, there has been many reports of similar cases[2,3,5,6]. This novel leukodystrophy has been synonyms: leukoencephalopathy with macrocephaly and mild clinical course. Van der knaap disease and Vacuoliting megalencephalic leukoencephalopathy. It is characterized by the development of macrocephaly within the first year of life. Early infantile development is usually normal or minimally delayed. However, after a delay of several years, a slow deterioration of motor function occurs with ataxia and spasticity. Cognitive function is less affected. Seizures occur in most patients but are usually easily controlled with medication. Screening for inborn errors of metabolism that causes either megalencephaly or white matter disease is negative.

Since the report by Van der knaap in 1995, further family studies in several ethnic groups have suggested an autosomal recessive mode of inheritance. The disease occurs with relatively high frequency in an Asian-Indian tribe[3] and Turkish populations[6]. A locus of MLC was mapped to chromosome 22qtel[7]. Several mutations in the MLC1 gene, which encodes a putative CNS membrane transporter have been identified[8-11].

Histologically, the disease is characterized by the presence of numerous vacuoles between the outer lamellae of myelin sheaths suggesting splitting of these lamellae along the intraperiod line or incomplete compaction of the outermost myelin lamellae[4].

There is no biochemical diagnostic test for detection of the disease in asymptomatic stage. Only DNA test can be used for diagnosis, however it is not commercially available at the present time. And unfortunately, there is no specific treatment for this rare leukodystrophy.

Currently Magnetic Resonance Imaging is the most readily available diagnostic tool for evaluating this disease. The MRI features are characteristic and specific[1-3,5,6]. MRI typically demonstrates bilateral diffuse abnormal and swollen supratentorial hemispheric white matter,and subcortical cysts which are invariably present in the anterior-temporal, and often the frontoparietal regions.

Characteristic sparing of central white matter structures (corpus callosum, anterior limb of the internal capsule, occipital periventricular white matter, partially posterior limb of the internal capsule) and some sparing of subcortical white matter have been described[1,6]. No abnormal enhancement has been reported. Radiologists should be aware of this disorder since they may be the first to suggest the diagnosis based on the characteristic imaging findings. This may further prompt definitive genetic studies to confirm the diagnosis. On the basis of clinical and MRI criteria, our case is a typical example of Megalencephalic leukodystrophy with subcortical cysts. The clinical and MRI findings in our case are

similar to those previously described. However, we have serial imaging studies showing progression of cerebral atrophy with time. Swelling of the white matter was present in the early stage with gradual development of cerebral atrophy in late stage.

MRI is better than CT in identifying the white matter abnormality and subcortical cysts. However, MR findings do not reflect the clinical severity of disease (no change of follow up MRI studies, despite clinical progression of disease). In the study of van der knaap et al., MRS in four patients revealed decreased N-Acetyl aspartate (NAA), high Choline and normal myo Inositol (mI). In our case, NAA is decreased, Choline at the upper limits of normal, mI was not detected and a very small lactate doublet was identified (Figure 6). This MRS may be explained by loss of neurons, and tissue destruction.

The differential diagnosis of MLC includes other leukodystrophies that present with megalencephaly, cognitive decline and motor disability. Whereas megalencephaly is seen in the infantile form of Alexander disease, imaging studies are quite distinct, showing a frontal region preponderance of white matter change with abnormal enhancement and basal ganglia involvement, and the clinical course is much more rapidly progressive. Patients with Alexander disease can be diagnosed by GFAP (glial fibrillary acidic protein) gene mutation screening.

Canavan disease can present as megalencephaly and spasticity but is often accompanied by cortical blindness and much smaller subcortical cysts that are not as easily identifiable as the larger cysts seen in MLC. Canavan disease can also have involvement of basal ganglia and thalami. A deficiency of the enzyme aspartoacylase in cultured fibroblasts or characteristically high NAA peak on Magnetic Resonance Spectroscopy is diagnostic of Canavan Disease. Canavan disease also has rapid clinical course.

Similarly, glutaric aciduria type I can present with megalencephaly and variable clinical presentation (normal or slightly delayed development, dyskinesia, spasticity) but can be easily distinguished from MLC by the metabolic abnormality (metabolic acidosis/ketosis, hypoglycemia, aciduria) and MRI findings (Deep gray matter abnormality).

Conclusion

Megalocystic leukodystrophy is a rare disorder of infancy and childhood. The MR imaging findings are characteristic. The radiologist should therefore suggest this diagnosis when these classically located cysts are present in the setting of a leukodystrophy. MRS may also be helpful in making the diagnosis.

References

1. Van der Knaap MS, Barth PG, Stroink H, van Nieuwenhuizen O, Arts WFM, Hoogenraad F, Valk J. Leukoencephalopathy with swelling and discrepantly mild clinical course in eight children. Ann Neurol 1995;37: 324-34.
2. Goutiers F, Boulloche J, Bourgeois M, Aicardi J. Leukoencephalopathy, megalencephaly, and mild clinical course. A recent individualized familial leukodystrophy. Report on five new cases. J Child Neurol 1996;11:439-444.
3. Singhal BS, Gursahani RD, Udani VP, Biniwale AA. Megalencephalic leukodystrophy in an Asian ethnic group. Pediatr Neurol 1996;14:291-6.
4. Van der Knaap MS, Barth PG, Vrensen GFJM, Valk J. Histopathology of an infantile-onset spongiform leukoencephalopathy with a discrepantly mild clinical course. Acta Neuropathol 1996;92:206-12.
5. Mejaski-Bosnjak V, Besenski N, Brockmann K, Pouwels PJ, Frahm J, Hanefeld FA. Cystic leukoencephalopathy in a megalencephalic child: Clinical and magnetic resonance

imaging/magnetic resonance spectroscopy findings. Pediatr Neurol 1997;16:347-50.

6. Topcu M, Saatci K, Topcuoglu MA, Kose G, Kunak B. Megalencephaly and leukodystrophy with mild clinical course: a report on 12 new cases. Brain Dev 1998; 20:142-53.
7. Topcu M, Gartioux C, Ribierre F, et al. Vacuoliting megalencephalic leukoencephalopathy with subcortical systs, mapped to chromosome 22qtel. Am J Hum Genet 2000; 66:733-9.
8. Leegwater PA, Yuan BQ, van der Steen J, et al. Mutations of MLC1 (KIAA0027), encoding a putative membrane protein, cause megalencephalic leukoencephalopathy with subcortical cysts. Am J Hum Genet 2001;68:831-8.
9. Leegwater PA, Boor PK, Yuan BQ, et al. Identification of novel mutations in MLC1 responsible for megalencephalic leukoencephalopathy with subcortical cysts. Am J Hum Genet 2002;110:279-83.
10. Ben-Zeev B, Levy-Nissenbaum E, Lahat H, Anikster Y, et al. Megalencephalic leukoencephalopathy with subcortical cysts: a founder effect in Israeli patients and a higher than expected carrier rate among Libyan Jews. Hum Genet 2002;111:214-8.
11. Gorospe JR, Singhal BS, Kainu T, et al. Indian Agarwal megalencephalic leukodystrophy with cysts is caused by a common MLC1 mutation. Neurology 2004; 62:878-82.

Instructions for Authors

1. The Asean Journal of Radiology publishes the papers on Radiological Sciences, such as research work, reviews articles case reports, innovations in medical Sciences related to all branches of Radiology, and letters to the editor. The aforementioned materials can be written in English only.
2. The authors have to submit 2 copies of the manuscript and a CD :to Assoc. Prof. Sirintara Singhara Na Ayudya, Department of Radiology, Faculty of medicine, Ramathibodi hospital 270, Rama VI Road, Toong Phayathai, Ratchathewi, Bangkok, 10400. Tel 02-2011259#110, Fax 02-2011297, E-mail Sirintarapongpech2@hotmail.com
3. The original copy to be submitted must be typed in a double space on one of the page 8.5"x11" (A4) paper.
4. The format of the article must include:
   a. Title page and address of the author (s)
   b. Abstract (Objective, Methods, Results and conclusion)
   c. Introduction
   d. Material and Method
   e. Results and discussion
   f. Acknowledgment (if any)
   g. References (Follow the Vancouver style)
5. We will provide 5 copies of reprints for the author (s) an article for publication in the Asean Journal.
6. The illustrations and table must be clearly prepared with legends in English as they are the art works to be reproduced
7. The authors are responsible for the contents of the article as to its facts and findings.
8. Ethics

Paper reporting studies which might be interpreted as human experimentation (e.g. controlled trials) should conform to the standards of the Declaration of Hilsinki (see British Medical Journal 1964:2:177) and should indicate that, approval that such studies may proceed, has been granted by the local or hospital Ethics Committee.

When reporting experiments on animal indicate whether the institution's or the National Research Council's guide for, or any national law on, the care and use of laboratory animals was followed.

AGILITY

TRUFILL Detachable Coil DCS Orbit

Codman enterprise™

vascular reconstruction device

PROWLER®

PROWLER™ PLUS

PROWLER® SELECT™ Plus

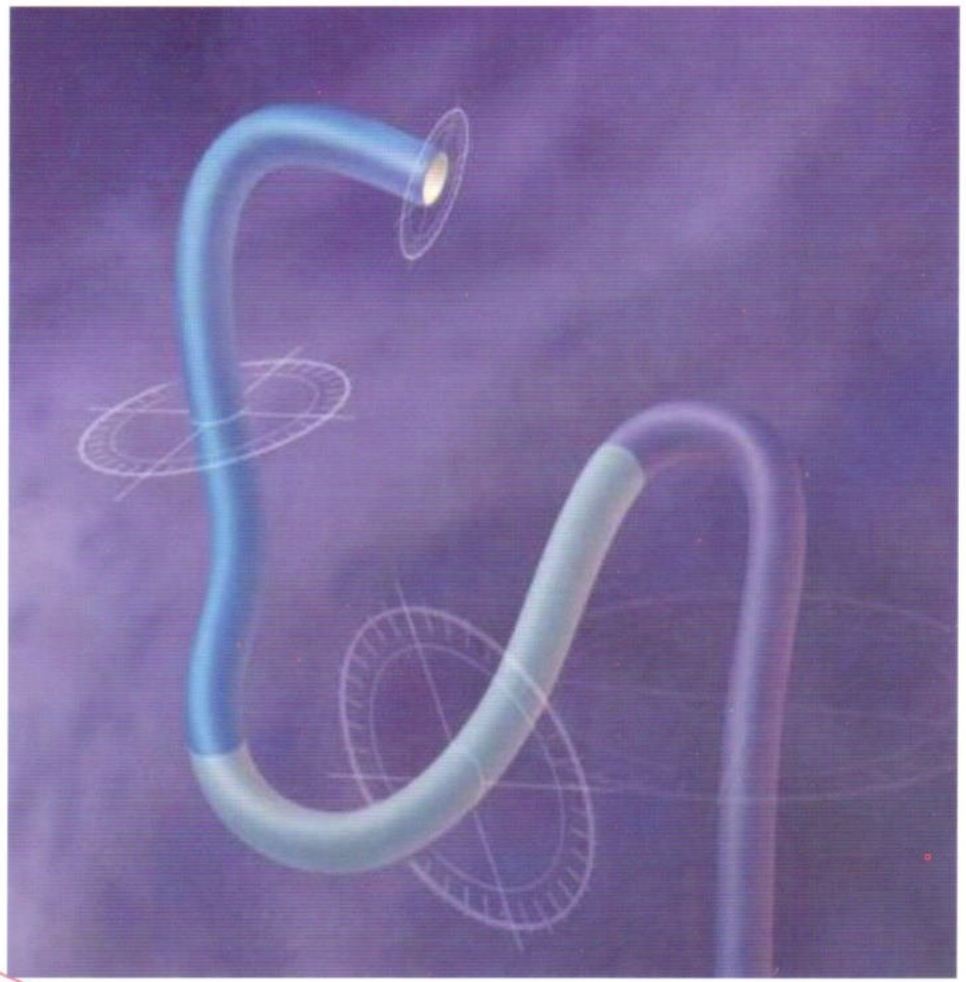

Codman

a Johnson & Johnson company

NEUROVASCULAR

never stop moving™

บริษัท จอห์นสันแอนด์จอห์นสัน (ไทย) จำกัด
106 หมู่ 4 นิคมอุตสาหกรรมลาดกระบัง
ถนนฉลองกรุง แขวงลำปลาทิว
ลาดกระบัง กทม 10520
โทร 02-3260902